Haploid Reporter Screens Aimed at Identification of NF-kappaB Regulators
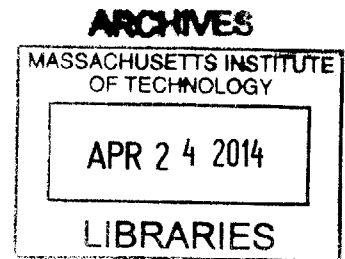
by

Clarissa Ci Lee

B.A., Molecular and Cell Biology
University of California, Berkeley, 2007

SUBMITTED TO THE DEPARTMENT OF BIOLOGY IN PARTIAL FULFILLMENT OF
THE REQUIREMENTS FOR THE DEGREE OF

DOCTOR OF PHILOSOPHY IN BIOLOGY
AT THE
MASSACHUSETTS INSTITUTE OF TECHNOLOGY

JUNE 2014

Signature redacted

Signature of Author: _____
Department of Biology
April 18, 2014

Signature redacted

Certified by: _____
Hidde L. Ploegh
Professor of Biology
Member, Whitehead Institute for Biomedical Research
Thesis Supervisor

Signature redacted

Accepted by: _____
Amy Keating
Associate Professor of Biology
Co-Chair, Committee for Graduate Students

1

Haploid Reporter Screens Aimed at Identification of NF-kappaB Regulators

by

Clarissa Ci Lee

Submitted to the Department of Biology on April 18, 2014 in Partial Fulfillment of the
Requirements for the Degree of Doctor of Philosophy in Biology

ABSTRACT

Nuclear factor-kappaB (NF-κB) is a family of transcription factors that are essential for execution of both the innate and the adaptive immune response. NF-κB regulates hundreds of genes involved in critical processes such as cell survival, differentiation, proliferation, and inflammation. Consequently, NF-κB activity must be tightly regulated and a failure to do so causes diseases such as inflammatory disorders and cancer. The identification of novel NF-κB regulators can increase our understanding of the elaborate regulatory networks that control the NF-kB response and influence the design of therapeutic interventions directed at NF-kB. A classical approach for identifying new members in a pathway is the forward genetic screen. Human haploid genetic screens represent a recent advance in this approach. I have attempted to expand the utility of human haploid genetic screens through the use of transcriptional reporters and developed human haploid reporter screens for the specific purpose of identifying regulators of NF-kB. To identify constitutive inhibitors of NF-kB, I utilized a NF-κB-blasticidin S resistance gene (*BSR*) reporter and identified *CYLD*, a known negative regulator of NF-κB, demonstrating that in principle this approach works. In the same screen, two members of the poorly characterized leucine-rich repeat-containing 8 (LRRC8) family of proteins appeared as significant hits. I determined that *LRRC8D* is not required for NF-κB regulation, but rather for import of blasticidin, the selecting agent used in the screen. Thus, quite serendipitously, I identified the first mammalian protein that mediates import of the antibiotic blasticidin. My further characterization of LRRC8D provides new insight into the function of LRRC8 proteins. I developed a second screen, using a NF-κB-GFP reporter, to identify genes required to activate NF-κB in response to the TLR2/6 ligand, FSL-1. This screen successfully identified known components of the TLR2/6 pathway and identified many other candidate genes for further study.

Thesis Supervisor: Hidde L. Ploegh
Title: Professor of Biology, MIT; Member, Whitehead Institute for Biomedical Research

Acknowledgements

My deepest thanks extend to ...

For my parents

Table of Contents

Chapter 4: A Human Haploid Reporter Screen for Genes Required to Activate NF-κB in Response to TLR2/6 Signaling

Chapter 5: Future Directions

Appendix 1: Proteolytic cleavage in an endolysosomal compartment is required for activation of Toll-like receptor 9

Appendix 2: Accessory molecules for Toll-like receptors and their Function

Introduction

Nuclear factor-κB (NF-κB) is a family of transcription factors that was originally discovered as regulators of κB light chain expression in mature B and plasma cells (Sen and Baltimore, 1986a; 1986b). Work since then has demonstrated that NF-κB is expressed in almost all cell types and regulates hundreds of genes in response to > 150 different stimuli (Hoffmann et al., 2006; Pahl, 1999) (Figure 1). Among the processes influenced by NF-κB are inflammation, immunity, cell proliferation, differentiation, and survival. Given its involvement in such critical processes, dysregulation of NF-κB has been implicated in a number of pathologies including cancer, diabetes, and inflammatory disorders. Determining the mechanisms by which NF-κB is regulated will thus be crucial for understanding how NF-κB-related pathologies develop and how best to design therapeutic interventions.

NF-κB Signaling Pathways

The mammalian NF-κB transcription factor family consists of five members: p65 (RelA), RelB, c-Rel, p50 (NF-κB1), and p52 (NF-κB2) that can form homo- or heterodimeric complexes with distinct functions. All five members posses an N-terminal Rel homology domain (RHD) required for dimerization and DNA binding (Hayden and Ghosh, 2012). p65, RelB, and c-Rel also posses a transcription activation domain (TAD) that confers the ability to initiate transcription. p50 and p52 lack TADs, but can positively regulate transcription by heterodimerization with TAD-containing NF-κB members or by interaction with other proteins that have transactivating abilities. The primary mechanism by which inducible activation of NF-κB is achieved is through binding of NF-κB dimers to Inhibitor of κB (IκB) proteins which sequester NF-κB dimers in the cytoplasm at steady-state. Cellular stimulation results in phosphorylation, ubiquitylation, and proteasome-mediated proteolysis of the NF-κB-bound IκB, which allows NF-κB to translocate to the nucleus and bind to DNA.

The NF-κB signaling pathways have been broadly classified into two types: canonical and noncanonical (Figure 2). A wide range of stimuli can activate NF-κB in the canonical pathway. In a typical example, ligand binding to a cell surface receptor (e.g. TNF receptor, IL-1 receptor, Toll-like receptors, and antigen receptors) leads to a

conformational change in the receptor and initiates the recruitment of a series of adapter proteins, which possess protein-protein interaction domains. Domains that are commonly used in NF-κB signaling cascades are death domains (DDs), caspase activation and recruitment domains (CARDs), RIP homotypic interaction motifs (RHIMs), and Toll/IL-1 (TIR) domains. Adapter proteins then recruit kinases to the receptor complex to form a large signaling platform, which mediates the activation of the IKK complex, containing two highly homologous kinase subunits, IKKα, IKKβ, and a regulatory subunit, NEMO. The activated IKK complex then phosphorylates the IκB proteins IκBα, IκBβ, IκBε, which leads to their proteasomal degradation and the release of their NF-κB bound dimers.

Unlike the canonical pathway, which can be activated by diverse receptors, the noncanonical pathway is induced by specific members of the TNF cytokine family, such as BAFF, lymphotoxin-β, or CD40 ligand (Hayden and Ghosh, 2012; Razani et al., 2011). Following receptor ligation, NF-κB-inducing kinase (NIK) protein, which is normally subject to constitutive ubiquitylation and subsequent degradation, is stabilized (Liao, 2004). NIK can then phosphorylate and activate IKKα, which in turn phosphorylates p100, thus initiating processing of p100 to p52. RelB/p52 dimers can then enter the nucleus and regulate target genes that are distinctly regulated by the noncanonical pathway.

Toll-like Receptors and Activation of NF-κB

Toll-like receptors (TLRs) are pattern–recognition receptors (PRRs) that recognize pathogen-associated molecular patterns (PAMPs) from microorganisms or danger-associated molecular patterns (DAMPs) from damaged tissue. TLRs trigger innate immune responses and also prime antigen-specific adaptive immunity. TLRs are type I transmembrane proteins that possess an extracellular leucine-rich repeat (LRR) domain for ligand binding, and an intracellular Toll/IL-1receptor (TIR) domain that mediates signal transduction through the recruitment of adapter proteins. So far, 10 and 12 functional TLRs have been identified in humans and mice, respectively. Each TLR has a distinct function in terms of PAMP recognition and immune responses. TLRs form heterodimers or homodimers as a means of triggering a signal. Most TLRs form homodimers, with a few exceptions. For example, TLR2 forms heterodimers with TLR1 or TLR6, which enables differential recognition of bacterial lipopeptides: TLR1–TLR2

recognizes triacylated lipopeptides, whereas TLR2–TLR6 responds to diacylated lipopeptides (Jin et al., 2007; Kang et al., 2009).

TLRs can be divided into two subgroups based upon their cellular localization. TLR1, TLR2, TLR4, TLR5, TLR6, and TLR11 traffic from the ER to the cell surface and mainly recognize PAMPs derived from the surface of microorganisms including LPS, lipoproteins, and flagellin (Kawai and Akira, 2010; Takeuchi and Akira, 2010). TLR3, TLR7, TLR8, and TLR9 on the other hand, traffic to endolysosome compartments where they recognize microbial nucleic acids (Kawai and Akira, 2010; Takeuchi and Akira, 2010). Several proteins mediate the trafficking of TLRs to their final destination. Gp96, a paralogue of the heat-shock protein 90 (HSP90) chaperone, mediates the folding of several TLRs in the ER. Gp96 is necessary for the function of TLR1, TLR2, TLR4, TLR5, TLR7 and TLR9 and is required for the surface expression of TLR1, TLR2 and TLR4 and for the maturation and cleavage of TLR9 in the endolysosome (Liu and Li, 2008; Liu et al., 2010; Randow and Seed, 2001; Yang et al., 2007). PRAT4A, an ER luminal protein, appears to function together with Gp96 to mediate maturation of TLRs in the ER (Liu et al., 2010). Knockdown of PRAT4A expression impeded the passage of TLR1 and TLR4 through the Golgi and prevented ligand-induced trafficking of TLR9 from the ER to endolysosomes (Takahashi et al., 2007). UNC93B1 is an ER-resident glycoprotein that is predicted to span the membrane 12 times (Tabeta et al., 2006). Mice homozygous for an *UNC93B1* missense mutation (H412R) that prevents interaction with TLR3, TLR7, TLR8, and TLR9 have impaired signaling via TLR3, TLR7 and TLR9. Bone marrow-derived macrophages from these mice show defective ligand-induced trafficking of UNC93B1, TLR7 and TLR9 to endolysosomal compartments (Brinkmann et al., 2007; Kim et al., 2008; Tabeta et al., 2006).

TLRs can also be classified by the signaling pathways they activate (Figure 3). The MyD88-dependent pathway is used by all TLRs except TLR3 and results in the activation of NF-κB and mitogen-activated protein kinases (MAPKs) to induce inflammatory cytokines (Kawai and Akira, 2010). The TRIF-dependent pathway is used by TLR3 and TLR4 and activates NF-κB and interferon-regulatory factors (IRFs) to yield inflammatory cytokines and type I interferon (Kawai and Akira, 2010). MyD88 and TRIF are adapter molecules required in their respective pathways. While several TLRs can recruit MyD88 or TRIF directly through their TIR domain, others require additional adapter molecules to bridge the interaction. The TLR1–TLR2, TLR2–TLR6, and TLR4–

TLR4 dimers require the adapter TIRAP, also known as MAL, to recruit MyD88 (O'Neill and Bowie, 2007; O'Neill et al.). Alternatively, TLR4–TLR4 homodimers can utilize the adapter TRAM to recruit TRIF (O'Neill and Bowie, 2007; O'Neill et al.).

In the MyD88-dependent pathway, MyD88 recruits the IL-1 receptor-associated kinases IRAK4, IRAK1, and IRAK2 to TLRs (Kawai and Akira, 2010). IRAK4 is activated first, which in turn phosphorylates IRAK1 and IRAK2 (Kawai and Akira, 2007; 2010). The activated IRAKs then interact with TRAF6, an E3 ligase that attaches K63-linked polyubiquitin chains onto target proteins with the assistance of the E2 ubiquitin-conjugating enzyme complex comprising Ubc13 and Uev1A (Kawai and Akira, 2007; 2010). In a poorly understood manner, the synthesis of K63-linked polyubiquitin chains by TRAF6 recruits a complex of TAK1, TAB2, and TAB3 (Kawai and Akira, 2007; 2010). TAK1 can phosphorylate IKK, but whether this is the final event required for IKK activation and subsequent activation of NF-κB, is not completely understood (Hayden and Ghosh, 2008). Deletion of TAK1 impairs TLR4-mediated activation of NF-κB in macrophages, B cells, and fibroblasts, but not in neutrophils (Alagbala Ajibade et al., 2012; Sato et al., 2005; Schuman et al., 2009). Activation of the IKK complex requires phosphorylation of T loop serines of at least one of the IKK subunits (Hayden and Ghosh, 2008). Whether this phosphorylation event is catalyzed by TAK1, a downstream target of TAK1, or whether IKK transautophosphorylation is induced by oligomerization of a signaling scaffold is still a matter of debate. All TLRs that use the MyD88-dependent pathway can activate NF-κB. In dendritic cells, the endosomal TLRs can also activate IRFs in a MyD88-dependent manner (Honda et al., 2004; Negishi et al., 2006; Schmitz et al., 2007; Schoenemeyer et al., 2005).

In the TRIF-dependent pathway, TRIF can recruit TRAF6, TRAF3, or RIP1 (Takeuchi and Akira, 2010). TRAF6 and RIP1 are thought to mediate activation of NF-κB through mechanisms similar to those of the MyD88-dependent pathway. TRAF3 is important for activating two IKK-related kinases, TBK1 and IKKε (Häcker et al., 2006; Oganesyan et al.), TBK1 and IKKε phosphorylate IRF3 and IRF7, promoting their homodimerization and translocation to the nucleus (Takeuchi and Akira, 2010).

Regulation of NF-κB Transcriptional Specificity

NF-κB dimers bind to DNA κB sites in promoters and enhancers that have the highly degenerate sequence 5' GGGRNWYYCC 3' (where N is any base, R is purine, W

is adenine or thymine, and Y is pyrimidine) (Hayden and Ghosh, 2012). In addition, they have been found to bind sites that deviate from this consensus sequence (Natoli et al., 2005). The degenerate nature of the sequences to which NF-κB can bind means that there are many sites across the genome recognized by NF-κB. However, often, NF-κB activation leads to the expression of only a subset of genes it is capable of activating. Many other layers of regulation may influence NF-κB target gene regulation, including selective dimer combinations, chromatin environment, post-translational modifications of NF-κB, cross-talk between signaling pathways, and cell state.

Context-dependent assembly of NF-κB family members into selective dimer combinations that regulate unique sets of target genes could influence the specificity of an NF-κB response. Specificity of dimer formation has been difficult to study because of considerable redundancy between NF-κB dimer combinations and because each NF-κB family member can participate in many different dimers. Nevertheless, the RelB/p52 heterodimer used by the noncanonical pathway provides one clear example of an NF-κB dimer selectively activating a unique set of target genes in response to a specific stimulus (Ghosh and Hayden, 2008).

The kinetics of NF-κB recruitment to target genes are complex – some genes recruit NF-κB shortly after its nuclear entry whereas others take hours to do so (Saccani et al., 2001; 2004). NF-κB target genes vary in their dependence for chromatin modification for expression, which may account for this phenomenon (Natoli et al., 2005). Genes that do not require chromatin modification may be expressed more quickly in response to a stimulus, whereas genes that require chromatin modification are expressed later (Ramirez-Carrozzi et al., 2006; Saccani et al., 2001). In LPS-stimulated macrophages, the catalytic BRG1/BRM subunits of the SWI/SNF class of ATP-dependent nucleosome remodeling complexes are required for the activation of secondary response genes and primary response genes induced with delayed kinetics, but not for rapidly induced primary response genes. Pharmacological inhibition of BET proteins that govern the assembly of histone acetylation-dependent chromatin complexes suppresses transcriptional activation of only a subset of NF-κB target genes in LPS-stimulated macrophages (Nicodeme et al., 2010)

All NF-κB family members can be extensively modified. Selective modification and co-dependent regulatory interactions may control target gene expression in different physiological contexts (Smale, 2011). Phosphorylation of Ser 276 of p65 by PKA

promotes the interaction of p65 with the histone acetyltransferases (HATs), CBP and p300 (Zhong et al., 1998). Knock-in mutation of Rel S276A leads to defective activation of a subset of NF-κB target genes suggesting that recruitment of HATs is differentially required at NF-κB target genes (Dong et al., 2008). Other kinases such as MSK1 and MSK2 have also been reported to phosphorylate Ser276 of p65 and *MSK1$^{-/-}$ MSK2$^{-/-}$* cells have diminished transcriptional activity in response to TNF (Vermeulen et al., 2003). Acetylation of p65 promotes association with HATs and is associated with increased transcription (Chen and Greene, 2004). Methylation of p65 by the Set9 methyltransferase has been reported although there is a lack of consensus on the functional outcome of this post-translational modification. Set9 has been shown to target Lys37 of RelA in response to cytokine stimulation and is required for the expression of a subset of NF-κB target genes (Ea and Baltimore, 2009; Li et al., 2008). However, in another report that demonstrated methylation of RelA Lys 314 and 315 by Set9, Set9 was required for the termination of NF-κB responses (Yang et al., 2009). The observed differences may be due to the use of different cell lines and the examination of different target genes.

Often an inflammatory stimulus will induce signaling pathways that result in the activation of multiple transcription factors. Stimulus-specific NF-κB transcriptional programs may be achieved through cooperative binding of NF-κB with other transcription factors at promoters and enhancer of genes. One well-characterized example of this is the enhanceosome complex for the gene that encodes interferon-β, which involves several transcription factors induced by viral infection (NF-κB, ATF-2–c-Jun, and IRF3 or IRF7)(Agalioti et al., 2000; Panne et al., 2004; 2007). In this case, transcriptional synergy is conferred by both cooperative DNA binding and recruitment of coactivators. Additional factors for which synergistic interaction with NF-κB have been reported are Sp1, AP1, STAT3, and CEBP/β (Oeckinghaus et al., 2011).

NF-κB activation in different cell types can result in different transcriptional programs. While both TNF and LPS activate NF-κB in human dendritic cells, only LPS is capable of inducing recruitment of NF-κB to the *IL6* promoter (Natoli et al., 2005). In contrast, both TNF and LPS result in efficient recruitment of NF-κB to the *IL6* promoter in fibroblasts. Cell-type specificity of the NF-κB response is likely linked to the pathways and factors that control cell differentiation and development. The deposition of chromatin barriers at specific sets of NF-κB target genes during development may dictate which

genes will be activated in response to a stimulus (De Santa et al., 2009; 2007; Saccani and Natoli, 2002; van Essen et al., 2010). The relative expression levels of NF-κB dimer combinations and signaling pathway components would also contribute to distinct NF-κB responses in different cell types.

Termination of the NF-κB Response

Prompt activation of NF-κB is critical for host defense against pathogens during an infection. However, after the danger has been eliminated, NF-κB responses must be properly terminated to avoid inflammation, autoimmune disorders, and tumorigenesis. The most studied and best understood mechanism for termination of the NF-κB response involves the rapid resynthesis of IκB proteins, induced by activated NF-κB (Andrea Oeckinghaus, 2009; Ruland, 2011). Newly synthesized IκBα can enter the nucleus, remove NF-κB from the DNA, and relocalize it to the cytosol (Kearns et al., 2006; Oeckinghaus et al., 2011; Ruland, 2011). Similar to IκB, PIAS1 and PIAS4 have been implicated in the displacement of RelA dimers from DNA although the exact mechanism is unknown (Bin Liu et al., 2004; Liu et al., 2005). An additional layer of regulation in the nucleus involves ubiquitin-dependent proteasomal degradation of promoter-bound p65 (Ryo et al., 2003; Tanaka et al., 2007).

Acting further upstream in the signaling pathway, several deubiquitinase (DUB) enzymes are involved in the negative regulation of canonical NF-κB signaling. The best characterized DUB that down-modulates NF-κB is A20 (Hymowitz and Wertz, 2010; Ruland, 2011). Like IκBs, A20 expression is directly induced by NF-κB activity in a negative feedback loop (Dixit et al., 1990; Hymowitz and Wertz, 2010). Once activated, the DUB domain of A20 removes K63-linked polyubiquitin chains from RIP1, TRAF6, NEMO, RIP2, and MALT1, all of which are signaling components upstream of or part of the IKK complex (Boone et al., 2004; Düwel et al., 2009; Hitotsumatsu et al., 2008; Mauro et al., 2006). Cezanne, another DUB whose expression is induced by NF-κB activation, is involved in negatively regulating the TNFR pathway. A third DUB, CYLD, deubiquitinates K63-linked polyubiquitin chains from a wide range of activators including RIP1, TRAF2, TRAF6, TRAF7, TAK1, and NEMO, but it is unclear if deubiquitination of all these targets is necessary for NF-κB regulation (Ruland, 2011; Sun, 2009). Whether CYLD functions at steady-state in the absence of stimulus or after stimulus-dependent NF-κB activation has occurred is incompletely understood. Inducible expression of CYLD

seems to be cell type- and stimuli-dependent. In mouse bone marrow-derived macrophages, CYLD expression is strongly induced by RANKL, but not by TNF or LPS (Jin et al., 2008). Yet TNF can induce CYLD expression in HeLa cells and human bronchial epithelial cells (Jono et al., 2004). CYLD undergoes phosphorylation in response to TNF and LPS. This modification appears to negatively regulate its ability to deubiquitinate TRAF2 (Reiley et al., 2005). The phosphorylation is mediated by IKK, suggesting that CYLD may not be involved in feedback control of NF-κB, but may function instead as a negative regulator at steady-state to prevent aberrant, spontaneous activation of NF-κB (Reiley et al., 2005).

A signal-specific layer for the negative regulation of NF-κB response is provided by dominant-negative adaptors that interfere with protein-protein interactions between signaling components upstream of IKK. These have been best characterized in the TLR pathway and include the MyD88s isoform, IRAK-M, and SARM, all of which are inducibly generated or expressed following an appropriate stimulus (Burns et al., 2003; Carty et al., 2006; Escoll et al., 2003; Janssens et al., 2003; Kobayashi et al., 2002). MyD88s, IRAM-M, and SARM specifically inhibit the TLR pathway as they directly interact with adapter molecules that are selectively required for TLR signaling.

NF-κB in Disease

NF-κB regulates the expression of hundreds of genes involved in key processes, including cell proliferation, cell survival, inflammation, and innate immunity, often as a means to deal with cellular or organismal stress. Thus, not surprisingly, either defective or excessive NF-κB activity can lead to a range of human disease such as immunodeficiency, inflammatory disorders, and cancer.

A number of inherited human diseases due to mutations in components of the core NF-κB signaling pathway have been described. Mutations in the IKK complex regulator subunit NEMO can produce diverse and variable defects in humans, including severe immunodeficiency, osteopetrosis, skin defects, and colitis (Courtois and Gilmore, 2006; Pasparakis, 2009). The exact mechanism by which these NEMO mutations impact NF-κB on a molecular level remain to be fully understood. Two patients have been identified with a heterozygous missense mutation in IkBα that abolished its ability to be phosphorylated by IKK and accordingly resulted in impaired IkBα degradation. Both patients exhibited symptoms of severe immunodeficiency, including an impaired innate

immune response and a T-cell proliferation defect that resulted in a lack of memory cells (Courtois et al., 2003; Janssen et al., 2004). Mutations that affect the kinase domain of IRAK4, either resulting in its truncation or impairing its activity, have been identified in patients with recurrent bacterial infections (Medvedev et al., 2003; Picard et al., 2003). IRAK4 is a protein kinase that is essential for IL-1 and TLR signaling pathways and consequently these patients show defective responses to IL-1 and various TLR ligands. Germline mutations in an inhibitor of NF-κB have also been identified. Cylindromatosis, a rare recessive genetic disease characterized by the formation of benign skin tumors, mostly on the scalp, is caused by mutations in CYLD, a DUB that negatively regulates NF-κB (Bignell et al., 2000; Brummelkamp et al., 2003; Kovalenko et al., 2003; Trompouki et al., 2003).

Somatic cell mutations in NF-κB signaling components have been identified in lymphomas, glioblastoma, multiple myeloma, breast cancer, and prostate cancer (Annunziata et al., 2007; Ben-Neriah and Karin, 2011; Bredel et al., 2011; Chapman et al., 2011; Courtois and Gilmore, 2006). However, the number of tumors with activated NF-κB signaling is much larger than the fraction of malignancies with confirmed mutations, likely due to epigenetic changes within the cancer cells and/or microenvironmental factors (Ben-Neriah and Karin, 2011). NF-κB-mediated inflammation can contribute to tumor initiation by increasing mutation rates and by causing genomic instability (Grivennikov et al., 2010). Once tumor cells have formed, inflammation enhances their survival as well as their proliferation, and further promotes angiogenesis, invasion, and metastasis (Grivennikov et al., 2010). Nonetheless, the role of NF-κB in tumorigenesis is not always positive. For example, overexpression of IκBα promotes oncogenic Ras-induced invasive epidermal growth resembling squamous cell carcinoma (Dajee et al., 2003). While NF-κB appears to promote inflammation-associated hepatocellular carcinoma, it seems to prevent carcinogen-induced hepatocellular carcinoma (Ben-Neriah and Karin, 2011). Thus, the role of NF-κB in tumorigenesis is complex and may depend on cell-type and the status of tumor suppressor mechanisms in the cell (Perkins, 2012). Understanding the regulation of NF-κB in cancers will be key to the development of therapies that intervene in a way that inhibits tumorigenesis with the least amount of side effects.

Due to its critical role in controlling the inflammatory response, NF-κB has been implicated in the development of inflammatory-related disorders besides cancer.

Activated NF-κB has also been detected in many chronic inflammatory conditions, including inflammatory bowel disease, rheumatoid arthritis, and psoriasis (Ben-Neriah and Karin, 2011; Courtois and Gilmore, 2006). It is now recognized that NF-κB-mediated inflammation plays a role in the development of many metabolic disorders including obesity, type 2 diabetes, and atherosclerosis (Baker et al., 2011; Tornatore et al., 2012). Thus, the development of drugs that interfere with NF-κB-driven inflammation could provide relief to a number of serious human diseases.

Genetic Screens for Components of NF-κB Signaling Pathways

Since the discovery of NF-κB, genetic screens have led to novel discoveries in NF-κB signaling and regulation. Although NF-κB is evolutionarily conserved between *Drosophila* and humans, there are important differences in their NF-κB signaling pathways including the mechanism by which NF-κB is activated (Silverman and Maniatis, 2001). For this reason, screens that seek to understand human innate immune signaling generally use either mice or mammalian cells in culture.

Forward genetic screens in mice have been particularly important in contributing to our understanding of how TLRs sense and respond to microbial components. TLR4 was the first human TLR to have a function assigned to it. Its identification as a pattern recognition receptor for LPS was accomplished through positional cloning of a spontaneous mutation that occurred in C3H/HeJ in mice that rendered them resistant to LPS toxicity (Poltorak et al., 1998). Shortly afterwards, Bruce Beutler's group began treating mice with the mutagen *N*-ethyl-*N*-nitrosourea and testing the ability of immune cells from these mice for their ability to respond to TLR ligands. This endeavor resulted in the further functional identification of TRIF as a TLR adapter molecule, CD36 as a co-factor for TLR2/6, and UNC93B1 as a chaperone that mediates endosomal TLR trafficking (Brinkmann et al., 2007; Hoebe et al., 2003; 2005; Kim et al., 2008; Tabeta et al., 2006). While genetic screens in mice have provided fruitful insight into TLR signaling and important mouse models for future studies, this approach is time-consuming and expensive.

Genetic screens for NF-κB signaling pathway components have also been performed with mammalian cells grown in tissue culture. A screen involving chemical mutagenesis of a diploid cell line containing a NF-κB-GFP reporter identified Gp96 as an essential chaperone of TLRs (Randow and Seed, 2001). To identify activators of NF-κB,

random activation of gene expression (RAGE) technology was used to generate a limited protein expression library in a transgenic NF-κB reporter cell line. The library was then selected for cells that constitutively activated the reporter. Thus TAB3 was identified as a positive regulator of NF-κB (Jin et al., 2004). More recently, a large number of RNAi screens for activators and inhibitors of NF-κB have been performed (Brummelkamp et al., 2003; Chiang et al., 2012; Choudhary et al., 2011; Gewurz et al., 2012; Li et al., 2006; Nickles et al., 2012; Warner et al., 2013). While RNAi screens hold much promise, difficulties with low signal to noise values limit their utility. Secondary screens or secondary selection criteria are often required to winnow candidate lists that even then may include hundreds of genes. In a genome-wide siRNA screen to identify regulators of the NOD2 pattern recognition receptor signaling pathway, only 25% of putative positive regulators and 33% of putative negative regulators identified in the primary screen scored positive in a secondary screen (Warner et al., 2013). Targeted screens using RNAi pools against genes with specific functions (e.g. kinase, phosphatases) tend to give less ambiguous results than genome-wide screens. In one extreme example of this, a screen to identify de-ubiquitylating enzymes (DUBs) that negatively regulate NF-κB started with 200 knock-down vectors against 50 DUBs and identified only a single candidate gene (Brummelkamp et al., 2003). That gene was *CYLD* and was concurrently, but separately confirmed to be a negative regulator of NF-κB by two other groups (Kovalenko et al., 2003; Trompouki et al., 2003). Although targeted RNAi screens may provide higher specificity they also bias the screen and may prevent the identification of genes that are involved in your pathway of interest.

Introduction to the Work Presented in this Thesis

The isolation of human cells lines that are nearly or completely haploid and the subsequent development of genetic screens using these cells have provided an alternative genetic approach towards dissecting biological processes relevant to human biology. Human haploid screens have led to the identification of a number of host factors exploited by serious human pathogens, including Ebola virus, and identified transporters that are required for the import of toxic molecules, such as tunicamycin (Carette et al., 2011; Reiling et al., 2011). However, the majority of human haploid screens reported to date have involved the selection of mutant cells that are resistant to a lethal agent. The biological pathways amenable to study by human haploid screens are currently limited.

In this thesis, I will describe work that has sought to expand the utility of haploid screen through the use of transcriptional reporters. Given the critical role of NF-κB in diverse biological processes and the number of human diseases that are connected with aberrant NF-κB regulation, human haploid reporter screens were developed with the aim of identifying positive and negative regulators of NF-κB.

The first chapter describes the development of a human haploid reporter screen that was designed to identify constitutive inhibitors of NF-κB. This screen utilized a NF-κB-blasticidin S resistance gene (*BSR*) reporter and identified *CYLD*, a known negative regulator of NF-κB, demonstrating that in principle our approach works. Also identified in the screen were two members of the leucine-rich repeat-containing 8 (LRRC8) family of proteins and *HEATR7A*. The second chapter describes the characterization of LRRC8 family members and demonstrate that the most significant hit in the screen for NF-κB inhibitors, *LRRC8D*, is not required for NF-κB regulation, but rather for the import of blasticidin, the selecting agent used in the screen. While LRRC8s were not our intended target, their appearance in our screen provided new insight into the function of this family of proteins. The third chapter focuses on the development of a screen using a NF-κB-GFP reporter. The use of a NF-κB-GFP reporter eliminates the possibility of identifying transporters and it provides the ability to screen for both inhibitors and activators of NF-κB. In this chapter, I describe a screen for genes required for NF-κB activation in response to the TLR2/6 ligand, FSL-1. This screen successfully identified known components of the TLR2/6 pathway and identified many other candidate genes for further study.

Figures

Antigen receptors
TCR
BCR

Cytokines
TNFα
IL-1

Infection
LPS
dsRNA

Genotoxic stress
UV-, γ-radiation
reactive oxygen
intermediates (ROI)

NF-κB

Immunregulatory proteins

Serum amyloid protein,
C3 complement

VCAM,
ICAM

TCRα, β
MHC I

Cytokines

TNFα, IL-1,
IL-6, IL-12

Rel/IκB proteins

IκBα, c-Rel,
p105

Cyclins, growth factors

G-CSF,
M-CSF

Regulators of apoptosis

Bcl-XL,
IAPs

**APOTOSIS/
CELL SURVIVAL**

IMMUNE RESPONSE/INFLAMMATION

**NF-κB
REGULATION**

PROLIFERATION

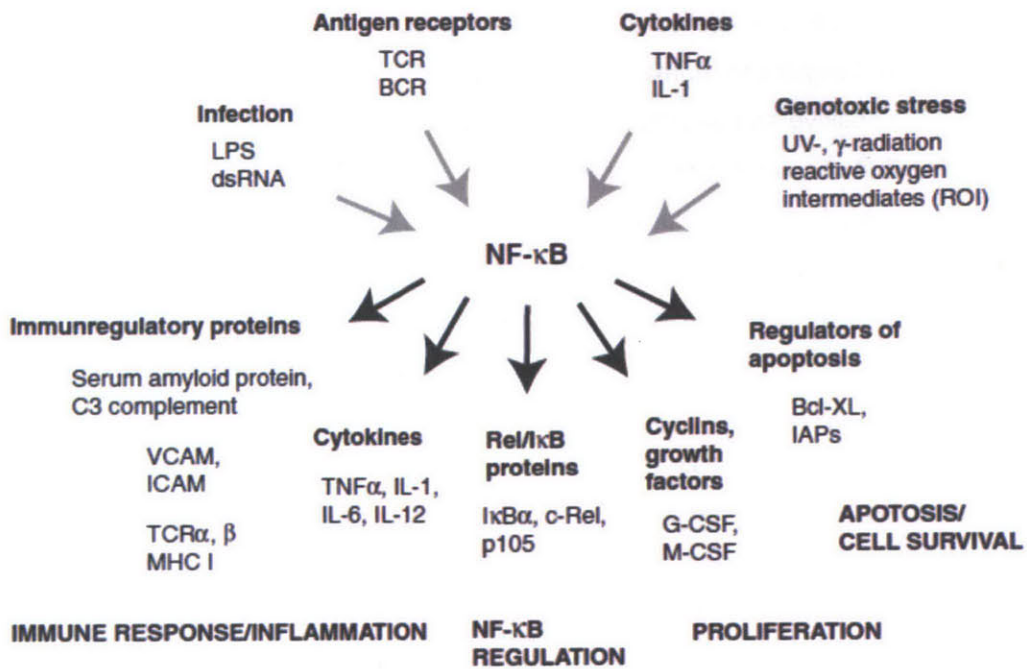**Figure 1. NF-κB stimuli and target genes.** In response to diverse stimuli that often occur during infection or cellular stress, NF-κB can activate target genes important for inflammation, proliferation, and cell survival. Since prolonged NF-κB can result in tissue damage and disease, activation of NF-κB also results in the activation of a number of negative feedback loops. Adapted from (Andrea Oeckinghaus, 2009).
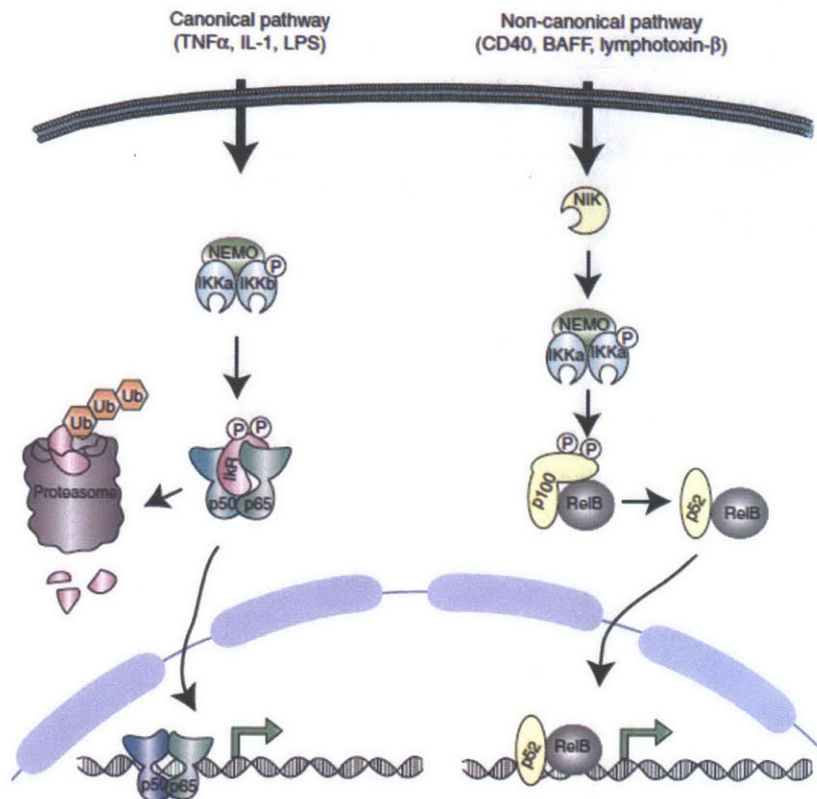
Figure 2. Canonical and noncanonical activation of NF-κB. In the canonical pathway, a wide range of stimuli can activate cell surface receptors (e.g. TNF receptor, IL-1 receptor, Toll-like receptors, and antigen receptors) that then recruit a large number of adapter proteins in order to activate the IKK complex. This complex contains IKKα, IKKβ, and NEMO. The activated IKK complex then phosphorylates the classical IκB proteins IκBα, IκBβ, IκBε, which leads to their proteasomal degradation and the release of their NF-κB bound dimers. The noncanonical pathway is induced by specific members of the TNF cytokine family, such as BAFF, lymphotoxin-β, or CD40 ligand. Following receptor ligation, NF-κB-inducing kinase (NIK) protein, normally subject to constitutive ubiquitylation and subsequent degradation, is stabilized. NIK can then phosphorylate and activate IKKα, which in turn phosphorylates p100, to initiate processing of p100 to p52. RelB/p52 dimers can then enter the nucleus and regulate target genes that are distinctly regulated by the noncanonical pathway. Adapted from (Andrea Oeckinghaus, 2009).
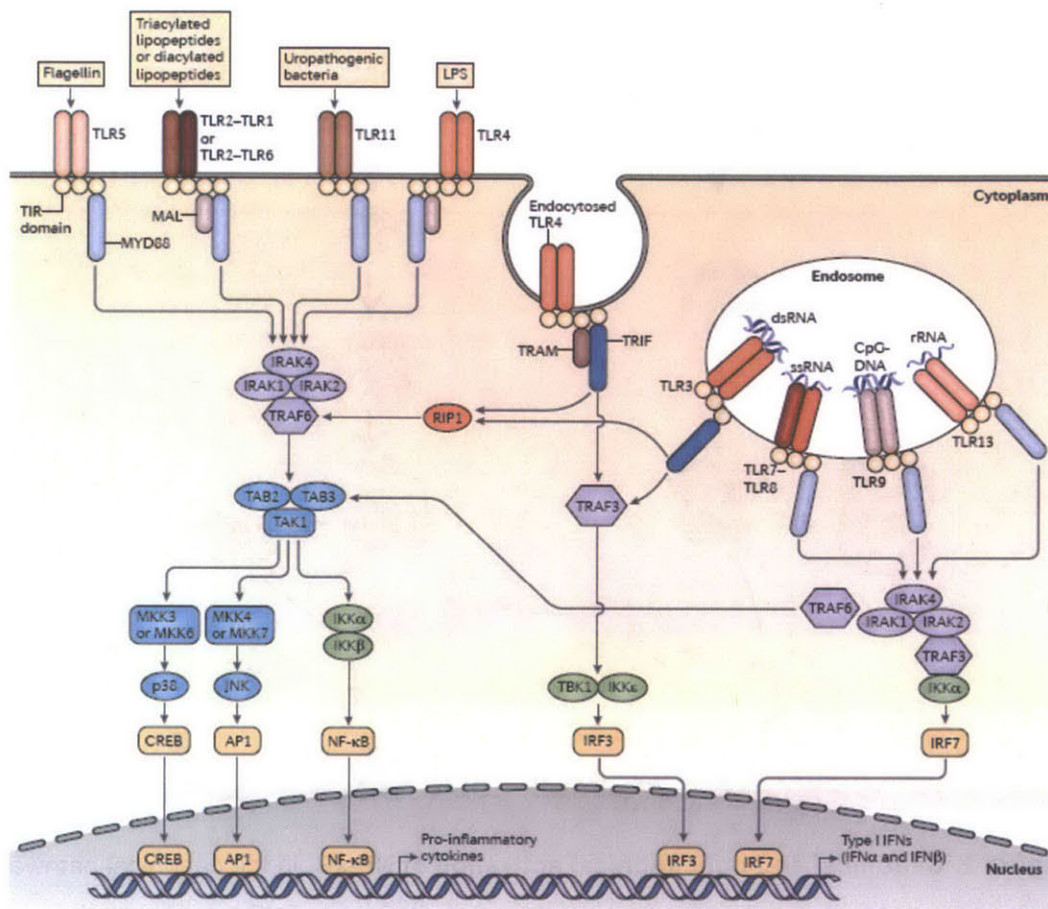
Figure 3. Mammalian TLR signaling pathways. Upon ligand-induced dimerization, TLRs recruit adapter proteins (MyD88, MAL/TIRAP, TRIF, TRAM), which in turn recruit IL-1R-associated kinases (IRAKs), TNF receptor-associated factors (TRAFs), and other molecules to activate mitogen-activated protein kinases (MAPKS) or IκB kinases (IKKs). Combined, these activate transcription factors including NF-κB and interferon-regulatory factors (IRFs). Adapted from (O'Neill et al.).

References

Agalioti, T., Lomvardas, S., Parekh, B., Yie, J., Maniatis, T., and Thanos, D. (2000). Ordered recruitment of chromatin modifying and general transcription factors to the IFN-beta promoter. Cell *103*, 667–678.

Alagbala Ajibade, A., Wang, Q., Cui, J., Zou, J., Xia, X., Wang, M., Tong, Y., Hui, W., Liu, D., Su, B., et al. (2012). TAK1 Negatively Regulates NF-κB and p38 MAP Kinase Activation in Gr-1+CD11b+ Neutrophils. Immunity *36*, 43–54.

Andrea Oeckinghaus, S.G. (2009). The NF-κB Family of Transcription Factors and Its Regulation. Cold Spring Harb Perspect Biol *1*, a000034–a000034.

Annunziata, C.M., Davis, R.E., Demchenko, Y., Bellamy, W., Gabrea, A., Zhan, F., Lenz, G., Hanamura, I., Wright, G., Xiao, W., et al. (2007). Frequent engagement of the classical and alternative NF-kappaB pathways by diverse genetic abnormalities in multiple myeloma. Cancer Cell *12*, 115–130.

Baker, R.G., Hayden, M.S., and Ghosh, S. (2011). NF-κB, inflammation, and metabolic disease. Cell Metab. *13*, 11–22.

Ben-Neriah, Y., and Karin, M. (2011). Inflammation meets cancer, with NF-κB as the matchmaker. Nat Immunol *12*, 715–723.

Bignell, G.R., Warren, W., Seal, S., Takahashi, M., Rapley, E., Barfoot, R., Green, H., Brown, C., Biggs, P.J., Lakhani, S.R., et al. (2000). Identification of the familial cylindromatosis tumour-suppressor gene. Nat Immunol *25*, 160–165.

Bin Liu, Mink, S., Wong, K.A., Stein, N., Getman, C., Dempsey, P.W., Wu, H., and Shuai, K. (2004). PIAS1 selectively inhibits interferon-inducible genes and is important in innate immunity. Nat Immunol *5*, 891–898.

Boone, D.L., Turer, E.E., Lee, E.G., Ahmad, R.-C., Wheeler, M.T., Tsui, C., Hurley, P.,

Chien, M., Chai, S., Hitotsumatsu, O., et al. (2004). The ubiquitin-modifying enzyme A20 is required for termination of Toll-like receptor responses. Nat Immunol *5*, 1052–1060.

Bredel, M., Scholtens, D.M., Yadav, A.K., Alvarez, A.A., Renfrow, J.J., Chandler, J.P., Yu, I.L.Y., Carro, M.S., Dai, F., Tagge, M.J., et al. (2011). NFKBIADeletion in Glioblastomas. N Engl J Med *364*, 627–637.

Brinkmann, M.M., Spooner, E., Hoebe, K., Beutler, B., Ploegh, H.L., and Kim, Y.-M. (2007). The interaction between the ER membrane protein UNC93B and TLR3, 7, and 9 is crucial for TLR signaling. J Cell Biol *177*, 265–275.

Brummelkamp, T.R., Nijman, S.M.B., Dirac, A.M.G., and Bernards, R. (2003). Loss of the cylindromatosis tumour suppressor inhibits apoptosis by activating NF-kappaB. Nature *424*, 797–801.

Burns, K., Janssens, S., Brissoni, B., Olivos, N., Beyaert, R., and Tschopp, J. (2003). Inhibition of interleukin 1 receptor/Toll-like receptor signaling through the alternatively spliced, short form of MyD88 is due to its failure to recruit IRAK-4. J Exp Med *197*, 263–268.

Carette, J.E., Raaben, M., Wong, A.C., Herbert, A.S., Obernosterer, G., Mulherkar, N., Kuehne, A.I., Kranzusch, P.J., Griffin, A.M., Ruthel, G., et al. (2011). Ebola virus entry requires the cholesterol transporter Niemann–Pick C1. Nature *477*, 340–343.

Carty, M., Goodbody, R., Schröder, M., Stack, J., Moynagh, P.N., and Bowie, A.G. (2006). The human adaptor SARM negatively regulates adaptor protein TRIF-dependent Toll-like receptor signaling. Nat Immunol *7*, 1074–1081.

Chapman, M.A., Lawrence, M.S., Keats, J.J., Cibulskis, K., Sougnez, C., Schinzel, A.C., Harview, C.L., Brunet, J.-P., Ahmann, G.J., Adli, M., et al. (2011). Initial genome sequencing and analysis of multiple myeloma. Nature *471*, 467–472.

Chen, L.-F., and Greene, W.C. (2004). Shaping the nuclear action of NF-kappaB. Nat Rev Mol Cell Biol *5*, 392–401.

Chiang, C.-Y., Engel, A., Opaluch, A.M., Ramos, I., Maestre, A.M., Secundino, I., De Jesus, P.D., Nguyen, Q.T., Welch, G., Bonamy, G.M.C., et al. (2012). Cofactors Required for TLR7- and TLR9-Dependent Innate Immune Responses. Cell Host & Microbe *11*, 306–318.

Choudhary, S., Rosenblatt, K.P., Fang, L., Tian, B., Wu, Z.-H., and Brasier, A.R. (2011). High throughput siRNA screening of the human kinome identifies novel kinases controlling the canonical NF-kB activation pathway. Journal of Biological Chemistry *286*, jbc.M111.224923–jbc.M111.237195.

Courtois, G., and Gilmore, T.D. (2006). Mutations in the NF-I[kappa]IB signaling pathway: implications for human disease. Oncogene *25*, 6831–6843.

Courtois, G., Smahi, A., Reichenbach, J., Döffinger, R., Cancrini, C., Bonnet, M., Puel, A., Chable-Bessia, C., Yamaoka, S., Feinberg, J., et al. (2003). A hypermorphic IkBα mutation is associated with autosomal dominant anhidrotic ectodermal dysplasia and T cell immunodeficiency. J Clin Invest *112*, 1108–1115.

Dajee, M., Lazarov, M., Zhang, J.Y., Cai, T., Green, C.L., Russell, A.J., Marinkovich, M.P., Tao, S., Lin, Q., Kubo, Y., et al. (2003). NF-kappaB blockade and oncogenic Ras trigger invasive human epidermal neoplasia. Nature *421*, 639–643.

De Santa, F., Narang, V., Yap, Z.H., Tusi, B.K., Burgold, T., Austenaa, L., Bucci, G., Caganova, M., Notarbartolo, S., Casola, S., et al. (2009). Jmjd3 contributes to the control of gene expression in LPS-activated macrophages. Embo J *28*, 3341–3352.

De Santa, F., Totaro, M.G., Prosperini, E., Notarbartolo, S., Testa, G., and Natoli, G. (2007). The histone H3 lysine-27 demethylase Jmjd3 links inflammation to inhibition of polycomb-mediated gene silencing. Cell *130*, 1083–1094.

Dixit, V.M., Green, S., Sarma, V., Holzman, L.B., Wolf, F.W., O'Rourke, K., Ward, P.A., Prochownik, E.V., and Marks, R.M. (1990). Tumor necrosis factor-alpha induction of novel gene products in human endothelial cells including a macrophage-specific chemotaxin. J Biol Chem *265*, 2973–2978.

Dong, J., Jimi, E., Zhong, H., Hayden, M.S., and Ghosh, S. (2008). Repression of gene expression by unphosphorylated NF-kappaB p65 through epigenetic mechanisms. Genes & Development *22*, 1159–1173.

Düwel, M., Welteke, V., Oeckinghaus, A., Baens, M., Kloo, B., Ferch, U., Darnay, B.G., Ruland, J., Marynen, P., and Krappmann, D. (2009). A20 negatively regulates T cell receptor signaling to NF-kappaB by cleaving Malt1 ubiquitin chains. The Journal of Immunology *182*, 7718–7728.

Ea, C.-K., and Baltimore, D. (2009). Regulation of NF-kappaB activity through lysine monomethylation of p65. Proc Natl Acad Sci USA *106*, 18972–18977.

Escoll, P., del Fresno, C., García, L., Vallés, G., Lendínez, M.J., Arnalich, F., and López-Collazo, E. (2003). Rapid up-regulation of IRAK-M expression following a second endotoxin challenge in human monocytes and in monocytes isolated from septic patients. Biochem Biophys Res Commun *311*, 465–472.

Gewurz, B.E., Towfic, F., Mar, J.C., Shinners, N.P., Takasaki, K., Zhao, B., Cahir-McFarland, E.D., Quackenbush, J., Xavier, R.J., and Kieff, E. (2012). Genome-wide siRNA screen for mediat... [Proc Natl Acad Sci U S A. 2012] - PubMed - NCBI. Proc Natl Acad Sci USA *109*, 2467–2472.

Ghosh, S., and Hayden, M.S. (2008). New regulators of NF-kappaB in inflammation. Nat Rev Immunol *8*, 837–848.

Grivennikov, S.I., Greten, F.R., and Karin, M. (2010). Immunity, inflammation, and cancer. Cell *140*, 883–899.

Hayden, M.S., and Ghosh, S. (2008). Shared principles in NF-kappaB signaling. Cell *132*, 344–362.

Hayden, M.S., and Ghosh, S. (2012). NF-κB, the first quarter-century: remarkable progress and outstanding questions. Genes & Development *26*, 203–234.

Häcker, H., Redecke, V., Blagoev, B., Kratchmarova, I., Hsu, L.-C., Wang, G.G., Kamps, M.P., Raz, E., Wagner, H., Häcker, G., et al. (2006). Specificity in Toll-like receptor signalling through distinct effector functions of TRAF3 and TRAF6. Nature *439*, 204–207.

Hitotsumatsu, O., Ahmad, R.-C., Tavares, R., Wang, M., Philpott, D., Turer, E.E., Lee, B.L., Shiffin, N., Advincula, R., Malynn, B.A., et al. (2008). The Ubiquitin-Editing Enzyme A20 Restricts Nucleotide-Binding Oligomerization Domain Containing 2-Triggered Signals. Immunity *28*, 381–390.

Hoebe, K., Du, X., Georgel, P., Janssen, E., Tabeta, K., Kim, S.O., Goode, J., Lin, P.,

Mann, N., Mudd, S., et al. (2003). Identification of Lps2 as a key transducer of MyD88-independent TIR signalling. Nature *424*, 743–748.

Hoebe, K., Georgel, P., Rutschmann, S., Du, X., Mudd, S., Crozat, K., Sovath, S., Shamel, L., Hartung, T., Zähringer, U., et al. (2005). CD36 is a sensor of diacylglycerides. Nature *433*, 523–527.

Hoffmann, A., Natoli, G., and Ghosh, G. (2006). Transcriptional regulation via the NF-κB signaling module. Oncogene *25*, 6706–6716.

Honda, K., Yanai, H., Mizutani, T., Negishi, H., Shimada, N., Suzuki, N., Ohba, Y., Takaoka, A., Yeh, W.-C., and Taniguchi, T. (2004). Role of a transductional-transcriptional processor complex involving MyD88 and IRF-7 in Toll-like receptor signaling. Proc Natl Acad Sci USA *101*, 15416–15421.

Hymowitz, S.G., and Wertz, I.E. (2010). A20: from ubiquitin editing to tumour suppression. Nat Rev Cancer *10*, 332–341.

Janssen, R., van Wengen, A., Hoeve, M.A., Dam, ten, M., van der Burg, M., van Dongen, J., van de Vosse, E., van Tol, M., Bredius, R., Ottenhoff, T.H., et al. (2004). The same IkappaBalpha mutation in two related individuals leads to completely different clinical syndromes. J Exp Med *200*, 559–568.

Janssens, S., Burns, K., Vercammen, E., Tschopp, J., and Beyaert, R. (2003). MyD88S, a splice variant of MyD88, differentially modulates NF-κB- and AP-1-dependent gene expression. FEBS Lett *548*, 103–107.

Jin, G., Klika, A., Callahan, M., Faga, B., Danzig, J., Jiang, Z., Li, X., Stark, G.R., Harrington, J., and Sherf, B. (2004). Identification of a human NF-kappaB-activating protein, TAB3. Proc Natl Acad Sci USA *101*, 2028–2033.

Jin, M.S., Kim, S.E., Heo, J.Y., Lee, M.E., Kim, H.M., Paik, S.-G., Lee, H., and Lee, J.-O. (2007). Crystal structure of the TLR1-TLR2 heterodimer induced by binding of a tri-acylated lipopeptide. Cell *130*, 1071–1082.

Jin, W., Chang, M., Paul, E.M., Babu, G., Lee, A.J., Reiley, W., Wright, A., Zhang, M., You, J., and Sun, S.-C. (2008). Deubiquitinating enzyme CYLD negatively regulates RANK signaling and osteoclastogenesis in mice. J Clin Invest *118*, 1858–1866.

Jono, H., Lim, J.H., Chen, L.-F., Xu, H., Trompouki, E., Pan, Z.K., Mosialos, G., and Li, J.-D. (2004). NF-kappaB is essential for induction of CYLD, the negative regulator of NF-kappaB: evidence for a novel inducible autoregulatory feedback pathway. J Biol Chem *279*, 36171–36174.

Kang, J.Y., Nan, X., Jin, M.S., Youn, S.-J., Ryu, Y.H., Mah, S., Han, S.H., Lee, H., Paik, S.-G., and Lee, J.-O. (2009). Recognition of Lipopeptide Patterns by Toll-like Receptor 2-Toll-like Receptor 6 Heterodimer. Immunity.

Kawai, T., and Akira, S. (2007). Signaling to NF-kappaB by Toll-like receptors. Trends in

Molecular Medicine *13*, 460–469.

Kawai, T., and Akira, S. (2010). The role of pattern-recognition receptors in innate immunity: update on Toll-like receptors. Nat Immunol *11*, 373–384.

Kearns, J.D., Basak, S., Werner, S.L., Huang, C.S., and Hoffmann, A. (2006). IkappaBepsilon provides negative feedback to control NF-kappaB oscillations, signaling dynamics, and inflammatory gene expression. J Cell Biol *173*, 659–664.

Kim, Y.-M., Brinkmann, M.M., Paquet, M.-E., and Ploegh, H.L. (2008). UNC93B1 delivers nucleotide-sensing toll-like receptors to endolysosomes. Nature *452*, 234–238.

Kobayashi, K., Hernandez, L.D., Galán, J.E., Janeway, C.A., Jr., Medzhitov, R., and Flavell, R.A. (2002). IRAK-M Is a Negative Regulator of Toll-like Receptor Signaling. Cell *110*, 191–202.

Kovalenko, A., Chable-Bessia, C., Cantarella, G., Israël, A., Wallach, D., and Courtois, G. (2003). The tumour suppressor CYLD negatively regulates NF-kappaB signalling by deubiquitination. Nature *424*, 801–805.

Li, S., Wang, L., Berman, M.A., Zhang, Y., and Dorf, M.E. (2006). RNAi Screen in Mouse Astrocytes Identifies Phosphatases that Regulate NF-κB Signaling. Mol Cell *24*, 497–509.

Li, Y., Reddy, M.A., Miao, F., Shanmugam, N., Yee, J.-K., Hawkins, D., Ren, B., and Natarajan, R. (2008). Role of the histone H3 lysine 4 methyltransferase, SET7/9, in the regulation of NF-kappaB-dependent inflammatory genes. Relevance to diabetes and inflammation. J Biol Chem *283*, 26771–26781.

Liao, G. (2004). Regulation of the NF-kappaB-inducing kinase by tumor necrosis factor receptor-associated factor 3-induced degradation. J Biol Chem *279*, 26243–26250.

Liu, B., and Li, Z. (2008). Endoplasmic reticulum HSP90b1 (gp96, grp94) optimizes B-cell function via chaperoning integrin and TLR but not immunoglobulin. Blood *112*, 1223–1230.

Liu, B., Yang, Y., Qiu, Z., Staron, M., Hong, F., Li, Y., Wu, S., Li, Y., Hao, B., Bona, R., et al. (2010). Folding of Toll-like receptors by the HSP90 paralogue gp96 requires a substrate-specific cochaperone. Nat Commun *1*, 79.

Liu, B., Yang, R., Wong, K.A., Getman, C., Stein, N., Teitell, M.A., Cheng, G., Wu, H., and Shuai, K. (2005). Negative regulation of NF-kappaB signaling by PIAS1. Mol Cell Biol *25*, 1113–1123.

Mauro, C., Pacifico, F., Lavorgna, A., Mellone, S., Iannetti, A., Acquaviva, R., Formisano, S., Vito, P., and Leonardi, A. (2006). ABIN-1 Binds to NEMO/IKK and Co-operates with A20 in Inhibiting NF- B. Journal of Biological Chemistry *281*, 18482–18488.

Medvedev, A.E., Lentschat, A., Kuhns, D.B., Blanco, J.C.G., Salkowski, C., Zhang, S., Arditi, M., Gallin, J.I., and Vogel, S.N. (2003). Distinct mutations in IRAK-4 confer

hyporesponsiveness to lipopolysaccharide and interleukin-1 in a patient with recurrent bacterial infections. J Exp Med *198*, 521–531.

Natoli, G., Saccani, S., Bosisio, D., and Marazzi, I. (2005). Interactions of NF-kappaB with chromatin: the art of being at the right place at the right time. Nat Immunol *6*, 439–445.

Negishi, H., Fujita, Y., Yanai, H., Sakaguchi, S., Ouyang, X., Shinohara, M., Takayanagi, H., Ohba, Y., Taniguchi, T., and Honda, K. (2006). Evidence for licensing of IFN-gamma-induced IFN regulatory factor 1 transcription factor by MyD88 in Toll-like receptor-dependent gene induction program. Proc Natl Acad Sci USA *103*, 15136–15141.

Nickles, D., Falschlehner, C., Metzig, M., and Boutros, M. (2012). A genome-wide RNA interference screen identifies caspase 4 as a factor required for tumor necrosis factor alpha signaling. Mol Cell Biol *32*, 3372–3381.

Nicodeme, E., Jeffrey, K.L., Schaefer, U., Beinke, S., Dewell, S., Chung, C.-W., Chandwani, R., Marazzi, I., Wilson, P., Coste, H., et al. (2010). Suppression of inflammation by a synthetic histone mimic. Nature *468*, 1119–1123.

O'Neill, L.A.J., and Bowie, A.G. (2007). The family of five: TIR-domain-containing adaptors in Toll-like receptor signalling. Nat Rev Immunol *7*, 353–364.

O'Neill, L.A.J., Golenbock, D., and Bowie, A.G. The history of Toll-like receptors [mdash] redefining innate immunity : Nature Reviews Immunology : Nature Publishing Group. Nat Rev Immunol.

Oeckinghaus, A., Hayden, M.S., and Ghosh, S. (2011). Crosstalk in NF-κB signaling pathways. Nat Immunol *12*, 695–708.

Oganesyan, G., Saha, S.K., Guo, B., He, J.Q., Shahangian, A., Zarnegar, B., Perry, A., and Cheng, G. Critical role of TRAF3 in the Toll-like receptor-dependent and -independent antiviral response : Abstract : Nature. Nature.

Pahl, H.L. (1999). Activators and target genes of Rel/NF-I[kappa]IB transcription factors. , Published Online: 22 November 1999; I Doi:10.1038/Sj.Onc.1203239 *18*, 6853–6866.

Panne, D., Maniatis, T., and Harrison, S.C. (2004). Crystal structure of ATF-2/c-Jun and IRF-3 bound to the interferon-beta enhancer. Embo J *23*, 4384–4393.

Panne, D., Maniatis, T., and Harrison, S.C. (2007). An atomic model of the interferon-beta enhanceosome. Cell *129*, 1111–1123.

Pasparakis, M. (2009). Regulation of tissue homeostasis by NF-κB signalling: implications for inflammatory diseases. Nat Rev Immunol *9*, 778–788.

Perkins, N.D. (2012). The diverse and complex roles of NF-κB subunits in cancer. Nat Rev Cancer *12*, 121–132.

Picard, C., Puel, A., Bonnet, M., Ku, C.-L., Bustamante, J., Yang, K., Soudais, C., Dupuis, S., Feinberg, J., Fieschi, C., et al. (2003). Pyogenic bacterial infections in humans with IRAK-4 deficiency. Science *299*, 2076–2079.

Poltorak, A., He, X., Smirnova, I., Liu, M.Y., Van Huffel, C., Du, X., Birdwell, D., Alejos, E., Silva, M., Galanos, C., et al. (1998). Defective LPS signaling in C3H/HeJ and C57BL/10ScCr mice: mutations in Tlr4 gene. Science *282*, 2085–2088.

Ramirez-Carrozzi, V.R., Nazarian, A.A., Li, C.C., Gore, S.L., Sridharan, R., Imbalzano, A.N., and Smale, S.T. (2006). Selective and antagonistic functions of SWI/SNF and Mi-2beta nucleosome remodeling complexes during an inflammatory response. Genes & Development *20*, 282–296.

Randow, F., and Seed, B. (2001). Endoplasmic reticulum chaperone gp96 is required for innate immunity but not cell viability. Nat Cell Biol *3*, 891–896.

Razani, B., Reichardt, A.D., and Cheng, G. (2011). Non-canonical NF-κB signaling activation and regulation: principles and perspectives. Immunol Rev *244*, 44–54.

Reiley, W., Zhang, M., Wu, X., Granger, E., and Sun, S.-C. (2005). Regulation of the deubiquitinating enzyme CYLD by IkappaB kinase gamma-dependent phosphorylation. Mol Cell Biol *25*, 3886–3895.

Reiling, J.H., Clish, C.B., Carette, J.E., Varadarajan, M., Brummelkamp, T.R., and Sabatini, D.M. (2011). A haploid genetic screen identifies the major facilitator domain containing 2A (MFSD2A) transporter as a key mediator in the response to tunicamycin. Proc Natl Acad Sci USA *108*, 11756–11765.

Ruland, J. (2011). Return to homeostasis: downregulation of NF-κB responses. Nat Immunol *12*, 709–714.

Ryo, A., Suizu, F., Yoshida, Y., Perrem, K., Liou, Y.-C., Wulf, G., Rottapel, R., Yamaoka, S., and Lu, K.P. (2003). Regulation of NF-kappaB signaling by Pin1-dependent prolyl isomerization and ubiquitin-mediated proteolysis of p65/RelA. Mol Cell *12*, 1413–1426.

Saccani, S., Pantano, S., and Natoli, G. (2001). Two waves of nuclear factor kappaB recruitment to target promoters. J Exp Med *193*, 1351–1359.

Saccani, S., and Natoli, G. (2002). Dynamic changes in histone H3 Lys 9 methylation occurring at tightly regulated inducible inflammatory genes. Genes & Development *16*, 2219–2224.

Saccani, S., Marazzi, I., Beg, A.A., and Natoli, G. (2004). Degradation of promoter-bound p65/RelA is essential for the prompt termination of the nuclear factor kappaB response. J Exp Med *200*, 107–113.

Sato, S., Sanjo, H., Takeda, K., Ninomiya-Tsuji, J., Yamamoto, M., Kawai, T., Matsumoto, K., Takeuchi, O., and Akira, S. (2005). Essential function for the kinase TAK1 in innate and adaptive immune responses. Nat Immunol *6*, 1087–1095.

Schmitz, F., Heit, A., Guggemoos, S., Krug, A., Mages, J., Schiemann, M., Adler, H., Drexler, I., Haas, T., Lang, R., et al. (2007). Interferon-regulatory-factor 1 controls Toll-like receptor 9-mediated IFN-beta production in myeloid dendritic cells. Eur J Immunol *37*, 315–327.

Schoenemeyer, A., Barnes, B.J., Mancl, M.E., Latz, E., Goutagny, N., Pitha, P.M., Fitzgerald, K.A., and Golenbock, D.T. (2005). The interferon regulatory factor, IRF5, is a central mediator of toll-like receptor 7 signaling. J Biol Chem *280*, 17005–17012.

Schuman, J., Chen, Y., Podd, A., Yu, M., Liu, H.-H., Wen, R., Chen, Z.J., and Wang, D. (2009). A critical role of TAK1 in B-cell receptor-mediated nuclear factor kappaB activation. Blood *113*, 4566–4574.

Sen, R., and Baltimore, D. (1986a). Inducibility of κ immunoglobulin enhancer-binding protein NF-κB by a posttranslational mechanism. Cell *47*, 921–928.

Sen, R., and Baltimore, D. (1986b). Multiple nuclear factors interact with the immunoglobulin enhancer sequences. Cell *46*, 705–716.

Silverman, N., and Maniatis, T. (2001). NF-kappaB signaling pathways in mammalian and insect innate immunity. Genes & Development *15*, 2321–2342.

Smale, S.T. (2011). Hierarchies of NF-κB target-gene regulation. Nat Immunol *12*, 689–694.

Sun, S.C. (2009). CYLD: a tumor suppressor deubiquitinase regulating NF-κB activation and diverse biological processes. Cell Death Differ *17*, 25–34.

Tabeta, K., Hoebe, K., Janssen, E.M., Du, X., Georgel, P., Crozat, K., Mudd, S., Mann, N., Sovath, S., Goode, J., et al. (2006). The Unc93b1 mutation 3d disrupts exogenous antigen presentation and signaling via Toll-like receptors 3, 7 and 9. Nat Immunol *7*, 156–164.

Takahashi, K., Shibata, T., Akashi-Takamura, S., Kiyokawa, T., Wakabayashi, Y., Tanimura, N., Kobayashi, T., Matsumoto, F., Fukui, R., Kouro, T., et al. (2007). A protein associated with Toll-like receptor (TLR) 4 (PRAT4A) is required for TLR-dependent immune responses. J Exp Med *204*, 2963–2976.

Takeuchi, O., and Akira, S. (2010). Pattern Recognition Receptors and Inflammation. Cell *140*, 805–820.

Tanaka, T., Grusby, M.J., and Kaisho, T. (2007). PDLIM2-mediated termination of transcription factor NF-kappaB activation by intranuclear sequestration and degradation of the p65 subunit. Nat Immunol *8*, 584–591.

Tornatore, L., Thotakura, A.K., Bennett, J., Moretti, M., and Franzoso, G. (2012). The nuclear factor kappa B signaling pathway: integrating metabolism with inflammation. Trends Cell Biol. *22*, 557–566.

Trompouki, E., Hatzivassiliou, E., Tsichritzis, T., Farmer, H., Ashworth, A., and Mosialos, G. (2003). CYLD is a deubiquitinating enzyme that negatively regulates NF-kappaB activation by TNFR family members. Nature *424*, 793–796.

van Essen, D., Zhu, Y., and Saccani, S. (2010). A feed-forward circuit controlling inducible NF-κB target gene activation by promoter histone demethylation. Mol Cell *39*, 750–760.

Vermeulen, L., De Wilde, G., Van Damme, P., Vanden Berghe, W., and Haegeman, G. (2003). Transcriptional activation of the NF-kappaB p65 subunit by mitogen- and stress-activated protein kinase-1 (MSK1). Embo J *22*, 1313–1324.

Warner, N., Burberry, A., Franchi, L., Kim, Y.G., McDonald, C., Sartor, M.A., and Nunez, G. (2013). A genome-wide siRNA screen reveals positive and n... [Sci Signal. 2013] - PubMed - NCBI. Science Signaling *6*, rs3–rs3.

Yang, X.-D., Huang, B., Li, M., Lamb, A., Kelleher, N.L., and Chen, L.-F. (2009). Negative regulation of NF-kappaB action by Set9-mediated lysine methylation of the RelA subunit. Embo J *28*, 1055–1066.

Yang, Y., Liu, B., Dai, J., Srivastava, P.K., Zammit, D.J., Lefrançois, L., and Li, Z. (2007). Heat shock protein gp96 is a master chaperone for toll-like receptors and is important in the innate function of macrophages. Immunity *26*, 215–226.

Zhong, H., Voll, R.E., and Ghosh, S. (1998). Phosphorylation of NF-kappa B p65 by PKA stimulates transcriptional activity by promoting a novel bivalent interaction with the coactivator CBP/p300. Mol Cell *1*, 661–671.

Chapter 2

A Reporter Screen in a Human Haploid Cell Line Identifies CYLD as a Constitutive Inhibitor of NF-κB

Clarissa C. Lee [1,2], Jan E. Carette [1,3], Thijn R. Brummelkamp [1,4], Hidde L. Ploegh [1,2]

[1] Whitehead Institute for Biomedical Research, Cambridge, MA, USA

[2] Department of Biology, Massachusetts Institute of Technology, Cambridge, MA, USA

[3] Present address: Department of Microbiology and Immunology, Stanford University School of Medicine, Stanford, CA, USA

[4] Present address: Department of Biochemistry, Netherlands Cancer Institute, Amsterdam, The Netherlands

Abstract

The development of forward genetic screens in human haploid cells has the potential to transform our understanding of the genetic basis of cellular processes unique to man. So far, this approach has been limited mostly to the identification of genes that mediate cell death in response to a lethal agent, likely due to the ease with which this phenotype can be observed. Here, we perform the first reporter screen in the near-haploid KBM7 cell line to identify constitutive inhibitors of NF-κB. CYLD was the only currently known negative regulator of NF-κB to be identified, thus uniquely distinguishing this gene. Also identified were three genes with no previous known connection to NF-κB. Our results demonstrate that reporter screens in haploid human cells can be applied to investigate the many complex signaling pathways that converge upon transcription factors.

Introduction

Forward genetic screens are a powerful means to decipher a biological process
without any prior knowledge or assumptions. Typically such screens are performed in
yeast, Drosophila, Caenorhabditis elegans and other genetic model organisms to identify
new gene functions. Application of this method to human cultured cells allows the
dissection of pathways that are dissimilar or even absent in other model organisms. It
may also enable the discovery of novel drug targets to treat disease. Genetic screens in
human cells have been limited by the difficulties inherent in revealing recessive
phenotypes in diploid cells. While RNAi screens have been an important advance, they
are complicated by off-target effects and often do not completely eliminate the relevant
gene product. The recent isolation of human cells lines that are nearly or completely
haploid (KBM7 and HAP1, respectively) has revolutionized human forward genetic
screens and led to the identification of numerous human host factors required for
infection by pathogens and intoxication by bacterial toxins [1-7].

The majority of human haploid screens reported to date have involved the
selection of mutants that are resistant to an agent that is lethal to wild-type cells. The
one exception is a recent screen that used fluorescence activated-cell sorting (FACS) to
identify genes involved in MHC (major histocompatibility complex) class I antigen
presentation by sorting for mutants that were defective in surface expression of MHC-1
[8]. We sought to further expand the types of biological pathways that can be studied
using human haploid genetic screens by using a transcriptional reporter in conjunction
with selection for a lethal phenotype.

Transcription factors often lie at the terminus of complex signaling pathways and
control gene transcription programs that regulate diverse processes, ranging from
proliferation, differentiation, apoptosis, immune response, to metabolism. Given the
importance of transcription factors in facilitating vital aspects of cell biology, mutations in
-or aberrant regulation of- transcription factors have been associated with human
disease [9,10]. The identification of inhibitors or activators of transcription factors will
therefore not only illuminate the signaling pathways that regulate them, but could also

identify targets that may prove to be better drug targets than transcription factors themselves, or whose inhibition may provide a more selective therapeutic effect.

We chose to screen for inhibitors of NF-κB, a family of transcription factors that in mammals plays a central role in regulating immune responses, development, cell proliferation, and survival [11]. The NF-κB family consists of five members: RelA/p65, RelB, c-Rel, NF-κB1 (p50 and its precursor p105) and NF-κB2 (p52 and its precursor p100). They form dimers and are normally kept inactive in the cytoplasm. Activation of a wide variety of receptors, including antigen receptors, pattern-recognition receptors and cytokine receptors leads to translocation of NF-κB dimers into the nucleus. Here the dimers bind to DNA κB sites in promoters and enhancers of target genes. Activation of NF-κB needs to be tightly controlled and rapidly curtailed following the initial stimulus to prevent uncontrolled tissue damage and/or disease.

Here we performed the first reporter screen in KBM7 cells to identify constitutive inhibitors of NF-κB. The identification of CYLD, a known negative regulator of NF-κB, demonstrates the utility of using human haploid cells to dissect a variety of biological processes.

Results

All screens in human haploid cells performed to date have relied on intrinsic phenotypes, such as sensitivity to toxins or protein surface expression, both of which can be easily observed at a cellular level. To provide a clear phenotypic readout for abrogation of NF-κB inhibitor function -and thus improper activation of NF-κB- we generated a NF-κB reporter cell line (Fig. 1). We transduced KBM7 cells, which are haploid for all chromosomes but chromosome 8, with a reporter construct that contains a NF-κB transcriptional response element (TRE) and a minimum cytomegalovirus (mCMV) promoter upstream of the blasticidin S resistance gene (*BSR*) from *Bacillus cereus*. Thus, insertional inactivation of genes that normally repress activation of NF-κB would render the reporter cells resistant to blasticidin and provide an easy means to distinguish them from wild-type cells. To ensure that the selected clonal reporter cell line had intact NF-κB regulation, we stimulated both KBM7 cells and the NF-κB reporter cell line with TNF (Fig. 2). We saw that both cells displayed similar IκBα degradation kinetics. The selected clonal reporter cell line survived in the presence of blasticidin only when stimulated with NF-κB activators, demonstrating that the reporter functioned properly (Fig. 3A). The NF-κB reporter cell line was then mutagenized with a retroviral gene-trap vector, using an established protocol that generally yields a library containing mutations in approximately 98% of genes expressed in KBM7 cells [1]. Mutagenized NF-κB reporter cells were exposed to blasticidin and the survivors were pooled and expanded. The selected mutant population was markedly more resistant to blasticidin than the parental reporter cell line and wild-type KBM7 cells in the absence of any stimulus, suggesting that the survivors contain mutations that cause constitutive activation of NF-κB (Fig. 3B). To identify the mutations in the selected mutant population, genomic DNA was harvested from the survivors. The DNA sequences that flank gene-trap insertion sites were amplified, sequenced in parallel, and mapped to the human genome. We identified four genes significantly enriched (p-value < 0.01) for disruptive mutations in our blasticidin-selected population, as compared to a control population of unselected mutagenized cells (Fig. 4). In the blasticidin-resistant population, *CYLD, HEATR7A, LRRC8A*, and *LRRC8D* were represented with 4, 8, 3, and 26 independent inactivating gene-trap

insertions (sense orientation or present in an exon), respectively (respective P-values of 6.91×10^{-5}, 1.09×10^{-12}, 7.88×10^{-4}, and 9.71×10^{-37}) (Figs. 4 and 5).

CYLD encodes a deubiquitylase (DUB) that targets NF-κB signaling factors and is known to negatively regulate NF-κB activation [12-14]. CYLD is expressed and active at steady-state and it is thought to be constitutively required to prevent spontaneous ubiquitylation of its targets and inappropriate activation of NF-κB in the absence of stimulus [15]. To confirm that CYLD is constitutively required for proper regulation of NF-κB in KBM7 cells, we employed shRNA-mediated knockdown of *CYLD* in NF-κB reporter cells (Fig. 6A). In the absence of any stimulus, steady-state IκBα levels are lower in CYLD-depleted cells as compared to cells expressing a control hairpin against luciferase (Fig. 6B). Upon TNF stimulation, IκBα expression is lost more rapidly in CYLD-depleted cells. The ability of our screen to specifically identify CYLD, but not other established NF-κB inhibitors that are not required in the absence of stimulus, validates the use of haploid reporter screens to identify particular components of signaling pathways.

HEATR7A is predicted to encode a protein of 1,641 amino acids and has no known function. It contains seven HEAT (**H**untington, **e**longation Factor 3, protein phosphatase 2**A**, **T**OR1) domains, a protein fold found in a variety of proteins including the four that its name derives from. *HEATR7A* is located on chromosome 8, the only chromosome to be present in two copies in KBM7 cells suggesting that the mutations caused by the gene trap insertions in *HEATR7A* are of a dominant nature.

LRRC8A and LRRC8D represent two of five members of the leucine-rich repeat-containing 8 (LRRC8) family of proteins that are composed of four transmembrane domains at the N-terminus, followed by up to 17 leucine-rich repeats [16]. Their function is poorly understood, but LRRC8A and LRRC8C have been implicated in B cell development and adipocyte differentiation, respectively [17-19]. Thus it is not inconceivable that there may exist a link between LRRC8s and NF-κB, given the established function of NF-κB in lymphocyte differentiation and its emerging role in metabolic disorders [11,20,21]. Given that LRRC8D was identified with high confidence in our screen, we sought to examine its function by isolating two clones that carry gene trap insertions in the *LRRC8D* gene. While the LRRC8D mutant cell lines were notably resistant to blasticidin, examination by immunoblotting revealed no obvious impact of LRRC8D deficiency on IκBα and p100 degradation (data not shown). Our attempts to

demonstrate a possible effect of the LRRC8D disruptions on blasticidin import as an explanation for the observed level of resistance were inconclusive, as the fluorescently labeled or biotinylated versions of blasticidin we prepared were themselves inactive on KBM7 cells. Thus we can neither exclude the possibility that resistance is conferred by differences in intracellular blasticidin levels, nor discount the possibility of alternative modes of NF-κB activation not accounted for by degradation of IkBα and p100 [22].

Discussion

Most genetic screens performed in human haploid cells have sought to identify components in pathways required for cell death in response to a lethal insult. Here we have demonstrated that KBM7 cells can be modified with genetically encoded transcriptional reporters to study more diverse cellular processes. While we chose to screen for regulators -specifically, inhibitors- of NF-κB, our method could presumably be applied to study the approximately 1,391 human sequence specific DNA binding transcription factors, many of whose binding site profiles have recently been described [9,23].

By using resistance to blasticidin as our reporter read-out, we were able to perform a selection -a genetic screen where only mutants of interest survive- to identify mutants that constitutively turned on the reporter. In principle, one could perform a screen in a reversed fashion, in which only mutants that fail to turn on the reporter survive, for example by exploiting thymidine kinase or some other protein whose expression could induce cell death. Identification of positive regulators of transcription factors should thus be possible. Fluorescent reporters could likewise be used in screens for both positive and negative transcriptional regulators. Since stringency in this type of screen would be more adjustable than in a lethal screen, mutations that result in intermediate phenotypes might be more easily recovered.

While the identification of CYLD validated our approach, we were unable to identify mutations in other known negative regulators of NF-κB. Perhaps the selection we performed was particularly stringent. Presumably, only mutations that resulted in constitutive activation of NF-κB could be recovered. Thus, inhibitors whose function or expression is induced by NF-κB in a negative feedback loop, such as A20 and Cezanne, may not meet that criterion. In addition, loss-of-function mutations in dominant-negative adaptors such as MyD88s, IRAK-M, and SARM would not result in constitutive activation of NF-κB. We did not recover mutations in IκBs, possibly because there is some redundancy in function in KBM7 cells and removal of just one IκB is not sufficient for constitutive activation of NF-κB. In contrast, CYLD qualifies as a constitutively active inhibitor that prevents spontaneous ubiquitylation of its targets [15]. CYLD mutations are

associated with constitutive activation of NF-κB in multiple myeloma cells and B cells from mice deficient for wild-type CYLD exhibited constitutive activation of NF-κB [15,24,25].

Our haploid reporter screen confirms the absolute requirement of CYLD function for proper regulation of NF-κB and further supports constitutive NF-κB activity as the mechanism underlying the development of human diseases associated with CYLD mutations. Our screen identified genes not previously known to be involved with NF-κB regulation. Their exact role remains to be determined. The ability to perform haploid reporter screens in human cultured cells opens up many new cellular processes for investigation.

Figures
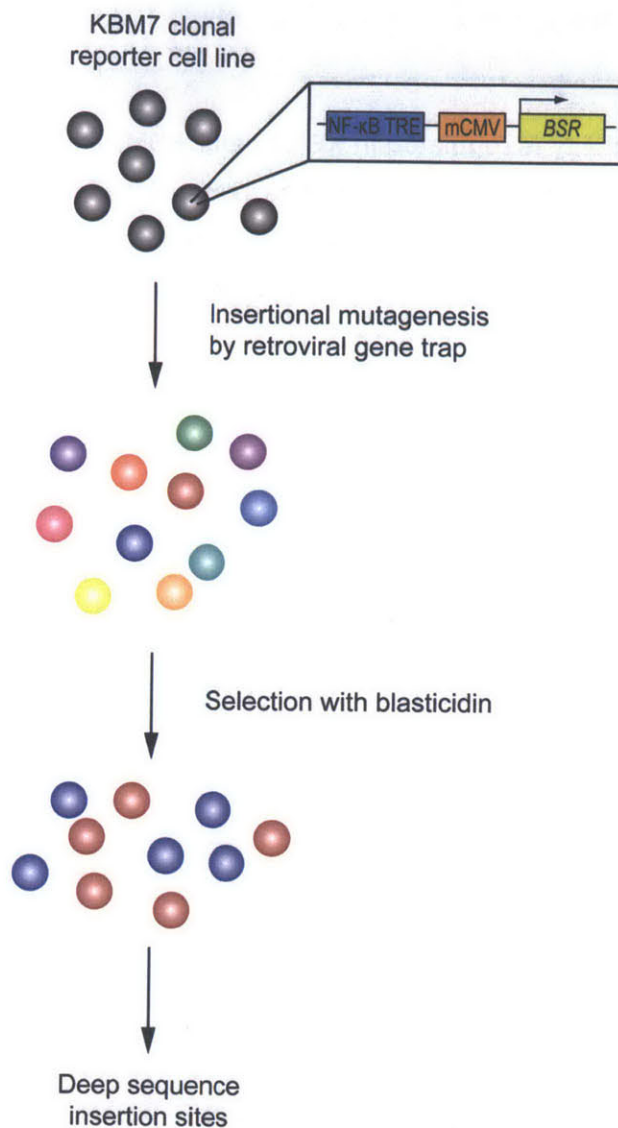
Figure 1. NF-κB reporter haploid genetic screen. KBM7 cells were transduced with a reporter containing a NF-κB transcriptional response element (TRE) and a minimum CMV (mCMV) promoter upstream of the blasticidin S resistance gene (*BSR*) from *Bacillus cereus*. A clonal reporter cell line was mutagenized by infection with a gene-trap virus. The resulting cells were treated with blasticin. Survivors were expanded and DNA was extracted. DNA sequences flanking gene-trap insertion sites were amplified and sequenced in parallel.
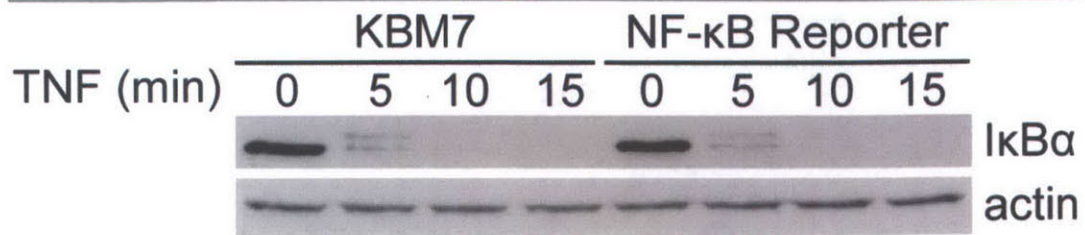
Figure 2. NF-κB activity is regulated in KBM7 cells. KBM7 and NF-κB reporter cells were stimulated with 10 ng/mL TNF for the times indicated. Lysates were analyzed by immunoblot with anti-IκBα. After stripping, the membrane was reprobed with anti-actin antibodies to provide a loading control. Data are representative of two independent experiments.
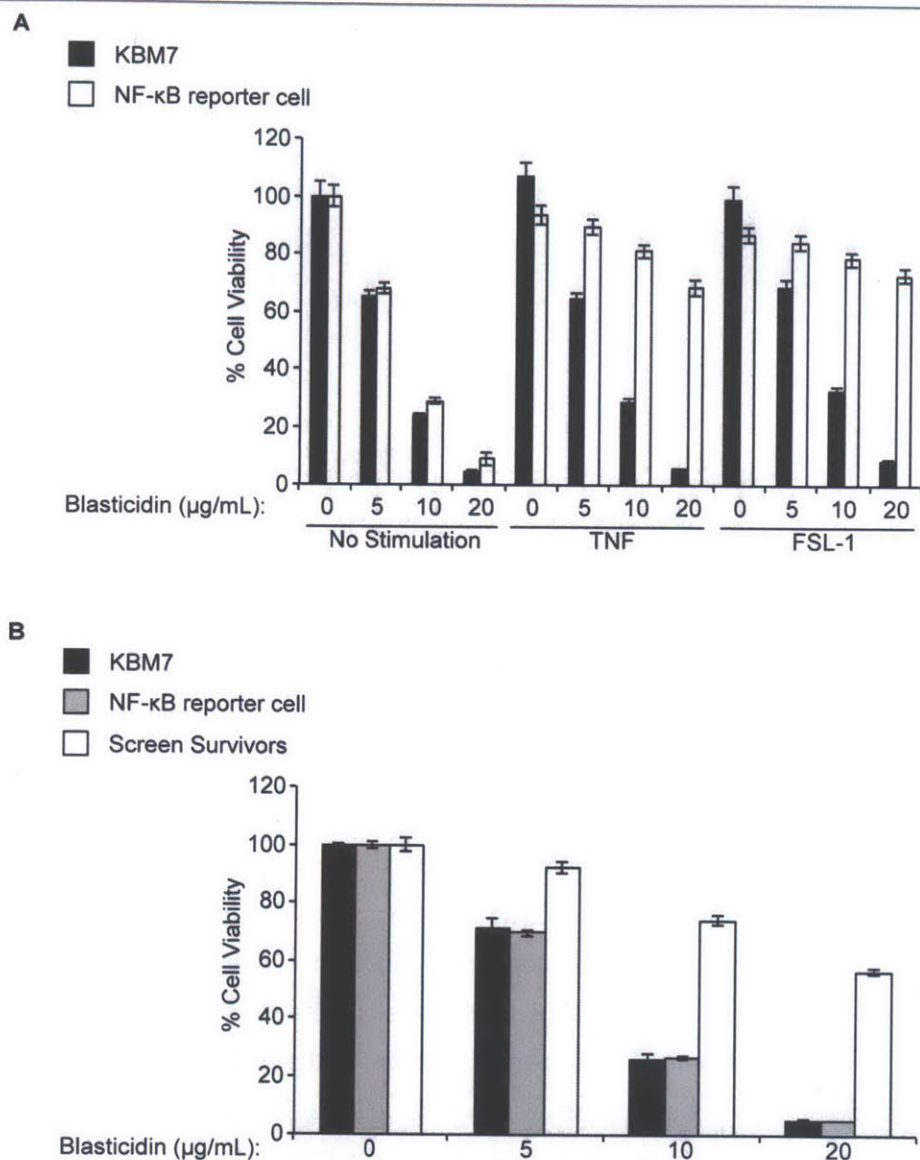
Figure 3. Demonstration of NF-κB reporter function. A. Wild-type KBM7 and the clonal NF-κB reporter cell line were treated with varying concentrations of blasticidin in the absence or presence of NF-κB activators (TNF, FSL-1). **B**. Wild-type KBM7, the clonal NF-κB reporter cell line, and the polyclonal screen survivor population were treated with varying concentrations of blasticidin. Cell viability was determined after 24 hours of treatment using the CellTiter Glo assay and results are plotted as percent viability of treated cells compared with untreated cells. Results are mean ± SEM of triplicates and are representative of 3 independent experiments.
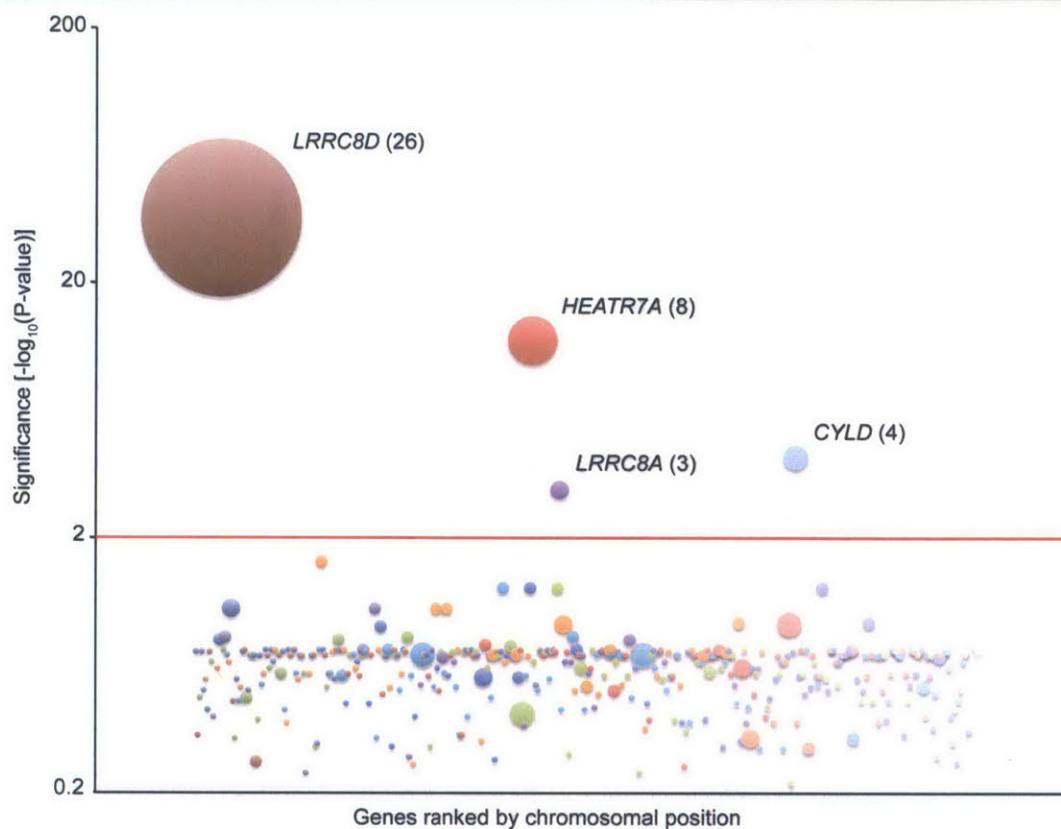
Figure 4. Haploid reporter screen for constitutive inhibitors of NF-κB identifies CYLD. Genes with sequenced inactivating mutations are depicted as circles, the size of which corresponds to the number of independent insertions. Genes are ranked on the x-axis according to their chromosomal position and along the y-axis according to the significance of the enrichment of gene-trap insertions in the indicated gene compared to an unselected control dataset. Genes with a p-value lower than 0.01 are labeled and the number of independent inactivating mutations is indicated between brackets.
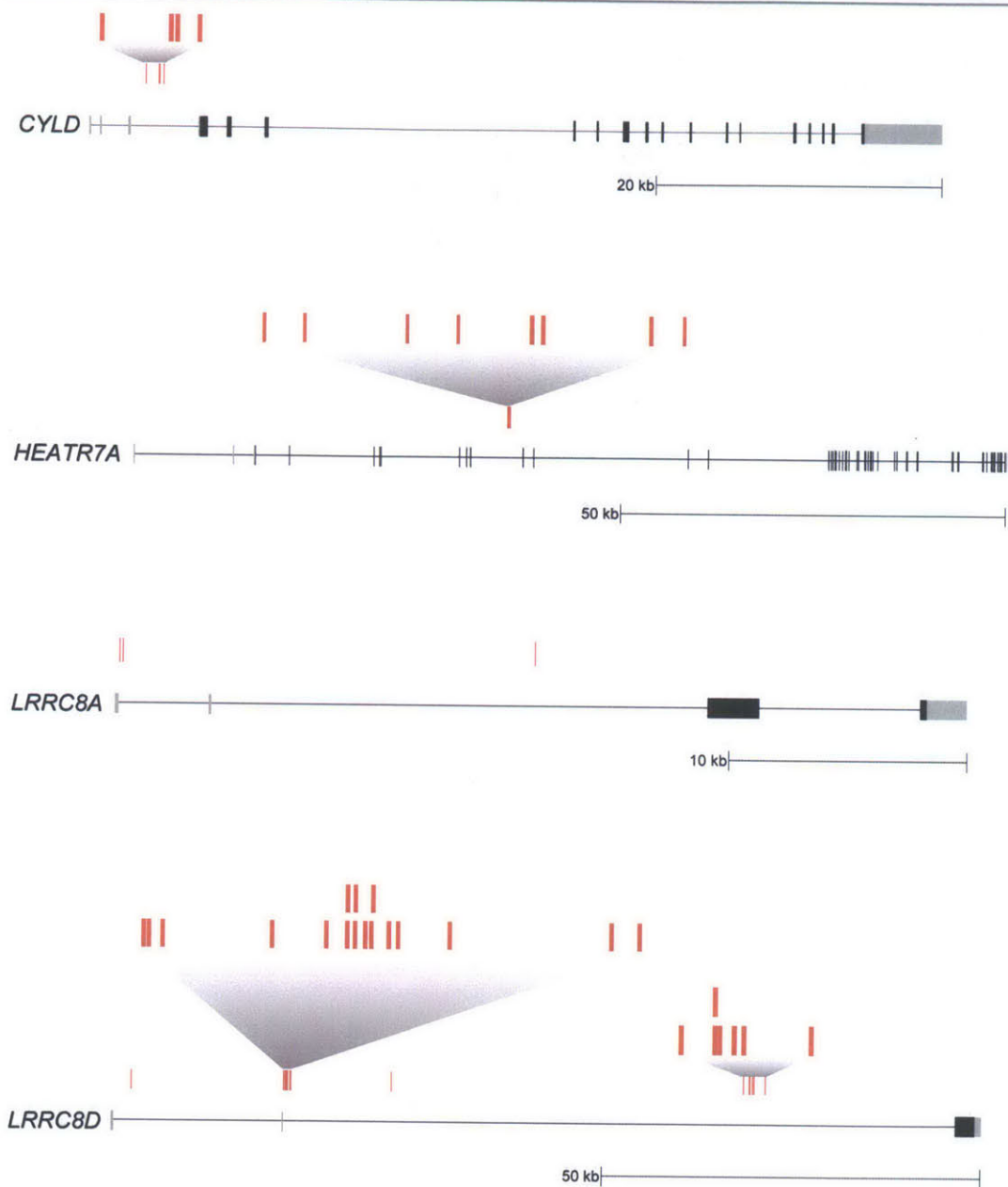
Figure 5. Schematic diagram of inactivating gene-trap insertion sites. The loci of *CYLD* (NM_015247.2), *HEATR7A* (NM_032450.2), *LRRC8A* (NM_019594.3), and *LRRC8D* (NM_001134479.1) are depicted with unique inactivating gene-trap insertion sites (sense orientation or present in an exon) shown in red. For regions where there were many unique insertion sites, the areas are blown up to reveal all unique sites. Gray boxes denote the 5' and 3' untranslated regions, and black boxes denote coding exons.
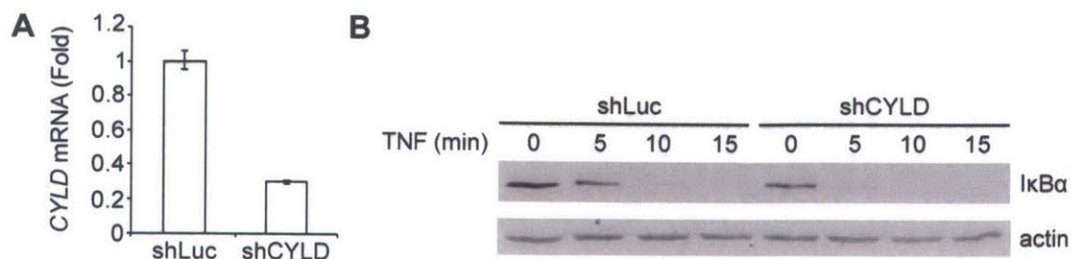
Figure 6. CYLD is constitutively required for normal NF-κB function. A. NF-κB reporter cells were infected with a control hairpin against luciferase (shLuc) or a hairpin against *CYLD* (shCYLD). *CYLD* mRNA levels (mean of triplicates) were determined by quantitative real-time PCR. **B.** NF-κB reporter cells expressing either shLuc or shCYLD were stimulated with 10 ng/mL TNF for various time points. Lysates were analyzed by immunoblot with anti-IκBα. After stripping, the membrane was reprobed with anti-actin antibody to provide a loading control. Data are representative of three independent experiments.

Materials and Methods

Plasmids

The NF-κB reporter was created by digesting pTRH1-NF-κB-dscGFP (System Biosciences) with SpeI and SalI to remove the dscGFP. The same restriction sites were used to insert a synthesized DNA fragment encoding mCMV-NheI-Kozak sequence-BamHI-*Bacillus cereus BSR*-Thosea asigna virus 2A sequence-XbaI-Rabbit *CYP4B1*. Lentiviral shRNAs were obtained from The RNAi Consortium (TRC) collection of the Broad Institute. The TRC numbers for the shRNAs used are TRCN0000072245 (shLuc) and TRCN0000039632 (shCYLD).

Cells

KBM7 cells were grown in Iscove's modified Dulbecco's medium (IMDM) with 10% heat-inactivated fetal serum (IFS) [3,26]. A NF-κB reporter cell line was created by transducing KBM7 cells with the NF-κB reporter construct described above and single cells were sorted into individual wells of 96 well plates. A clone that remained haploid and that died in the presence of blasticidin S (Invivogen), but survived in blasticidin when stimulated with NF-κB agonists was selected for the screen.

Reporter haploid genetic screen

The screening procedure has been described previously [1-6]. Briefly, 100 million NF-κB reporter cells were infected with gene-trap retrovirus to create a mutagenized library. 200 million mutagenized cells were then plated 100,000 cells/well in 96 well plates with half in 10 ug/mL blasticidin S (Invivogen) and half in 15 ug/mL blasticidin S for 6 days. After 6 days, the media above the cells was replaced with antibiotic-free IMDM. Survivors were allowed to expand for about three additional weeks before harvest. DNA was harvested from ~30 million cells from each of the two blasticidin conditions.

Sequence analysis of gene-trap insertion sites

The mapping of the insertion sites was done as previously described [1-6]. In short, DNA sequences flanking gene-trap insertions sites were amplified using an inverse PCR

protocol followed by sequencing using the Genome Analyzer platform (Illumina). The
sequences were then aligned to the human genome. The number of inactivating
mutations (that is, sense orientation or present in exon) per individual gene was counted
as well as the total number of inactivating insertions for all genes. Enrichment of a gene
in the screen was calculated by comparing how often that gene was mutated in the
screen compared to how often the gene carries an insertion in the control data set. For
each gene, a P-value (corrected for false discovery rate) was calculated using the one-
sided Fisher exact test.

Immunoblot analysis of TNF stimulated cells

Two million cells were used per condition. Cells were washed once in ice-cold PBS and
then lysed in buffer containing 50 mM Tris-HCl pH 7.4, 150 mM NaCl, 0.5 mM EDTA,
protease inhibitors (Roche) and 1% (v/v) NP40. Protein concentrations of lysates were
determined by Bio-Rad Protein Assay and then normalized across samples. Proteins
from total lysates were resolved by 10% SDS-PAGE and analyzed by immunoblotting
with primary antibodies: mouse anti-IκBα (BD #610690) at 1:500 dilution and mouse
anti-actin (BD #612656) at 1:10,000. Horseradish peroxidase (HRP)-conjugated sheep
anti-mouse IgG (GE NXA931) was used at 1:5,000 dilution. Restore PLUS Western Blot
Stripping Buffer (Thermo) was used to strip the membranes between probing for IκBα
and actin.

Cell viability assay

CellTiter-Glo Luminescent Cell Viability Assay (Promega) was used to quantify cell
viability. 200,000 cells were seeded per well in Optilux clear-bottom 96-well plates (BD
Falcon) in IMDM or IMDM supplemented with varying concentrations of Blasticidin S
(Invivogen), TNF-α (Invivogen), FSL-1 (Invivogen) for 24 hours before reading on a
Luminoskan Ascent luminometer (Thermo Scientific).

Quantitative real-time PCR

RNA was extracted using a RNAeasy kit (QIAGEN) followed by on-column DNase I
(QIAGEN) digestion. SuperScript III First-Strand Synthesis System (Invitrogen) was used
for the reverse transcription reaction using Oligo dT primers. SYBR Green PCR Master

Mix (Applied Biosystems) was used according to manufacturer's instructions. Real-time

PCR reactions were run on an ABI 7900HT machine. PCR volume was 20 uL (96-well

plate), and data values were derived from three replicates using the comparative Ct

method. Primers used for *CYLD* were 5' GGTAATCCGTTGGATCGGTCAGC 3' and 5'

TGCAAACCTAGAGTCAGGCCTGC 3'. Primers used for *GAPDH* were 5'

ACCCACTCCTCCACCTTTGACG 3' and 5' CACCCTGTTGCTGTAGCCAAATTCG 3'.

References

1. Carette JE, Guimaraes CP, Wuethrich I, Blomen VA, Varadarajan M, et al. (2011) Global gene disruption in human cells to assign genes to phenotypes by deep sequencing. Nat Biotech 29: 542–546. doi:10.1038/nbt.1857.

2. Carette JE, Raaben M, Wong AC, Herbert AS, Obernosterer G, et al. (2011) Ebola virus entry requires the cholesterol transporter Niemann–Pick C1. Nature 477: 340–343. doi:10.1038/nature10348.

3. Carette JE, Guimaraes CP, Varadarajan M, Park AS, Wuethrich I, et al. (2009) Haploid Genetic Screens in Human Cells Identify Host Factors Used by Pathogens. Science 326: 1231–1235. doi:10.1126/science.1178955.

4. Rosmarin DM, Carette JE, Olive AJ, Starnbach MN, Brummelkamp TR, et al. (2012) Attachment of Chlamydia trachomatis L2 to host cells requires sulfation. Proc Natl Acad Sci USA 109: 10059–10064. doi:10.1073/pnas.1120244109.

5. Guimaraes CP, Carette JE, Varadarajan M, Antos J, Popp MW, et al. (2011) Identification of host cell factors required for intoxication through use of modified cholera toxin. J Cell Biol 195: 751–764. doi:10.1083/jcb.201108103.

6. Papatheodorou P, Carette JE, Bell GW, Schwan C, Guttenberg G, et al. (2011) Lipolysis-stimulated lipoprotein receptor (LSR) is the host receptor for the binary toxin Clostridium difficile transferase (CDT). Proc Natl Acad Sci USA 108: 16422–16427. doi:10.1073/pnas.1109772108.

7. Jae LT, Raaben M, Riemersma M, van Beusekom E, Blomen VA, et al. (2013) Deciphering the glycosylome of dystroglycanopathies using haploid screens for lassa virus entry. Science 340: 479–483. doi:10.1126/science.1233675.

8. Duncan LM, Timms RT, Zavodszky E, Cano F, Dougan G, et al. (2012) Fluorescence-based phenotypic selection allows forward genetic screens in haploid human cells. PLoS ONE 7: e39651. doi:10.1371/journal.pone.0039651.

9. Vaquerizas JM, Kummerfeld SK, Teichmann SA, Luscombe NM (2009) A census of human transcription factors: function, expression and evolution. Nat Rev Genet 10: 252–263. doi:10.1038/nrg2538.

10. Maston GA, Evans SK, Green MR (2006) Transcriptional regulatory elements in the human genome. Annu Rev Genomics Hum Genet 7: 29–59. doi:10.1146/annurev.genom.7.080505.115623.

11. Vallabhapurapu S, Karin M (2009) Regulation and Function of NF-κB Transcription Factors in the Immune System. Annu Rev Immunol 27: 693–733. doi:10.1146/annurev.immunol.021908.132641.

12. Trompouki E, Hatzivassiliou E, Tsichritzis T, Farmer H, Ashworth A, et al. (2003) CYLD is a deubiquitinating enzyme that negatively regulates NF-kappaB activation by TNFR family members. Nature 424: 793–796. doi:10.1038/nature01803.

13. Kovalenko A, Chable-Bessia C, Cantarella G, Israël A, Wallach D, et al. (2003) The tumour suppressor CYLD negatively regulates NF-kappaB signalling by deubiquitination. Nature 424: 801–805. doi:10.1038/nature01802.

14. Brummelkamp TR, Nijman SMB, Dirac AMG, Bernards R (2003) Loss of the cylindromatosis tumour suppressor inhibits apoptosis by activating NF-kappaB. Nature 424: 797–801. doi:10.1038/nature01811.

15. Sun SC (2009) CYLD: a tumor suppressor deubiquitinase regulating NF-κB activation and diverse biological processes. Cell Death Differ 17: 25–34. doi:10.1038/cdd.2009.43.

16. Abascal F, Zardoya R (2012) LRRC8 proteins share a common ancestor with pannexins, and may form hexameric channels involved in cell-cell communication. Bioessays. doi:10.1002/bies.201100173.

17. Hayashi T, Nozaki Y, Nishizuka M, Ikawa M, Osada S, et al. (2011) Factor for adipocyte differentiation 158 gene disruption prevents the body weight gain and insulin resistance induced by a high-fat diet. Biol Pharm Bull 34: 1257–1263.

18. Tominaga K, Kondo C, Kagata T, Hishida T, Nishizuka M, et al. (2004) The novel gene fad158, having a transmembrane domain and leucine-rich repeat, stimulates adipocyte differentiation. J Biol Chem 279: 34840–34848. doi:10.1074/jbc.M312927200.

19. Sawada A, Takihara Y, Kim JY, Matsuda-Hashii Y, Tokimasa S, et al. (2003) A congenital mutation of the novel gene LRRC8 causes agammaglobulinemia in humans. J Clin Invest 112: 1707–1713. doi:10.1172/JCI18937.

20. Tornatore L, Thotakura AK, Bennett J, Moretti M, Franzoso G (2012) The nuclear factor kappa B signaling pathway: integrating metabolism with inflammation. Trends Cell Biol 22: 557–566. doi:10.1016/j.tcb.2012.08.001.

21. Baker RG, Hayden MS, Ghosh S (2011) NF-κB, inflammation, and metabolic disease. Cell Metab 13: 11–22. doi:10.1016/j.cmet.2010.12.008.

22. Hayden MS, Ghosh S (2012) NF-κB, the first quarter-century: remarkable progress and outstanding questions. Genes & Development 26: 203–234. doi:10.1101/gad.183434.111.

23. Jolma A, Yan J, Whitington T, Toivonen J, Nitta KR, et al. (2013) DNA-binding specificities of human transcription factors. Cell 152: 327–339.

doi:10.1016/j.cell.2012.12.009.

24. Jin W, Reiley WR, Lee AJ, Wright A, Wu X, et al. (2007) Deubiquitinating enzyme CYLD regulates the peripheral development and naive phenotype maintenance of B cells. J Biol Chem 282: 15884–15893. doi:10.1074/jbc.M609952200.

25. Hövelmeyer N, Wunderlich FT, Massoumi R, Jakobsen CG, Song J, et al. (2007) Regulation of B cell homeostasis and activation by the tumor suppressor gene CYLD. J Exp Med 204: 2615–2627. doi:10.1084/jem.20070318.

26. Kotecki M, Reddy PS, Cochran BH (1999) Isolation and characterization of a near-haploid human cell line. Exp Cell Res 252: 273–280. doi:10.1006/excr.1999.4656.

Chapter 3

The Protein Synthesis Inhibitor Blasticidin S Enters Mammalian Cells via Leucine-Rich Repeat-Containing Protein 8D

Clarissa C. Lee [1,2], Elizaveta Freinkman [2], David M. Sabatini [1,2,3,4], Hidde L. Ploegh [1,2]

[1] Whitehead Institute for Biomedical Research, Cambridge, MA, USA

[2] Department of Biology, Massachusetts Institute of Technology (MIT), Cambridge, MA, USA

[3] David H. Koch Institute for Integrative Cancer Research at MIT, Cambridge, MA, USA

[4] Broad Institute, Cambridge, MA, USA

[5] Howard Hughes Medical Institute, MIT, Cambridge, MA, USA

E.F. performed the targeted mass-spectrometry of blasticidin in Figure 2. C.C.L. performed all other experiments.

Abstract

Leucine-rich repeat-containing 8 (LRRC8) proteins have been identified as putative receptors involved in lymphocyte development and adipocyte differentiation. They remain poorly characterized and no specific function has been assigned to them. There is no consensus on how this family of proteins might function, because homology searches suggest that members of the LRRC8 family act not as plasma membrane receptors, but rather as channels that mediate cell-cell signaling. Here we provide experimental evidence that supports a role for LRRC8s in the transport of small molecules. We show that LRRC8D is a mammalian protein required for the import of the antibiotic blasticidin S. We characterize localization and topology of LRRC8A and LRRC8D and demonstrate that LRRC8D interacts with LRRC8A, LRRC8B, and LRRC8C. Given the suggested involvement in solute transport, our results support a model in which LRRC8s form one or more complexes that may mediate cell-cell communication by transporting small solutes.

Introduction

The leucine-rich repeat-containing 8 (LRRC8) family of proteins comprises five members, named LRRC8A, LRRC8B, LRRC8C, LRRC8D, and LRRC8E. Each member comprises four predicted transmembrane domains at the N-terminus and up to 17 leucine-rich repeats (LRR) at the C-terminus [1,2]. While LRRC8A and LRRC8C have been implicated in lymphocyte development and adipocyte differentiation, respectively, their mechanism of function remains unknown and the other members of the family remain poorly characterized [3-5].

The founding member of the family, LRRC8A, was identified when white blood cells from a patient suffering from congenital agammaglobulinemia showed a balanced chromosomal translocation t(9;20)(q33.2;q12) that resulted in the expression of both a normal copy of LRRC8A and a truncated form of LRRC8A that lacks the last two and a half LRR domains [3]. Forced expression of the truncated version of LRRC8A in murine bone marrow cells inhibited B cell development and confirmed that the patient's B-cell deficiency was due to the mutation in LRRC8A. Given the dominant nature of the mutation and the presence of LRRs in the extracellular binding domain of diverse receptors (Toll-like receptors, follicle-stimulating hormone receptor, high affinity nerve growth factor receptor), LRRC8A was proposed to function as a cell surface receptor that oligomerizes upon binding an unknown ligand important for B cell development [6].

The only other functional studies on LRRC8s concern adipocyte development. *LRRC8C*, also known as *FAD158*, was identified as a gene whose expression is induced in the early stage of adipocyte differentiation [4]. Knock-down and overexpression studies supported a role for LRRC8C in adipocyte differentiation. When *LRRC8C-/-* and wild-type mice were fed a high-fat diet, *LRRC8C-/-* mice had significantly lower body weights and fat mass [5]. How exactly LRRC8C is involved in adipocyte differentiation and the development of obesity in response to a high-fat diet remains unclear.

A recent hypothesis paper, based exclusively on a bioinformatics approach, proposed that LRRC8s evolved from the combination of a pannexin and an LRR domain prior to the diversification of chordates [2]. Sequence similarity and inferred homology between LRRC8s and pannexins would place the LRR domains of LRRC8s facing the

cytoplasm rather than the outside of the cell, in contrast to the report by Sawada et al. [3].

Pannexins are a family of communication channels composed of four α-helical transmembrane domains. They are thought to function primarily in transporting intracellular molecules to the extracellular space [7]. While pannexins could participate in many biological processes, evidence is strongest for a role of pannexin 1 (Panx1) in the release of 'find-me' signals, specifically ATP and UTP, by apoptotic cells to recruit phagocytes [7-9]. While LRRC8s, like pannexins, might form channels and participate in cell-cell communication, there has been no experimental evidence to support such a role.

Here we show that LRRC8D is required for the import of the antibiotic blasticidin S (BlaS) by mammalian cells and is the first protein implicated in this process, supporting a role for LRRC8s in solute transport. We further provide evidence that the LRR domains of LRRC8A and LRRC8D face the cytoplasm rather than extracellular space and that LRRC8D interacts with LRRC8A, LRRC8B, and LRRC8C.

Results

LRRC8D-deficient cells are resistant to BlaS

We identified LRRC8D and LRRC8A as hits in a haploid reporter genetic screen aimed at discovering inhibitors of NF-κB[10]. We performed the screen with cells carrying a NF-κB transcriptional reporter that drives expression of the blasticidin S-resistance gene (*BSR*), so that cells in which the NF-κB pathway is activated would survive in the presence of BlaS (Fig. 1A).

After insertional mutagenesis, reporter cells that survived in the presence of BlaS were selected, with the expectation that they would contain mutations in NF-κB inhibitors and thus show constitutive expression of the NF-κB-BSR reporter. Indeed, one of the significant hits in the screen, CYLD, is a known negative regulator of NF-κB. We confirmed that CYLD is required at steady-state to prevent aberrant activation of NF-κB[10]. To further characterize LRRC8D, we isolated 2 clonal cell lines from the screen, LRRC8D^{GT1} and LRRC8D^{GT2}, that have gene-trap insertion sites located in the intron between exon 2 and exon 3 (Fig 1B). Neither LRRC8D^{GT1} nor LRRC8D^{GT2} cell lines express full-length *LRRC8D* mRNA (Fig. 1C). Consistent with the design of the gene trap vector, this suggests that in LRRC8D^{GT1} and LRRC8D^{GT2} cells, exon 2 is not splicing to exon 3, but rather to the splice acceptor site in the gene-trap, which terminates the transcript. Thus, none of the protein coding sequence for LRRC8D, fully contained in exon 3, is expressed in LRRC8D^{GT1} and LRRC8D^{GT2} cell lines.

We determined that both LRRC8D^{GT1} and LRRC8D^{GT2} cell lines are indeed resistant to BlaS (Fig. 1D). We hypothesized that LRRC8D deficiency results in constitutive activation of the NF-κB-BSR reporter and therefore confers BlaS resistance. To our surprise we were unable to demonstrate a defect in NF-κB regulation in LRRC8D^{GT1} and LRRC8D^{GT2} cells (data not shown). Previous haploid genetic screens with tunicamycin and 3-bromopyruvate as the selecting agents identified transporters for these small molecules [11,12]. We then considered the possibility that resistance of LRRC8D^{GT1} and LRRC8D^{GT2} cells to BlaS was attributable to defective import of the antibiotic rather than altered NF-κB signaling.

LRRC8D mediates transport of BlaS

How BlaS enters mammalian cells is not known, but given its polar nature (Fig. 1A), it is unlikely to cross the plasma membrane unaided. There is no easy path to the synthesis of radiolabeled BlaS that could then be used for cellular uptake experiments. We generated a biotinylated version of BlaS for that purpose, but found that it lacked biological activity when applied to intact cells and therefore could not be used as a BlaS analog to measure transport. We resorted to a liquid chromatography/mass spectroscopy-based assay to directly measure BlaS levels in extracts from BlaS-exposed cells. To determine if LRRC8D is required for BlaS import, wild-type cells, LRRC8D^{GT1} cells, and LRRC8D^{GT2} cells were incubated with varying concentrations of BlaS for three hours. BlaS levels in extracts made from BlaS-treated cells were measured by targeted mass spectrometry. While BlaS was easily detected in wild-type cells, it was either absent from, or present in only trace amounts in LRRC8D^{GT1} and LRRC8D^{GT2} cells, thus demonstrating that LRRC8D deficiency results in defective BlaS import (Fig. 2).

Localization of LRRC8A and LRRC8D

We next sought to determine where LRRC8A and LRRC8D are located in the cell. If they are transporters for BlaS and other molecules, one would expect to see them most likely at the plasma membrane. In Hela cells stably expressing LRRC8A equipped with a C-terminal HA tag, LRRC8A-HA was present at the plasma membrane (Fig. 3). In Hela cells that stably express LRRC8D-HA, LRRC8D-HA appeared less prominently at the plasma membrane whereas the majority colocalized with calnexin in the ER. Surface display of LRRC8D may require the involvement of a partner protein present in limiting amounts. Overexpression of LRRC8D on its own in the absence of such cofactors would then prevent a major portion of LRRC8D from reaching the plasma membrane.

LRR domains of LRRC8A and LRRC8D face the cytoplasm

LRR domains are widespread and often mediate protein-protein interactions[6]. The LRR domain of LRRC8A was initially reported to face the outside of cells, but this assertion has recently been questioned based on sequence similarity between LRRC8s and pannexins, a family of communication channels [2,3]. If LRRC8s have the same

topology as pannexins, then the LRR domains of LRRC8s would face the cytoplasm and have access to very different interaction partners than on the outside of cells.

To determine the topology of LRRC8A and LRRC8D we performed a flow cytometry experiment. Hela cells that stably express either empty vector or C-terminally HA-tagged Kell (KEL-HA), Glycophorin A (GYPA-HA), LRRC8A, or LRRC8D were incubated with Alexa Fluor 488-conjugated anti-HA in the absence or presence of the detergent saponin (Fig. 4, A and B). Kell, a mammalian type II transmembrane protein, and Glycophorin A, a mammalian type I transmembrane protein, are expressed on the cell surface and were used as controls [13,14]. As expected, HA was detected on intact cells expressing KEL-HA. Permeabilization with saponin allowed detection of both the plasma membrane and intracellular populations of KEL. In contrast, for cells that express GYPA-HA, the HA-tag could be detected only when the cells were permeabilized due to the cytosolic exposure of the tag. Similarly, for cells that express LRRC8A-HA and LRRC8D-HA, the HA-tag could be detected only when the cells were permeabilized, suggesting that their LRR domains face the cytosol.

Since the expression level of LRRC8D-HA was lower than that of LRRC8A-HA in the stable cell lines used for flow cytometry, and since LRRC8D-HA was not as prominently displayed at the plasma membrane in our immunofluorescence experiments, we sought to verify the topology of LRRC8D biochemically with a protease protection assay (Fig. 4, C and D). We used SEL1L and AUP1, members of an ER complex required for the dislocation of misfolded proteins, as controls [15]. The N-terminus and bulk of SEL1L are located in the ER lumen, whereas AUP1 is a monotypic membrane protein that has both termini facing the cytosol [15-17]. Microsome-containing fractions from 293T transfectants expressing HA-SEL1L, AUP1-GFP, and LRRC8D-HA were incubated with proteinase K in the absence or presence of Triton X-100. Proteinase K-treated samples were then analyzed by immunoblot. Consistent with the known topology of SEL1L and AUP1, detection of HA-SEL1L was lost only upon addition of both detergent and proteinase K, whereas detection of AUP1-GFP was lost with the addition of proteinase K even in the absence of detergent. Similar to AUP1-GFP, detection of LRRC8D-HA was lost with the addition of proteinase K even in the absence of detergent, thus confirming that the LRR domain of LRRC8D faces the cytosol.

LRRC8D interacts with other members of the LRRC8 family

Given that the LRR domain of LRRC8s faces the cytosol rather than extracellular space, we hypothesized that the LRR domain could be mediating interactions with cytoplasmic proteins or molecules that affect the opening or closing of a channel of which the LRRC8s might be part. To identify potential interacting partners of LRRC8A and LRRC8D, lysates from RAW 264.7 macrophages that stably express murine LRRC8A-HA, LRRC8D-HA, or empty vector were incubated with anti-HA agarose beads and the immunoprecipitated proteins were identified by mass spectrometry (Table 1). The results indicate that LRRC8A and LRRC8D interact with each other as well as with LRRC8C. A similar experiment with KBM7 cells showed that LRRC8A and LRRC8D interact with LRRC8B as well (data not shown). We verified that LRRC8D interacts with LRRC8A, LRRC8B, and LRRC8C by co-expressing epitope-tagged versions of the proteins in 293T cells, immunoprecipitating for LRRC8A-Myc, LRRC8B-V5, and LRRC8C-Flag and blotting for LRRC8D-HA in the co-immunoprecipitating fractions (Fig. 5).

We demonstrated that the interaction between LRRC8s does not occur post-lysis by using transfectants that each express a single epitope-tagged LRRC8 member. Lysates from LRRC8A-Myc, LRRC8B-V5, and LRRC8C-Flag transfectants were each combined with lysates from LRRC8D-HA transfectants. When LRRC8A-Myc, LRRC8B-V5, and LRRC8C-Flag were immunoprecipitated from these combined lysates, LRRC8D-HA did not appear in the co-immunoprecipitating fractions. We did not verify the interaction of LRRC8D with the other proteins identified by mass spectrometry, as they were identified with modest peptide coverage. We have found that several of these hits occur as common contaminants in immunoprecipitation-mass spectrometry experiments.

Discussion

Defective *LRRC8D* expression results in BlaS resistance due to a defect in BlaS import. Since import of a toxic molecule is not a function that would be selected for by evolution, it is likely that there are as yet undiscovered physiological substrates that are normally transported by LRRC8D or the complex of which it is part. Since BlaS contains both a cytosine moiety and an arginine-like appendage, it is possible that nucleotides, amino acids, or short (modified) peptides could be substrates for LRRC8D. Pannexins, which display homology to LRRC8s, have often been linked to the release of ATP [7]. Thus ATP and other second messengers could be candidate substrates as well.

The discovery that LRRC8D has a role in the transport of a small molecule suggests that all members of the LRRC8 family, which are on average 45.92% identical, may have a similar function [2]. LRRC8A was initially proposed to be a cell surface receptor that initiates a signaling cascade in response to the binding of an extracellular ligand important for B cell development [3]. In light of our results, it is possible that instead of acting as a receptor, LRRC8A may act as a selective communication channel that mediates the import of a growth and/or differentiation factor secreted by nearby cells to allow continuation of B cell development. A similar mechanism may be at play for LRRC8C in adipocyte differentiation.

Contrary to what was reporter earlier, the LRR domains of LRRC8A and LRRC8D face the cytoplasm [3]. The topology inferred from our experiments is consistent with that of pannexins [2]. It has been proposed that LRRC8s are the evolutionary result of the combination of a pannexin and a LRR domain [2]. What could be the added benefit of the LRR domain? It is unclear whether LRRC8 channels are always open or if they selectively open when needed. Perhaps the LRR domain regulates the opening of the channel through an interaction with a protein or molecule that occurs in response to specific cellular needs. Alternatively, the LRR domain could bind to additional proteins that make up the scaffold of the transporter or it could recruit proteins that interact with incoming or outgoing substrates.

We discovered that LRRC8D interacts in stable fashion with other members of the LRRC8 family. Obviously, proteins that interact transiently or only under certain ligand-stimulated conditions would have been missed in our experimental conditions. In addition to future searches for such interactors, it would also be interesting to identify interactions that depend upon the LRR domain by comparing immunoprecipitates from full-length LRRC8s and LRRC8s missing their LRR domain. Panx1 oligomerizes into hexamers whereas PANX2 is thought to assemble into heptamers or octamers [7]. Some intermixing between Panx1, Panx2, and Panx3 has been observed, but the biological significance of this is currently unknown. It will be important to determine in future studies whether LRRC8s interact with each other in a single complex or if there are multiple complexes of distinct stoichiometry and composition.

Together our results provide clear experimental evidence for a functional link between members of the LRRC8 family and pannexins and shed new light on how LRRC8s could be mediating lymphocyte development and adipocyte differentiation.

Figures and Tables
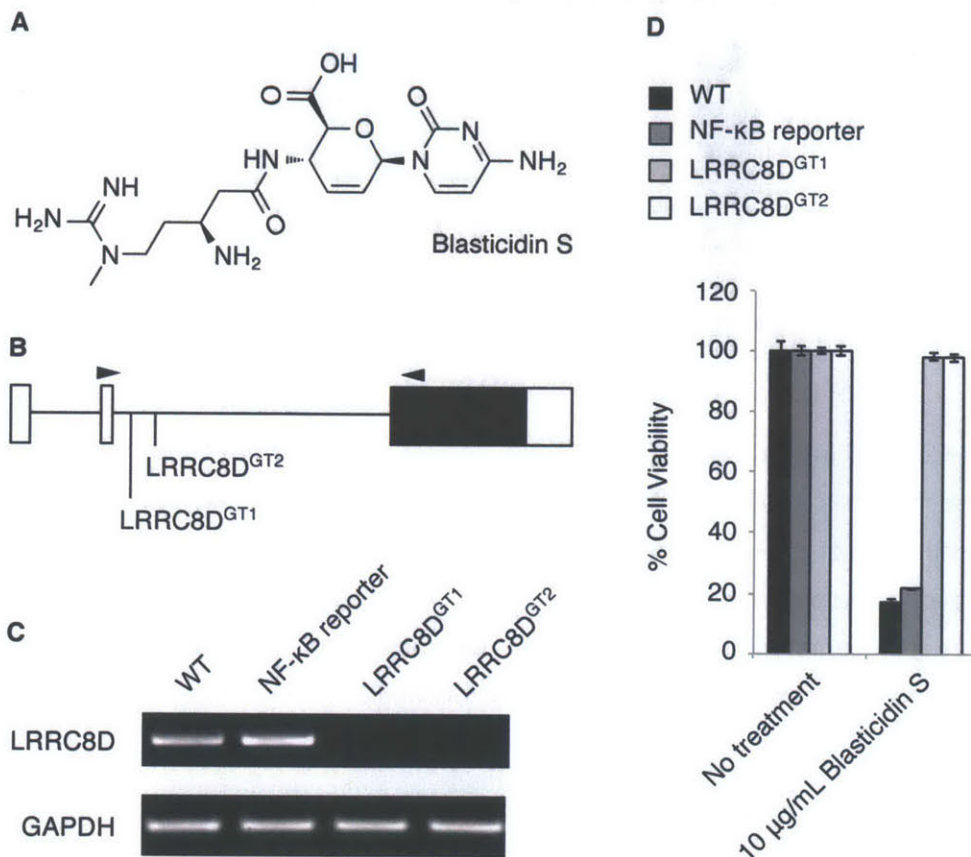
Figure 1. LRRC8D-deficient cells are resistant to blasticidin S.

A, Structure of BlaS B, Genomic locus of *LRRC8D* and the location of two gene-trap insertion sites. White boxes denote the 5' and 3' untranslated regions and the black box denotes the coding sequence, all of which is within exon three. Arrowheads indicate the binding sites of primers used for RT-PCR analysis C, RT-PCR analysis of WT KBM7 cells, WT NF-κB-BSR reporter cells, and two clonally derived cell lines containing gene-trap insertions in *LRRC8D* as indicated in (B). D, WT KBM7 cells, WT NF-κB reporter cells, *LRRC8D*^{GT1} cells, and *LRRC8D*^{GT2} cells were treated with varying concentrations of BlaS. Cell viability was determined after 24 hours of treatment using the CellTiter Glo assay and results are plotted as percent viability of treated cells compared with untreated cells. Results are mean ± SEM of triplicates and are representative of 3 independent experiments.
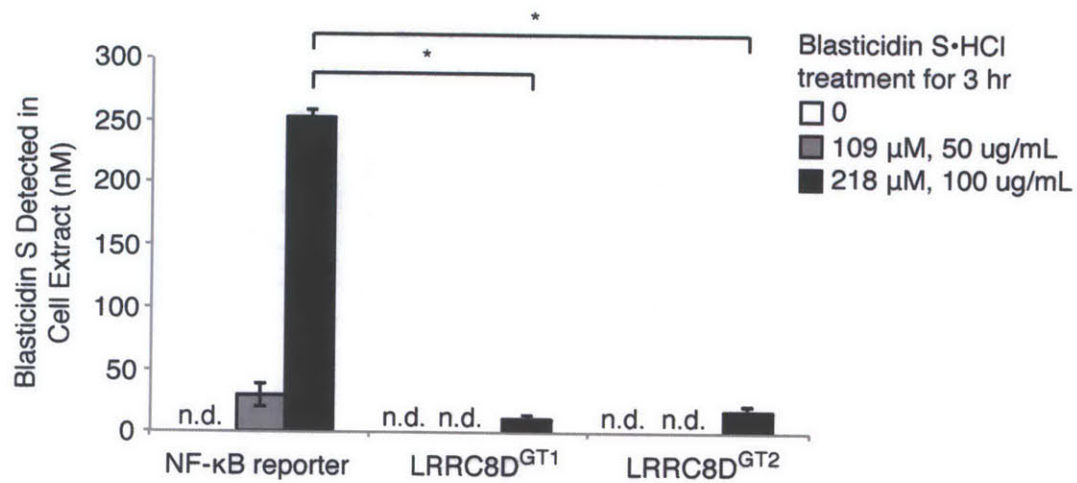
Figure 2. BlaS internalization is defective in LRRC8D deficient cells.

WT reporter cells, *LRRC8D*^{GT1} cells, and *LRRC8D*^{GT2} cells were treated with varying concentrations of BlaS for three hours. Extracts of polar metabolites from the cells were analyzed for the presence of BlaS using LC/MS. Results are mean ± SD of triplicates and are representative of three independent experiments. n.d., not detected. Statistical analysis was performed using the Welch test followed by a Bonferroni correction (*p < 0.0001).
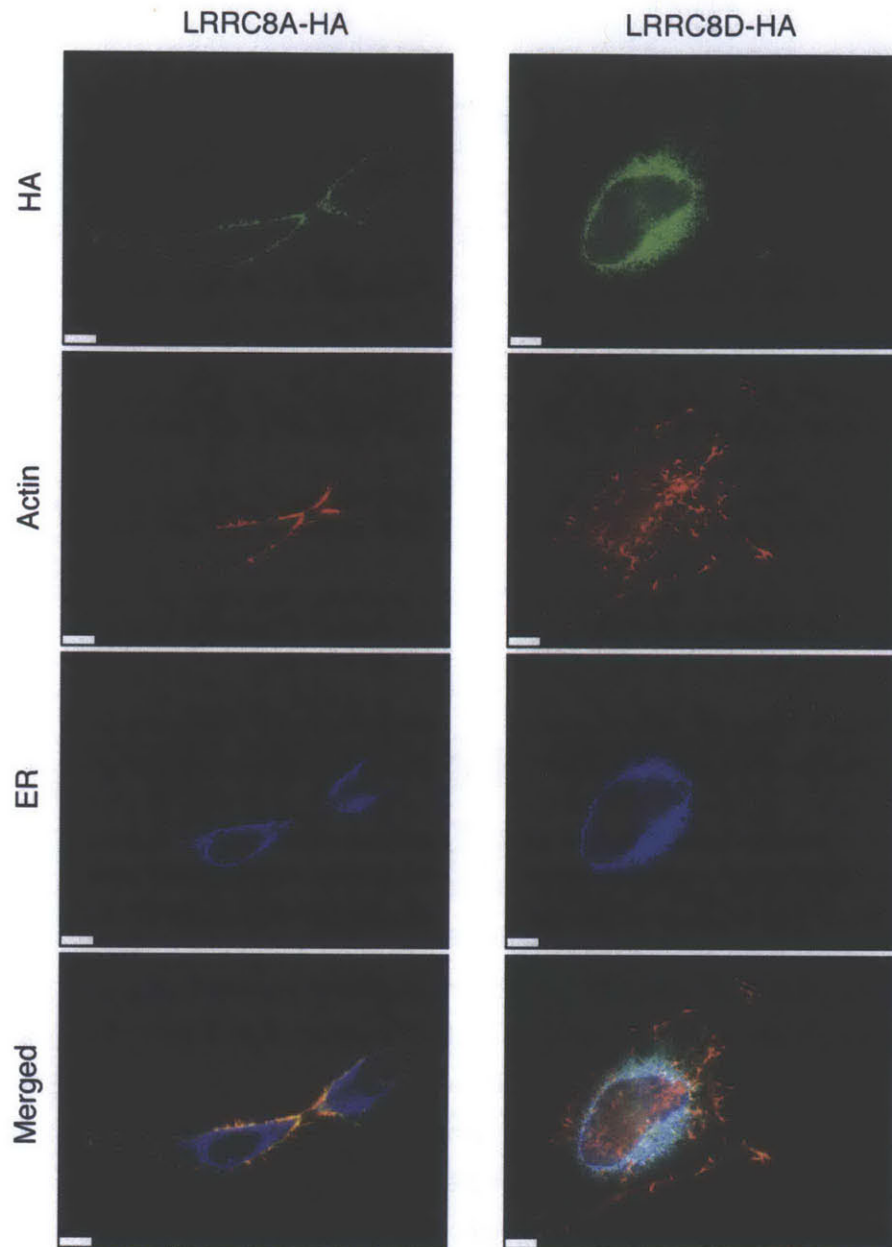
Figure 3. Localization of LRRC8A and LRRC8D.

Hela cells stably expressing human LRRC8A or LRRC8D C-terminally tagged with a HA epitope tag were stained for HA, the ER, and actin and examined by confocal microscopy. Images are representative of three independent experiments. Scale bar, 7 µm.
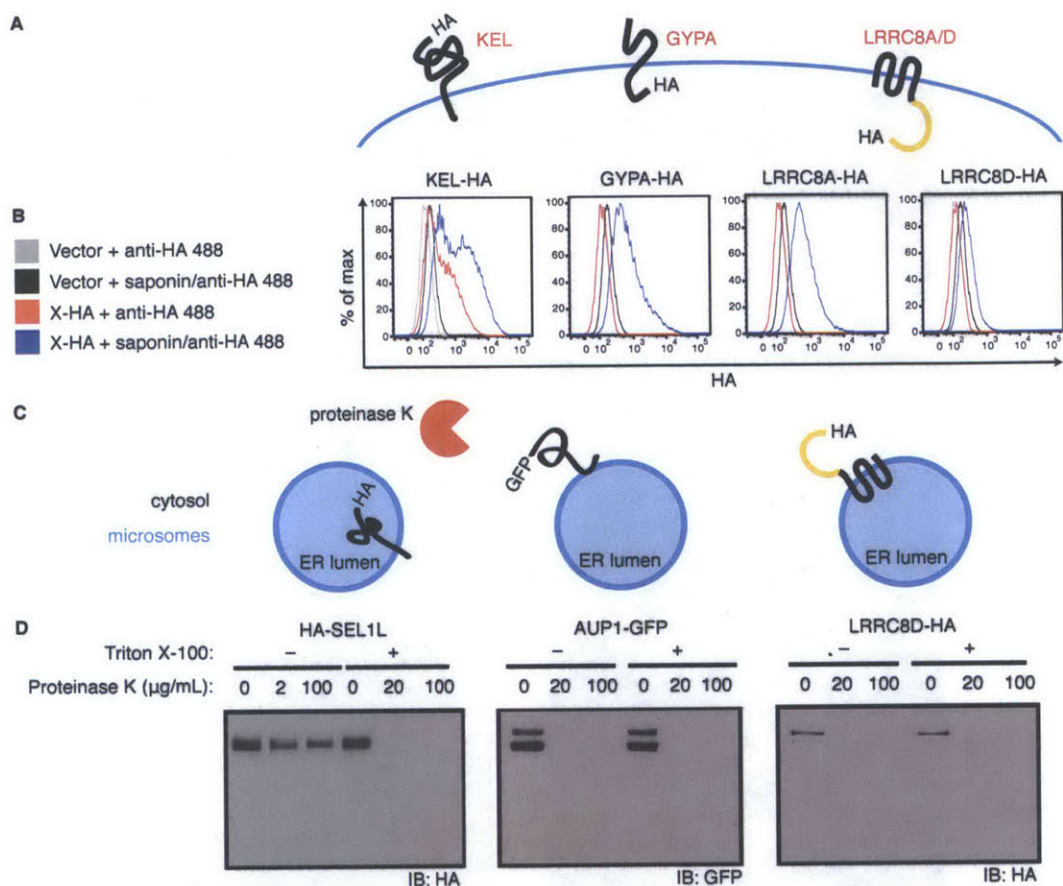
Figure 4. Topology of LRRC8A and LRRC8D.

A, Schematic depicting the topology of KEL-HA and GYPA-HA at the plasma membrane. Also depicted are the predicted topology of LRRC8A- and LRRC8D-HA at the plasma membrane based upon results in (B). B, Hela cells stably expressing either KEL-HA, GYPA-HA, LRRC8A-HA, LRRC8D-HA, or empty vector were incubated with Alexa Fluor 488-conjugated anti-HA in the absence or presence of saponin. C, Schematic depicting the experimental set-up in (D), the topology of HA-SEL1L and AUP1-GFP in the ER, and the predicted topology of LRRC8D-HA based upon results in (D). D, HA-SEL1L, AUP1-GFP, and LRRC8D-HA were transiently expressed in 293T cells. A microsome-containing fraction from these cells was exposed to proteinase K in the absence or presence of triton X-100 followed by immunoblot analysis. Results are representative of two (B) and three (D) independent experiments.

Figure 5. LRRC8D interacts with LRRC8A, B, and C.

293T cells were transiently transfected with murine LRRC8A-Myc, LRRC8B-V5, LRRC8C-Flag, and LRRC8D-HA. +, indicates constructs were co-expressed in the same cells. /, indicates constructs were independently expressed in separate cells and the lysates were combined post-lysis as a control. Blots are representative of two independent experiments.

Immunoprecipitated Protein	LRRC8D-HA		LRRC8A-HA	
	# Unique Peptides	% Coverage	# Unique Peptides	% Coverage
LRRC8D	31	41	19	27
LRRC8A	15	20	32	40
LRRC8C	10	14	15	20
serine hydroxymethyltransferase 2	7	16	6	12
carbamoyl-phosphate synthetase 2, aspartate transcarbamylase, and dihydroorotase	7	4.2	3	2.7
heterogeneous nuclear ribonucleoprotein A/B	6	18	4	14
60S acidic ribosomal protein P0	5	23	4	21
ADP/ATP translocase 2	5	14	3	11
aldehyde dehydrogenase 2	4	10	7	17
aspartate aminotransferase, mitochondrial	4	12	2	5.1

Table 1. Identification of potential LRRC8A and LRRC8D interacting partners. Lysates from RAW 264.7 macrophages stably expressing murine LRRC8A-HA, LRRC8D-HA, or empty vector were incubated with anti-HA agarose beads and the immunoprecipitated proteins were identified by mass spectrometry. Displayed are proteins that were immunoprecipitated from both LRRC8A-HA- and LRRC8D-HA-containing lysates, but not from the empty vector control. Proteins are listed in order of the number of unique peptides identified.

Materials and Methods

Constructs

cDNA was obtained from either RAW 264.7 macrophages or KBM7 cells for use as a cloning template. Murine LRRC8A-myc, LRRC8A-HA, LRRC8B-V5, LRRC8C-Flag, and LRRC8D-HA were cloned into LRCX vectors (Clontech). Human LRRC8A-myc, LRRC8B-V5, LRRC8C-Flag, and LRRC8D-HA, and LRRC8E-6xHis-T7 were cloned into pCDH vectors (System Biosciences). Human KEL-myc-LPETG-HA and human myc-GYPA-LPETG-HA were cloned into pCDH vectors. The HA-SEL1L and AUP1-GFP constructs were previously described in [15].

Isolation and characterization of LRRC8D mutant clones

The isolation of mutant clones has been previously described [18]. In brief, a subset of the survivors from the screen was FACS sorted into 96 well plates such that no more than a single cell was plated per well [10]. Clones were expanded and then assayed for a gene-trap insertion in the *LRRC8D* locus by PCR using the following primers: 5'-TCTCCAAATCTCGGTGGAAC-3' and 5'-CCAGACTAAACATCTCAGAACTCG-3'. To confirm that the cells were truly clonal and to confirm the absence of the wild-type DNA locus, a PCR was performed with the following primers: 5'-GGATCTCTCTAGCTCTTTCTCTCC-3' and 5'-CCAGACTAAACATCTCAGAACTCG-3'. Absence of the *LRRC8D* transcript in the isolated mutant clones was determined by RT-PCR. Total RNA was isolated using the RNeasy Mini kit (QIAGEN) and reverse transcribed using the SuperScriptTM III First-Strand synthesis system (Invitrogen). Amplification of *LRRC8D* was performed using the following primers: 5'-CGCCGTGGTTCCAGCCTCC-3' and 5'-CGCATGCTGTCTCAGACAACGC-3'and amplification of *GAPDH* was performed using the following primers: 5'-GCCTCCTGCACCACCAACTGC-3' and 5'-CCACTGACACGTTGGCAGTGGG-3'.

Antibodies

Anti-HA affinity matrix (Roche 11815016001), anti-HA HRP (Roche #12013819001), Alexa Fluor 488-conjugated anti-HA antibody (Life Technologies A-21287), anti-FLAG

M2 affinity gel (Sigma A2220), anti-FLAG HRP (Sigma A8592), anti-myc sepharose beads (Cell Signaling #3400), anti-V5 antibody (Life Technologies R96025), anti-V5 HRP (Life Technologies R96125), anti-actin (BD #612656), HRP-conjugated sheep anti-mouse IgG (GE NXA931), anti-calnexin (Santa Cruz sc11397), goat anti-Rb Alexa Fluor 568 (Molecular Probes A11011), Alexa Fluor 647 phalloidin (Life Technologies A22287).

Cell viability assay

CellTiter-Glo Luminescent Cell Viability Assay (Promega) was used to quantify the cell viability. 200,000 cells were seeded per well in clear-bottom 96-well plates (BD or Costar) in IMDM or IMDM supplemented with varying concentrations of Blasticidin S☐HCl (Invivogen), TNF-α (Invivogen), and FSL-1 (Invivogen).

Transfection and viral transduction

Transfections were accomplished using Trans-IT 293 (Mirus) for 293T cells. Transductions were accomplished using the pPACKH1 HIV Lentivector Packaging Kit (System Biosciences) according to its protocol.

Preparation of cell extracts for LC/MS analysis

4 million wild-type reporter cells, *LRRC8D^{GT1}* cells, and *LRRC8D^{GT2}* cells were treated with varying concentrations of BlaS for 3 hours in triplicate. Cells were washed two times in ice-cold IMDM and one time in ice-cold, filtered 0.9% NaCl. 200 uL of ice-cold extraction buffer (40% acetonitrile, 40% methanol, 20% water, 10 ng/mL phenylalanine-d$_8$, 10 ng/mL valine- d$_8$) was added to each cell pellet. Extracts were vortexed for 30 seconds and then spun at 14,000 rpm for 10 minutes at 4 °C in a table-top centrifuge. Extract supernatants were transferred to new eppendorf tubes and stored at -80 °C until analysis. Extract solvents were obtained from Fisher Scientific and were Optima LC/MS grade and phenylalanine-d$_8$ and valine- d$_8$ were purchased from Cambridge Isotope Laboratories.

LC analysis

Solvents were obtained from Fisher Scientific and were Optima LC/MS grade except where otherwise specified. An UltiMate 3000 UPLC system with autosampler (Dionex)

was used for this study. Biological triplicate samples (typically 10 μL) were injected onto a Luna-NH$_2$ 2 x 150 mm (3 μm particle size) column (Phenomenex) equipped with an inline particulate filter. The mobile phases were 5 mM ammonium acetate, 0.2% ammonium hydroxide, pH 9.9 (mobile phase A) and acetonitrile (mobile phase B). The flow rate was 0.25 ml/min and the column temperature was held at 15°C. The column was eluted with a gradient from 90% to 10% mobile phase B over 20 min., held at 10% mobile phase B for 5 min., returned to 90% mobile phase B over 1 min., and re-equilibrated at 90% mobile phase B for 8 min.

MS analysis

The UPLC system was coupled to a QExactive orbitrap mass spectrometer equipped with a HESI II probe (Thermo Fisher Scientific) operating in positive ion mode. The spray voltage was set to 3.9 kV, the heated capillary was held at 335°C, and the HESI probe was held at 350°C. The sheath gas flow was set to 35 units, the auxiliary gas flow was set to 7 units, and the sweep gas flow was set to 0 units. External mass calibration was performed every 7 days. The MS data acquisition was performed by targeted Selected Ion Monitoring (tSIM) of the metabolites of interest (BlaS and phenylalanine-d$_8$ as an internal standard), with the resolution set at 70,000, the AGC target at 5x10^4, the maximum injection time at 120 msec, and the isolation window at 1.0 m/z. Quantitation of the data was performed with XCalibur QuanBrowser 2.2 (Thermo Fisher Scientific) using a 5 ppm mass tolerance. Pure BlaS samples in extraction buffer (half-log serial dilution, 1 nM – 1 μM) were analyzed to confirm chromatographic retention times and generate standard curves for quantitation of each analytical batch. The limit of detection in sample matrix was 5 nM, as determined by addition of increasing concentrations of BlaS to a pooled BlaS-free cell extract.

Immunofluoresence

Cells were plated on #1.5, 18 mm round cover slips in 12-well plates. 24 hours later, the cells were washed one time with PBS, fixed with 4% paraformaldehyde in PBS, washed with PBS, incubated with a quenching solution containing 20 mM glycine and 50 mM NH$_4$Cl in PBS, washed with PBS, permeabilized with saponin binding buffer (PBS containing 0.1% (v/v) saponin and 0.2% (wt/v) BSA), incubated with primary antibodies

for 1 hour, washed five times with saponin binding buffer, incubated with secondary antibodies for 1 hour, washed five times with saponin binding buffer, twice with PBS, and once with water before mounting on glass slides using ProLong Gold with dapi (Life Technologies). Images were acquired with a PerkinElmer Ultraview Spinning Disk Confocal equipped with a Hammamatsu ORCA-ER CCD camera and analyzed with Volocity acquisition software.

Coimmunoprecipitation

Cells were washed one time in ice-cold PBS before lysing with NP40 lysis buffer containing 50 mM Tris pH 7.4, 150 mM NaCl, 0.5 mM EDTA, 1% (v/v) NP40, and protease inhibitors (Roche). Lysate concentrations were measured by Bradford Protein Assay (Bio-Rad) and normalized. Lysates were pre-cleared by incubating them with protein G agarose beads (Sigma P3296) for 1 hour at 4 °C. Pre-cleared lysates were then incubated with either anti-HA affinity matrix, anti-V5 antibody with protein G agarose beads, anti-FLAG M2 affinity gel, or anti-myc sepharose beads for 2 hours at 4 °C. Beads were washed three times with buffer containing 50 mM Tris pH 7.4, 150 mM NaCl, 0.5 mM EDTA, and 0.1% (v/v) NP40. Beads were then boiled in sample buffer and proteins in the supernatant were resolved by SDS-PAGE.

Affinity purification and mass spectrometry

After coimmunoprecipitation, eluted samples were separated by SDS-PAGE and polypeptides were visualized by silver staining. Bands of interest were excised, digested with trypsin, and analyzed by tandem mass spectrometry.

Immunoblot analysis

Proteins were separated by SDS-PAGE, transferred to nitrocellulose membranes, blocked with 5% (wt/vol) skim milk in PBS with 0.1% (vol/vol) Tween-20 and were probed with the appropriate primary antibodies. Membranes were washed three times with PBS with 0.1% (vol/vol) Tween-20 and were incubated with horseradish peroxidase–conjugated secondary antibodies if necessary. Proteins were visualized with an enhanced chemiluminescence detection reagent. Restore PLUS Western Blot Stripping Buffer (Thermo) was used to strip the membranes between probing.

Silver stain

Proteins were fixed in polyacrylamide gel by incubating the gel in 40% (vol/vol) ethanol, 10% (vol/vol) acetic acid. The gel was washed twice in 30% (vol/vol) ethanol and once in water. The gel was then sensitized in 0.02% (wt/vol) $Na_2S_2O_3$, washed three times in water, incubated in ice-cold 0.1% (wt/vol) $AgNO_3$, washed four more times in water, and developed in 3% (wt/vol) Na_2CO_3, 0.05% (vol/vol) formaldehyde. When protein bands became sufficiently visible, the gel was washed once in water and the staining process was terminated by incubating the gel in 5% (vol/vol) acetic acid. The gel was then washed a final three times in water.

FACS analysis of protein topology

Cells were washed one time in PBS. Cells were resuspended in staining solution containing 1 ug/mL antibody and 3% inactivated fetal calf serum in PBS and incubated in the dark at 4 °C for 30 minutes. Cells were washed twice in PBS containing 3% inactivated fetal calf serum (PBS/IFS). Cells were fixed with PBS containing 4% (v/v) formaldehyde for 30 minutes at room temperature in the dark. The protocol for permeabilized cells was similar except cells were first fixed, washed twice with PBS, permeabilized with 0.5% (wt/v) saponin in PBS/IFS, stained with 1 ug/mL antibody in 0.5% (wt/v) saponin in PBS/IFS, and then washed twice with PBS/IFS.

Protease digestion of epitope-tagged proteins in microsomes

293T cells expressing epitope-tagged proteins were washed once in ice-cold PBS and then incubated for 10 minutes in hypotonic buffer containing: 20 mM Hepes-KOH, pH 7.5, 5 mM KCl, 1.5 mM $MgCl_2$, 1 mM DTT. Cells were then broken open with a dounce homogenizer. NaCl was added to the lysates for a final concentration of 150 mM NaCl. Lysates were spun at 800 xg at 4 °C for 10 minutes. The supernatant was transferred to a new tube which was then spun at 10,000 xg at 4 °C for 10 minutes. Pellets were resuspended in buffer containing: 50 mM Hepes-KOH, pH 7.5, 50 mM KOAc, 2 mM $Mg(OAc)_2$, 250 mM sucrose and this microsome-containing mixture was equally aliquoted to tubes with or without triton X-100 (final 1% v/v). Proteinase K (NEB P8102S) was then added to the samples at varying concentrations and the samples

were incubated on ice for 30 minutes. PMSF was added to deactivate proteinase K.

Sample buffer was added and the samples were boiled. Proteins were resolved by SDS-

PAGE followed by immunoblot analysis.

Acknowledgements

References

1. Smits G, Kajava AV (2004) LRRC8 extracellular domain is composed of 17 leucine-rich repeats. Mol Immunol 41: 561–562. doi:10.1016/j.molimm.2004.04.001.

2. Abascal F, Zardoya R (2012) LRRC8 proteins share a common ancestor with pannexins, and may form hexameric channels involved in cell-cell communication. Bioessays. doi:10.1002/bies.201100173.

3. Sawada A, Takihara Y, Kim JY, Matsuda-Hashii Y, Tokimasa S, et al. (2003) A congenital mutation of the novel gene LRRC8 causes agammaglobulinemia in humans. J Clin Invest 112: 1707–1713. doi:10.1172/JCI18937.

4. Tominaga K, Kondo C, Kagata T, Hishida T, Nishizuka M, et al. (2004) The novel gene fad158, having a transmembrane domain and leucine-rich repeat, stimulates adipocyte differentiation. J Biol Chem 279: 34840–34848. doi:10.1074/jbc.M312927200.

5. Hayashi T, Nozaki Y, Nishizuka M, Ikawa M, Osada S, et al. (2011) Factor for adipocyte differentiation 158 gene disruption prevents the body weight gain and insulin resistance induced by a high-fat diet. Biol Pharm Bull 34: 1257–1263.

6. Bella J, Hindle KL, Lovell SC, McEwan PA (2008) The leucine-rich repeat structure. Cell Mol Life Sci 65: 2307–2333. doi:10.1007/s00018-008-8019-0.

7. Penuela S, Gehi R, Laird DW (2013) The biochemistry and function of pannexin channels. Biochim Biophys Acta 1828: 15–22. doi:10.1016/j.bbamem.2012.01.017.

8. Chekeni FB, Elliott MR, Sandilos JK, Walk SF, Kinchen JM, et al. (2010) Pannexin 1 channels mediate "find-me" signal release and membrane permeability during apoptosis. Nature 467: 863–867. doi:10.1038/nature09413.

9. Qu Y, Misaghi S, Newton K, Gilmour LL, Louie S, et al. (2011) Pannexin-1 is required for ATP release during apoptosis but not for inflammasome activation. The Journal of Immunology 186: 6553–6561. doi:10.4049/jimmunol.1100478.

10. Lee CC, Carette JE, Brummelkamp TR, Ploegh HL (2013) A Reporter Screen in a Human Haploid Cell Line Identifies CYLD as a Constitutive Inhibitor of NF-κB. PLoS ONE 8: e70339. doi:10.1371/journal.pone.0070339.

11. Birsoy K, Wang T, Possemato R, Yilmaz OH, Koch CE, et al. (2013) MCT1-mediated transport of a toxic molecule is an effective strategy for targeting glycolytic tumors. Nat Genet 45: 104–108. doi:10.1038/ng.2471.

12. Reiling JH, Clish CB, Carette JE, Varadarajan M, Brummelkamp TR, et al. (2011)

A haploid genetic screen identifies the major facilitator domain containing 2A (MFSD2A) transporter as a key mediator in the response to tunicamycin. Proc Natl Acad Sci USA 108: 11756–11765. doi:10.1073/pnas.1018098108.

13.   Redman CM, Lee S (1995) The Kell blood group system. Transfus Clin Biol 2: 243–249.

14.   Chasis JA, Mohandas N (1992) Red blood cell glycophorins. Blood 80: 1869–1879.

15.   Mueller B, Klemm EJ, Spooner E, Claessen JH, Ploegh HL (2008) SEL1L nucleates a protein complex required for dislocation of misfolded glycoproteins. Proc Natl Acad Sci USA 105: 12325–12330. doi:10.1073/pnas.0805371105.

16.   Klemm EJ, Spooner E, Ploegh HL (2011) Dual role of ancient ubiquitous protein 1 (AUP1) in lipid droplet accumulation and endoplasmic reticulum (ER) protein quality control. Journal of Biological Chemistry 286: 37602–37614. doi:10.1074/jbc.M111.284794.

17.   Spandl J, Lohmann D, Kuerschner L, Moessinger C, Thiele C (2011) Ancient ubiquitous protein 1 (AUP1) localizes to lipid droplets and binds the E2 ubiquitin conjugase G2 (Ube2g2) via its G2 binding region. Journal of Biological Chemistry 286: 5599–5606. doi:10.1074/jbc.M110.190785.

18.   Guimaraes CP, Carette JE, Varadarajan M, Antos J, Popp MW, et al. (2011) Identification of host cell factors required for intoxication through use of modified cholera toxin. J Cell Biol 195: 751–764. doi:10.1083/jcb.201108103.

Chapter 4

A Human Haploid Reporter Screen for Genes Required to Activate NF-κB in Response to TLR2/6 Signaling

Clarissa C. Lee [1,2], Jan E. Carette [1,3], Thijn R. Brummelkamp [1,4], Hidde L. Ploegh [1,2]

[1] Whitehead Institute for Biomedical Research, Cambridge, MA, USA

[2] Department of Biology, Massachusetts Institute of Technology, Cambridge, MA, USA

[3] Present address: Department of Microbiology and Immunology, Stanford University School of Medicine, Stanford, CA, USA

[4] Present address: Department of Biochemistry, Netherlands Cancer Institute, Amsterdam, The Netherlands

C.C.L. performed all experiments. J.E.C. cloned the gene-trap vector and assisted with the design of the screen and the analysis of the sequencing data.

Abstract

Forward genetic screens in human haploid cells have been limited mostly to the identification of genes that mediate cell death in response to a lethal agent. Here, we perform a reporter screen in the near-haploid KBM7 cell line to identify genes required for NF-κB-mediated transcription in response to the TLR2/6 ligand, FSL-1. Our screen identified 41 significant hits, including 5 known components of the TLR2/6 pathway. Fourteen hits have established or predicted roles in transcriptional regulation and may provide insight on how NF-κB promotes a specific transcriptional program in response to FSL-1. Seven of the genes encode protein or non-coding RNAs of unknown or poorly characterized function. Also identified as a candidate TLR2/6 pathway component was *TRIM8*, an E3 ubiquitin ligase with strong links to NF-κB regulation.

Introduction

The recent development of human haploid genetic screens offers an attractive alternative to RNAi-based screens which are often hampered by off-target effects and incomplete knock-down. Most haploid screens thus far have relied on the selection of mutants that are resistant to an agent that is lethal to wild-type cells [1-9]. While this has resulted in the identification of host factors that are exploited by pathogens and transporters that are required for the import of toxic molecules, the ability to dissect other types of biological processes has been limited, mostly because mutations in other cellular processes do not generally result in a cellular phenotype that is easily observable and selectable. To expand the types of biological pathways that can be studied using haploid genetic screens we previously developed a screen using a transcriptional reporter in conjunction with selection for a lethal phenotype [10]. In order to identify constitutive inhibitors of the transcription factor NF-κB, we created a haploid reporter cell line that expressed the blasticidin S resistance gene (*BSR*) under the control of a NF-κB transcriptional response element and selected for cells that could survive in the presence of blasiticidin, an antibiotic. While we were able to identify and validate *CYLD* as a constitutive inhibitor of NF-κB, the results of the screen were complicated by the unintended selection of mutants that had mutations in genes required for the import of blasticidin. The use of a NF-κB-GFP transcriptional reporter eliminates this confounding issue and provides the ability to screen for both activators and inhibitors of NF-κB.

NF-κB is activated by the engagement of a wide variety of receptors including Toll-like receptors (TLRs) [11]. TLRs are germline-encoded pattern recognition receptors (PRRs) that play a crucial role in pathogen sensing and subsequent initiation of innate immune responses to defend the host [12-14]. At the cell surface TLR2 and TLR6 form a heterodimer that recognizes diacylated lipopeptides from Gram-positive bacteria. Upon recognition of its ligand, TLR2/6 recruits the adapter molecules TIRAP and MyD88 to initiate downstream signaling events that ultimately result in the activation of the IKK complex, which targets IκB for degradation, allowing NF-κB to translocate to the nucleus and drive the expression of inflammatory cytokines. While much is known about the

signaling events that occur between ligand engagement and NF-κB activation, it is still unclear exactly how the IKK complex is activated [11]. It is also poorly understood how NF-κB mediates distinct cellular responses to different stimuli [15].

Here we performed a reporter haploid screen to identify genes required for NF-κB-mediated transcription in response to the TLR2/6 ligand, FSL-1. Among the hits identified in the screen is *TRIM8*, an E3 ubiquitin ligase required for NF-κB activity in response to TNF and IL-1β [16,17]. The screen identified many additional hits with a role in transcriptional regulation. Future work to validate the requirement of these genes in NF-κB-mediated transcription may provide insight on how NF-κB transcriptional specificity is determined.

Results and Discussion

To identify components required for TLR2/6 signaling, we transduced KBM7 cells, which are haploid for all chromosomes but chromosome 8, with a reporter construct that contains a NF-κB transcriptional response element (TRE) and a minimum cytomegalovirus (mCMV) promoter upstream of dscGFP, a gene that encodes a natural green monomeric GFP-like protein from a copepod, modified such that the half-life of the mature protein is ~1 hour (Fig. 1). Thus upon stimulation of cells with FSL-1, a synthetic diacylated lipoprotein, active transcription of NF-κB can be measured and cells containing inactivating mutations in genes normally required for NF-κB activation in the TLR2/6 signaling pathway can be isolated from wild-type cells by sorting for GFP negative cells. Transduction of KBM7 cells with the NF-κB-GFP reporter resulted in a polyclonal population of cells that individually displayed different reporter activation properties (Fig. 2). Since cells containing mutations in genes required for TLR2/6 signaling are isolated in the screen by their inability to turn on the reporter in response to FSL-1, it is essential that the reporter cell line selected for the screen robustly turns on the NF-κB-GFP reporter in response to a stimulus. One such clone that is non-fluorescent at steady-state, but that is strongly GFP-positive after FSL-1 stimulation was chosen for the screen (Fig. 2). The NF-κB-GFP reporter cell line was then mutagenized with a retroviral gene-trap vector containing a RFP marker, using an established protocol that generally yields a library containing mutations in approximately 98% of genes expressed in KBM7 cells [8]. Mutagenized NF-κB reporter cells were then stimulated with FSL-1 and sorted for a mutant population (RFP positive, GFP negative cells) and a control population (RFP positive cells). To identify gene-trap insertion sites, genomic DNA was harvested from both populations and the DNA sequences that flank gene-trap insertion sites were amplified, sequenced in parallel, and mapped to the human genome.

Of the 41 genes that appeared in the screen with a significant enrichment (p-value<0.05) of gene trap mutations in the mutant population compared to the control population, 5 are known components of the TLR2/6 pathway: *CNPY3* also known as *PRAT4A, IRAK1, IRAK4, MYD88,* and *TIRAP* (Fig. 3, Table 1) [12,18]. Fourteen of the significant hits have a gene summary in PubMed or a protein summary in UniProt

suggestive of a role in transcriptional regulation: *BAP1, BRMS1, CBX3, GATA2, LYL, MAZ, NCOA6, NFYA, SMARCA4, SPI1, STAT5A, STAT6, TP53*, and *WT1*. Three genes encode proteins of unknown function: *C10orf54, C14orf159, LRRC14* and four genes encode poorly characterized non-coding RNAs: *DKFZP686I15217, LOC100289341, MALAT1, NCRNA00095*. Of the remaining hits, one in particular, *TRIM8*, stands out as a putative member of the TLR2/6 pathway.

TRIM8 belongs to the tripartite motif-containing (TRIM) protein family whose members are characterized by the N-terminal possession of a RBCC motif [19]. The RBCC motif contains a RING domain, which often confers E3 ubiquitin ligase activity, followed by one or two B-box domains, which is then almost always followed by a coiled-coil domain that mediates homeric and heteromeric interactions [19]. Many members of the TRIM family are expressed in response to IFNs and have roles in innate immunity [19]. Several TRIM family members have been implicated in negative regulation of TLR signaling [20-22], but none have been implicated in positive regulation of TLR signaling. TRIM8 is required for NF-κB activation in response to TNF and IL-1β [16,17]. Knock-down of TRIM8 reduces K63-linked polyubiquitination of TAK1 and phosphorylation of TAK1, IKKα/β, and IκBα in response to TNF and IL-1β [17]. Given that these signaling components are also downstream of TLR2/6 engagement with FSL-1 and given the appearance of TRIM8 in our screen, it is highly likely that TRIM8 is a component of the TLR2/6 signaling pathway though this remains to be explicitly demonstrated.

It has become increasingly clear that recruitment of NF-κB to target genes and NF-κB induced transcription is a complex process that may require the coordinated function of many proteins including other transcription factors and co-activators in the context of a favorable chromatin environment [23,24]. These layers of regulation may provide specificity for distinct NF-κB-mediated transcriptional programs in different cell types and in response to different stimuli. Fittingly, approximately a third of the screen hits have a putative or established role in transcriptional regulation. Among this group are transcription factors like *GATA2, NFYA, SPI1, STAT5A, STAT6*, and *WT1* that have been previously linked to NF-κB function. GATA2 is required for NF-κB signaling in the absence of stimulus in non-small cell lung cancer cell (NSCLC) lines containing *KRAS* mutations [25]. Both NFYA and NF-κB have been shown to bind to the endogenous promoter of *Hspa1a* and *SND1* and are thought to work together along with other

transcription factors to regulate *Hspa1a* transcription [26,27]. Sp1, also known as PU.1, interacts with NF-κB to coordinate transcription of *HIV-1*, *MCP-1*, and *SOD2* [28-30]. A role for Sp1 in priming enhancers that confer cell-specific NF-κB-dependent gene expression has been described [31]. NF-κB interacts with both STAT5A and STAT6 and it is thought that the interaction between NF-κB and STATs may promote synergy between signaling pathways that activate the two families of transcription factors [32-34]. WT1 and NF-κB interact with each other and cooperatively regulate the expression of *NPHS1* and *KIRREL2* [35]. Also in this group of hits are *NCOA6* also known as *ASC-2*, a transcriptional co-activator and *SMARCA4* also known as *BRG1*, a member of the SWI/SNF chromatin remodeling complexes. Both NCoA6 and Brg1 interact with NF-κB and Brg1/Brm-dependent chromatin remodeling is required for most late-activated NF-κB-dependent genes [36-39]. Validation of these hits by RNAi knockdown or CRISPR/Cas genome engineering will be required to determine if they are indeed necessary for NF-κB-mediated transcription in response to TLR2/6 signaling. Since the NF-κB-GFP reporter in the KBM7 reporter cell line may be integrated in the genome in a non-physiologial context, it will be important to perform the validation in additional cell lines. ChIP-Seq of NF-κB and the screen hits after FSL-1 stimulation would also be informative.

While the screen identified 5 of the known components of the TLR2/6 signaling pathway, a surprising number of the known pathway components were not identified including the receptors themselves. Relatively few (6 to 12) unique, inactivating gene-trap insertion sites were sequenced in *TLR2* or *TLR6* in the selected and unselected populations suggesting that increasing the number of mutated cells in future screens may be required. Additional measures that may increase signal-to-noise include performing successive fluorescence activated cell sorting, optimizing the selection cut-off, and generating a new reporter cell line that contains multiple reporters, each expressing a different fluorescent protein, and sorting for mutant cells that do not express any of the reporters.

Also not identified as significant hits in the screen were NF-κB transcription factors (*RELA, RELB, REL, NFKB1, NFKB2*) and components of the IKK complex (*IKBKG, IKBKB, CHUK*). Few mutations were sequenced in the NF-κB transcription factors and no gene-trap insertion sites were sequenced in *NFKB2* or *RELB* in the

unselected population suggesting that either *NFKB2* and *RELB* are extremely difficult to mutagenize or more likely, that they are essential genes for the survival of KBM7 cells. An absence in myeloid cells was not observed in *NFKB2*^{-/-} or *RELB*^{-/-} mice suggesting that NF-κB signaling is not essential to the survival of normal myeloid cells [40-43]. The KBM7 cell line, however, was derived from a patient with chronic myeloid leukemia (CML) and possesses the *BCR-ABL* fusion oncogene, a hallmark of CML [9].

Overexpression of BCR-ABL in cell lines increases NF-κB-dependent gene expression and pharmacological inhibition of the NF-kB pathway decreases survival of Bcr-Abl-expressing cell lines [44-46]. While the NF-κB-GFP reporter cells show little if any GFP signal at steady-state, it is possible that low, persistent activity of NF-κB occurs and that this activity is required for promoting the expression of genes required for cell survival, while leaving the NF-κB-GFP reporter untouched. Thus it may be difficult to identify components that are generally and directly required for NF-κB function (e.g. NF-κB transcription factors, IKK complex) using haploid reporter screens. However, as demonstrated by the appearance of known components of the TLR2/6 signaling pathway in our screen, signaling components that are further upstream of NF-κB activation and/or genes that are required for NF-κB activity in particularly signaling contexts can be identified in haploid reporter screens. Signaling pathways that converge on transcription factors other than NF-κB may be more amenable to genetic dissection in KBM7 cells. In principle, a similar screen could be done with fluorescent reporters under different transcription response elements (TRE). As mentioned earlier, it may be useful and interesting to generate a reporter cell line that contains multiple fluorescent reporters either under the same TRE (to look for concordance of signal) or under different TREs (to study cross-talk between signaling pathways).

Figure and Tables
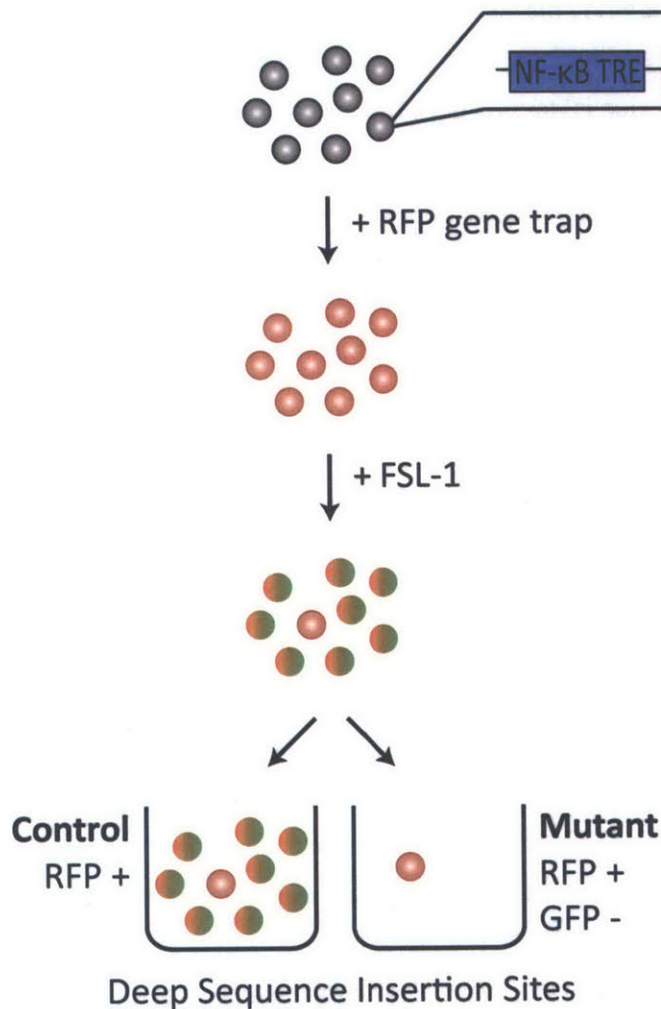
Figure 1. Schematic for a reporter haploid genetic screen for components of the TLR2/6 signaling pathway. KBM7 cells were transduced with a reporter containing a NF-κB transcriptional response element (TRE) and a minimum CMV (mCMV) promoter upstream of a modified green fluorescent protein gene from copepod (dsc*GFP*). A clonal reporter cell line was mutagenized by infection with a gene-trap virus containing a red fluorescent protein (RFP) marker. The mutagenized cells were stimulated with FSL-1. The indicated control population and mutant population were sorted by FACS and expanded. DNA was extracted and DNA sequences flanking gene-trap insertion sites were amplified and sequenced in parallel.
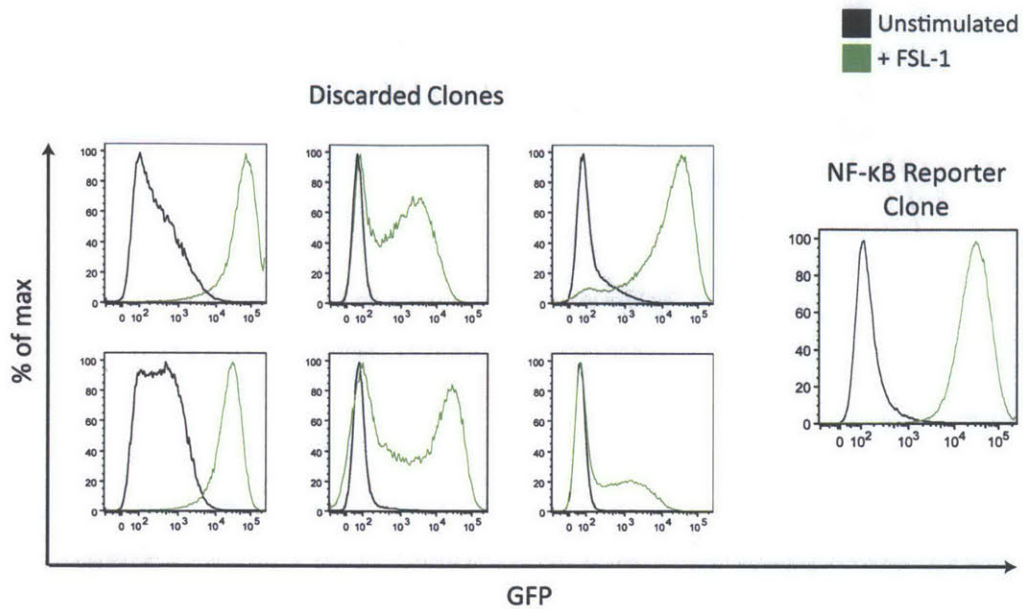
Figure 2. Isolation of a NF-κB Reporter Clone. KBM7 cells were transduced with a NF-κB–GFP reporter. Clones were then stimulated with 100-200 ng/mL FSL-1 for 24-30 hours. On the left, are plots for clones that were discarded because their GFP signal in unstimulated and stimulated conditions was not ideal. On the right, is the FACS plot for the NF-κB reporter clone that was selected for the screen.

Figure 3. Components of the TLR2/6 signaling pathway identified in the screen.
Known components of the TLR2/6 signaling pathway are indicated, with those that showed up in the screen with a p-value<0.05 highlighted in red. Additionally, TRIM8 is placed at the point in the pathway where it likely functions.

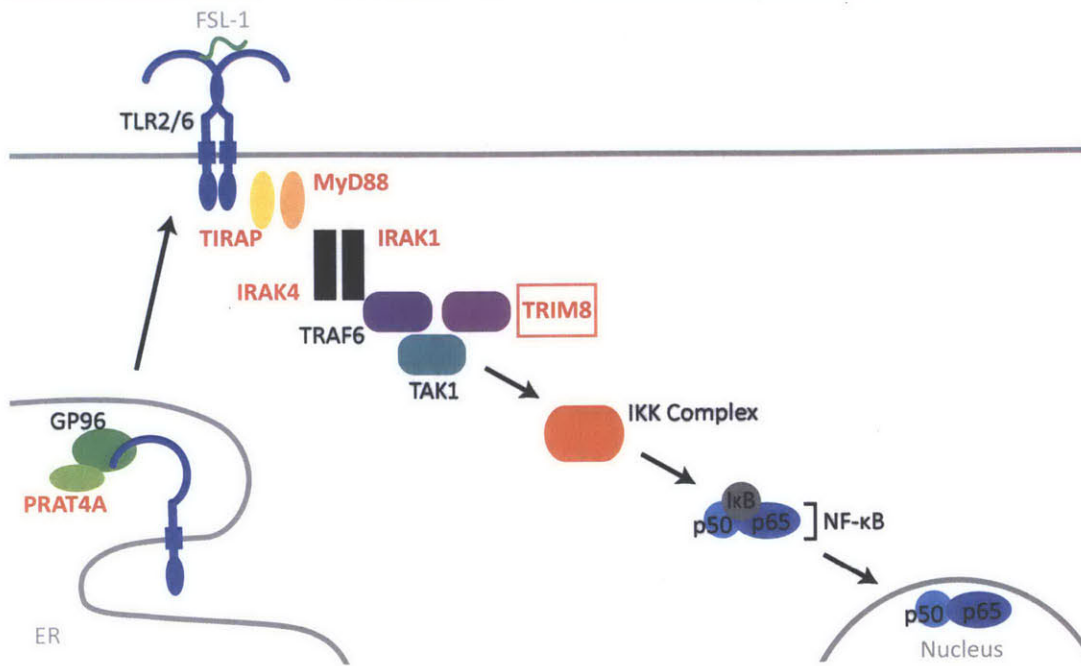| Gene name	# of inactivating mutations in gene	# of inactivating mutations in all other genes	# of all mutations in gene in control dataset	# of all mutations in all other genes in control dataset	p-value corrected for FDR
RANBP1	72	70395	53	302654	1.02E-17
TP53	137	70330	235	302472	2.11E-12
CNPY3	42	70425	24	302683	6.43E-12
WT1	315	70152	790	301917	1.43E-11
IRAK1	39	70428	23	302684	6.78E-11
BAP1	25	70442	7	302700	1.15E-09
SPN	80	70387	128	302579	5.72E-08
MAZ	40	70427	40	302667	4.60E-07
TIRAP	21	70446	11	302696	1.06E-05
MALAT1	67	70400	115	302592	1.16E-05
LINGO3	23	70444	15	302692	1.66E-05
IL17RE	29	70438	29	302678	7.86E-05
NCOA6	18	70449	11	302696	0.000298351
STAT6	25	70442	24	302683	0.000313387
SMARCA4	31	70436	39	302668	0.000709138
MYD88	15	70452	9	302698	0.002058787
LYL1	33	70434	49	302658	0.003726355
DDX28	24	70443	28	302679	0.00378369
FUT7	36	70431	57	302650	0.00378369
CBX3	29	70438	40	302667	0.003961094
NFYA	33	70434	50	302657	0.003961094
SPI1	38	70429	63	302644	0.003961094
C10orf54	80	70387	189	302518	0.005286266
FBXL15	20	70447	21	302686	0.006207301
TRIM8	18	70449	17	302690	0.006313529
LOC100289341	26	70441	35	302672	0.006873772
DKFZP686I15217	35	70432	61	302646	0.015577473
CCRL2	8	70459	2	302705	0.018804671
BRMS1	7	70460	1	302706	0.020136703
STAT5A	33	70434	57	302650	0.020136703
GATA2	31	70436	52	302655	0.021518852
C14orf159	51	70416	112	302595	0.033126454
IRAK4	10	70457	6	302701	0.045949902
MAEA	8	70459	3	302704	0.045949902
NCRNA00095	10	70457	6	302701	0.045949902
CSE1L	20	70447	27	302680	0.046580335
C8orf58	21	70446	30	302677	0.049546216
CORO1A	28	70439	48	302659	0.049546216
LRRC14	23	70444	35	302672	0.049546216
PTPN7	28	70439	48	302659	0.049546216
S1PR4	19	70448	25	302682	0.049546216

Table 1. Significant hits in a screen for TLR2/6 signaling components. Genes with a significant enrichment (p-value<0.05) of gene trap mutations in the mutant population compared to the control population are displayed. Genes that are already confirmed TLR2/6 signaling components are highlighted in blue. TRIM8, a putative member of the pathway, is highlighted in red.

Materials and Methods

Cells

KBM7 cells were grown in Iscove's modified Dulbecco's medium (IMDM) with 10% heat-inactivated fetal serum (IFS). A NF-κB reporter cell line was created by transducing KBM7 cells with pTRH1-NF-κB-dscGFP (System Biosciences) and single cells were sorted into individual wells of 96 well plates. A clone that remained haploid and that activated the reporter only when stimulated with FSL-1 was selected for the screen.

Flow cytometry

Analysis was done using a BD LSR II flow cytometer and FloJo software. Sorting was done using a FACSAria IIU or a MoFlo2.

Reporter haploid genetic screen

The screening procedure has been described previously [4-10]. Briefly, 100 million NF-κB reporter cells were infected with gene-trap retrovirus containing a RFP marker to create a mutagenized library. Seven days post-infection, 150 million mutagenized cells were stimulated with 250 ng/mL FSL-1 and then sorted for a mutant population (RFP positive, GFP negative cells) and a control population (RFP positive cells). Cells were allowed to expand for approximately 2 weeks before harvest.

Sequence analysis of gene-trap insertion sites

The mapping of the insertion sites was done as previously described [8]. In short, DNA sequences flanking gene-trap insertions sites were amplified using a linear amplication PCR (LAM-PCR) protocol followed by sequencing using the Genome Analyzer platform (Illumina). The sequences were then aligned to the human genome. The number of inactivating mutations (that is, sense orientation or present in exon) per individual gene was counted as well as the total number of inactivating insertions for all genes. Enrichment of a gene in the screen was calculated by comparing how often that gene was mutated in the screen compared to how often the gene carries an insertion in the control data set. For each gene, a P-value (corrected for false discovery rate) was calculated using the one-sided Fisher exact test.

References

1.   Jae LT, Raaben M, Riemersma M, van Beusekom E, Blomen VA, et al. (2013) Deciphering the glycosylome of dystroglycanopathies using haploid screens for lassa virus entry. Science 340: 479–483. doi:10.1126/science.1233675.

2.   Birsoy K, Wang T, Possemato R, Yilmaz OH, Koch CE, et al. (2013) MCT1-mediated transport of a toxic molecule is an effective strategy for targeting glycolytic tumors. Nat Genet 45: 104–108. doi:10.1038/ng.2471.

3.   Reiling JH, Clish CB, Carette JE, Varadarajan M, Brummelkamp TR, et al. (2011) A haploid genetic screen identifies the major facilitator domain containing 2A (MFSD2A) transporter as a key mediator in the response to tunicamycin. Proc Natl Acad Sci USA 108: 11756–11765. doi:10.1073/pnas.1018098108.

4.   Rosmarin DM, Carette JE, Olive AJ, Starnbach MN, Brummelkamp TR, et al. (2012) Attachment of Chlamydia trachomatis L2 to host cells requires sulfation. Proc Natl Acad Sci USA 109: 10059–10064. doi:10.1073/pnas.1120244109.

5.   Guimaraes CP, Carette JE, Varadarajan M, Antos J, Popp MW, et al. (2011) Identification of host cell factors required for intoxication through use of modified cholera toxin. J Cell Biol 195: 751–764. doi:10.1083/jcb.201108103.

6.   Papatheodorou P, Carette JE, Bell GW, Schwan C, Guttenberg G, et al. (2011) Lipolysis-stimulated lipoprotein receptor (LSR) is the host receptor for the binary toxin Clostridium difficile transferase (CDT). Proc Natl Acad Sci USA 108: 16422–16427. doi:10.1073/pnas.1109772108.

7.   Carette JE, Raaben M, Wong AC, Herbert AS, Obernosterer G, et al. (2011) Ebola virus entry requires the cholesterol transporter Niemann–Pick C1. Nature 477: 340–343. doi:10.1038/nature10348.

8.   Carette JE, Guimaraes CP, Wuethrich I, Blomen VA, Varadarajan M, et al. (2011) Global gene disruption in human cells to assign genes to phenotypes by deep sequencing. Nat Biotech 29: 542–546. doi:10.1038/nbt.1857.

9.   Carette JE, Guimaraes CP, Varadarajan M, Park AS, Wuethrich I, et al. (2009) Haploid Genetic Screens in Human Cells Identify Host Factors Used by Pathogens. Science 326: 1231–1235. doi:10.1126/science.1178955.

10.   Lee CC, Carette JE, Brummelkamp TR, Ploegh HL (2013) A Reporter Screen in a Human Haploid Cell Line Identifies CYLD as a Constitutive Inhibitor of NF-κB. PLoS ONE 8: e70339. doi:10.1371/journal.pone.0070339.

11.   Hayden MS, Ghosh S (2012) NF-κB, the first quarter-century: remarkable progress and outstanding questions. Genes & Development 26: 203–234. doi:10.1101/gad.183434.111.

12. Kawai T, Akira S (2010) The role of pattern-recognition receptors in innate immunity: update on Toll-like receptors. Nat Immunol 11: 373–384. doi:10.1038/ni.1863.

13. Akira S, Uematsu S, Takeuchi O (2006) Pathogen recognition and innate immunity. Cell 124: 783–801. doi:10.1016/j.cell.2006.02.015.

14. Takeuchi O, Akira S (2010) Pattern Recognition Receptors and Inflammation. Cell 140: 805–820. doi:10.1016/j.cell.2010.01.022.

15. Pahl HL (1999) Activators and target genes of Rel/NF-I[kappa]IB transcription factors. , Published online: 22 November 1999; I doi:101038/sjonc1203239 18: 6853–6866. doi:10.1038/sj.onc.1203239.

16. Tomar D, Sripada L, Prajapati P, Singh R, Singh AK, et al. (2012) Nucleo-Cytoplasmic Trafficking of TRIM8, a Novel Oncogene, Is Involved in Positive Regulation of TNF Induced NF-κB Pathway. PLoS ONE 7: e48662. doi:10.1371/journal.pone.0048662.

17. Li Q, Yan J, Mao A-P, Li C, Ran Y, et al. (2011) Tripartite motif 8 (TRIM8) modulates TNFα- and IL-1β-triggered NF-κB activation by targeting TAK1 for K63-linked polyubiquitination. Proc Natl Acad Sci USA 108: 19341–19346. doi:10.1073/pnas.1110946108.

18. Kawai T, Akira S (2011) Toll-like Receptors and Their Crosstalk with Other Innate Receptors in Infection and Immunity. Immunity 34: 637–650. doi:10.1016/j.immuni.2011.05.006.

19. Ozato K, Shin D-M, Chang T-H, Morse HC (2008) TRIM family proteins and their emerging roles in innate immunity. Nat Rev Immunol 8: 849–860. doi:10.1038/nri2413.

20. Zhao W, Wang L, Zhang M, Yuan C, Gao C (2012) E3 ubiquitin ligase tripartite motif 38 negatively regulates TLR-mediated immune responses by proteasomal degradation of TNF receptor-associated factor 6 in macrophages. The Journal of Immunology 188: 2567–2574. doi:10.4049/jimmunol.1103255.

21. Zha J, Han K-J, Xu L-G, He W, Zhou Q, et al. (2006) The Ret finger protein inhibits signaling mediated by the noncanonical and canonical IkappaB kinase family members. J Immunol 176: 1072–1080.

22. Shi M, Deng W, Bi E, Mao K, Ji Y, et al. (2008) TRIM30 alpha negatively regulates TLR-mediated NF-kappa B activation by targeting TAB2 and TAB3 for degradation. Nat Immunol 9: 369–377. doi:10.1038/ni1577.

23. Natoli G, Saccani S, Bosisio D, Marazzi I (2005) Interactions of NF-kappaB with chromatin: the art of being at the right place at the right time. Nat Immunol 6: 439–

445. doi:10.1038/ni1196.

24. Hoffmann A, Natoli G, Ghosh G (2006) Transcriptional regulation via the NF-κB signaling module. Oncogene 25: 6706–6716. doi:10.1038/sj.onc.1209933.

25. Kumar MS, Hancock DC, Molina-Arcas M, Steckel M, East P, et al. (2012) The GATA2 Transcriptional Network Is Requisite for RAS Oncogene-Driven Non-Small Cell Lung Cancer. Cell 149: 642–655. doi:10.1016/j.cell.2012.02.059.

26. Armengol S, Arretxe E, Rodríguez L, Ochoa B, Chico Y, et al. (2013) NF-κB, Sp1 and NF-Y as transcriptional regulators of human SND1 gene. Biochimie 95: 735–742. doi:10.1016/j.biochi.2012.10.029.

27. Sasi BK, Sonawane PJ, Gupta V, Sahu BS, Mahapatra NR (2014) Coordinated Transcriptional Regulation of Hspa1a Gene by Multiple Transcription Factors: Crucial Roles for HSF-1, NF-Y, NF-κB, and CREB. J Mol Biol 426: 116–135. doi:10.1016/j.jmb.2013.09.008.

28. Perkins ND, Agranoff AB, Pascal E, Nabel GJ (1994) An interaction between the DNA-binding domains of RelA(p65) and Sp1 mediates human immunodeficiency virus gene activation. Mol Cell Biol 14: 6570–6583.

29. Guo Z (2003) Role of the intronic enhancer in tumor necrosis factor-mediated induction of manganous superoxide dismutase. J Biol Chem 278: 23570–23578. doi:10.1074/jbc.M303431200.

30. Teferedegne B, Green MR, Guo Z, Boss JM (2006) Mechanism of action of a distal NF-kappaB-dependent enhancer. Mol Cell Biol 26: 5759–5770. doi:10.1128/MCB.00271-06.

31. Jin F, Li Y, Ren B, Natarajan R (2011) PU.1 and C/EBP(alpha) synergistically program distinct response to NF-kappaB activation through establishing monocyte specific enhancers. Proc Natl Acad Sci USA 108: 5290–5295. doi:10.1073/pnas.1017214108.

32. Musikacharoen T, Matsuguchi T, Kikuchi T, Yoshikai Y (2001) NF-kappa B and STAT5 play important roles in the regulation of mouse Toll-like receptor 2 gene expression. J Immunol 166: 4516–4524.

33. Ohmori Y, Schreiber RD, Hamilton TA (1997) Synergy between interferon-gamma and tumor necrosis factor-alpha in transcriptional activation is mediated by cooperation between signal transducer and activator of transcription 1 and nuclear factor kappaB. J Biol Chem 272: 14899–14907. doi:10.1074/jbc.272.23.14899.

34. Shen C-H, Stavnezer J (1998) Interaction of stat6 and NF-kappaB: direct association and synergistic activation of interleukin-4-induced transcription. Mol Cell Biol 18: 3395–3404.

35. Ristola M, Arpiainen S, Saleem MA, Holthöfer H, Lehtonen S (2012) Transcription of nephrin-Neph3 gene pair is synergistically activated by WT1 and NF-κB and silenced by DNA methylation. Nephrol Dial Transplant 27: 1737–1745. doi:10.1093/ndt/gfr576.

36. Ramirez-Carrozzi VR, Nazarian AA, Li CC, Gore SL, Sridharan R, et al. (2006) Selective and antagonistic functions of SWI/SNF and Mi-2beta nucleosome remodeling complexes during an inflammatory response. Genes & Development 20: 282–296. doi:10.1101/gad.1383206.

37. Limpert AS, Bai S, Narayan M, Wu J, Yoon SO, et al. (2013) NF-κB forms a complex with the chromatin remodeler BRG1 to regulate Schwann cell differentiation. J Neurosci 33: 2388–2397. doi:10.1523/JNEUROSCI.3223-12.2013.

38. Wurster AL, Precht P, Pazin MJ (2011) NF-κB and BRG1 bind a distal regulatory element in the IL-3/GM-CSF locus. Mol Immunol 48: 2178–2188. doi:10.1016/j.molimm.2011.07.016.

39. Lee SK, Na SY, Jung SY, Choi JE, Jhun BH, et al. (2000) Activating protein-1, nuclear factor-kappaB, and serum response factor as novel target molecules of the cancer-amplified transcription coactivator ASC-2. Mol Endocrinol 14: 915–925. doi:10.1210/mend.14.6.0471.

40. Burkly L, Hession C, Ogata L, Reilly C, Marconi LA, et al. (1995) Expression of relB is required for the development of thymic medulla and dendritic cells. Nature 373: 531–536. doi:10.1038/373531a0.

41. Weih F, Carrasco D, Durham SK, Barton DS, Rizzo CA, et al. (1995) Multiorgan inflammation and hematopoietic abnormalities in mice with a targeted disruption of RelB, a member of the NF-kappa B/Rel family. Cell 80: 331–340.

42. Caamaño JH, Rizzo CA, Durham SK, Barton DS, Raventós-Suárez C, et al. (1998) Nuclear factor (NF)-kappa B2 (p100/p52) is required for normal splenic microarchitecture and B cell-mediated immune responses. J Exp Med 187: 185–196. doi:10.1084/jem.187.2.185.

43. Franzoso G, Carlson L, Poljak L, Shores EW, Epstein S, et al. (1998) Mice deficient in nuclear factor (NF)-kappa B/p52 present with defects in humoral responses, germinal center reactions, and splenic microarchitecture. J Exp Med 187: 147–159. doi:10.1084/jem.187.2.147.

44. Reuther JY, Reuther GW, Cortez D, Pendergast AM, Albert S Baldwin J (1998) A requirement for NF-kappaB activation in Bcr-Abl-mediated transformation. Genes & Development 12: 968–981.

45. Hamdane M, David-Cordonnier M-H, D'Halluin JC (1997) Activation of p65 NF-I[kappa]IB protein by p210BCRI[thinsp]II[ndash]II[thinsp]IABL in a myeloid cell line

(P210BCR|[thinsp]|I[ndash]|II[thinsp]|ABL activates p65 NF-I[kappa]IB). ,
Published online: 22 November 1999; I doi:101038/sjonc1203239 15: 2267–2275.
doi:10.1038/sj.onc.1201411.

46.   Lounnas N, Frelin C, Gonthier N, Colosetti P, Sirvent A, et al. (2009) NF-κB
        inhibition triggers death of imatinib-sensitive and imatinib-resistant chronic
        myeloid leukemia cells including T315I Bcr-Abl mutants. International Journal of
        Cancer 125: 308–317. doi:10.1002/ijc.24294.

Future Directions

In this thesis, I presented the development of the first human haploid reporter screens. I sought to identify constitutive inhibitors of NF-κB as well as activators of NF-κB in the TLR2/6 pathway. Here I will summarize my findings and discuss areas for future study.

Human Haploid Reporter Genetic Screens

To identify constitutive inhibitors of NF-κB, I used a blasticidin S resistance gene (*BSR*) reporter under the control of a NF-κB transcriptional response element. This allowed reporter cells with constitutive NF-κB activity to survive in the presence of the antibiotic blasticidin. While this approach allowed for the selection of cells with mutations in *CYLD*, a constitutive inhibitor of NF-κB, it also allowed for the unanticipated selection of cells with mutations in *LRRC8D*, a gene I later demonstrated is required for blasticidin import. Only two other genes showed up significantly in this screen: *LRRC8A* and *HEATR7A*. Given the sequence homology and the physical interaction between LRRC8A and LRRC8D, the appearance of LRRC8A in the screen is likely due to a role in blasticidin import. It remains to be determined if *HEATR7A* has a role in NF-κB regulation or blasticidin import. Not much is known for *HEATR7A* except that it contains seven HEAT motifs, a domain found in diverse proteins including those that gave rise to its name: Huntingtin, elongation factor 3 (EF3), protein phosphatase 2A (PP2A), and the kinase TOR (Andrade et al., 2001). A HEAT domain consists of two helices that form a hairpin and this domain often occurs in tandem arrays. The HEAT domains of several proteins have been implicated in mediating protein-protein interactions and this domain may function generally as a scaffold for protein complexes (Groves et al., 1999; Neuwald and Hirano, 2000). Since eight unique inactivating mutations were sequenced in *HEATR7A* in the selected mutant population, it should be possible to isolate individual clones from the selected population with mutations in *HEATR7A*. Cells with mutations in HEART7A could then be used to determine if *HEATR7A* is required for NF-κB regulation or blasticidin import.

To eliminate the confounding issue of identifying transporters, I then switched to a screen with a NF-κB-GFP reporter. With this approach, I sought to identify genes required to activate NF-κB in the TLR2/6 pathway by sorting for cells that failed to turn GFP-positive in response to the TLR2/6 ligand, FSL-1. While the screen was able to identify five of the known components of the pathway, it was unable to identify TLR2 or TLR6 as bona fide hits in the screen. This suggests that the screen is not saturating and that future screens may need to start with a far larger pool of mutated cells. If large cell numbers become logistically problematic, cells could be infected with a higher MOI of gene-trap virus. Since coding DNA is < 2% of the genome, 2 mutations in a cell are unlikely to both occur in protein-coding genes (Lander et al., 2001; Venter et al., 2001). It is also unlikely that multiple random mutations in a cell would target the same pathway.

I observed that if I stimulated the sorted GFP-negative population of cells a second time with FSL-1, over half of the cells turned GFP-positive (data not shown). This suggests that the selected mutant population contains many false-positives. Due to negative feedback loops that turn NF-κB off after it has been turned on, NF-κB activity in response to a continuous stimulus has been observed to oscillate (Baltimore, 2011; Nelson et al., 2004). Thus, successive sorting for FSL-1-unresponsive cells over an extended period of time would prevent the collection of cells that at the moment of initial sorting had no or low NF-κB activity due to normal oscillation in NF-κB activity, rather than a mutation in the TLR2/6 pathway. Another strategy to decrease the number of false-positives is to perform the screen with a reporter cell line that contains multiple NF-κB reporters, each driving a different fluorescent protein. This would provide more confidence that cells that are non-fluorescent after FSL-1 treatment contain mutations in genes required to activate NF-κB in response to FSL-1.

Currently, the GFP in the NF-κB reporter has a destabilizing peptide at its C-terminus, which shortens the half-life of the mature protein to ~1 hour. While this feature is useful for studying kinetics of NF-κB activation and termination, it is not necessarily advantageous for identifying mutations that result in an absence of NF-κB activity. Removing the destabilizing peptide would result in a product that has a half-life ~26 hours (Corish and Tyler-Smith, 1999). Thus a long-lasting record would be produced for every activation event that results in transcription of the reporter and this could prevent the oscillating nature of NF-κB from confounding the sorting results.

Approximately a third of the hits from the screen for activators of NF-κB have a putative or established role in transcriptional regulation. It is possible that some of these genes may be specifically required for NF-κB-mediated transcription of target genes in response to the TLR2/6 ligand FSL-1. If knock-down and ChIP-Seq experiments confirm this to be true, screening for genes that are required for NF-κB-mediated transcription in response to other ligands (e.g. TNF, IL-1) could provide insight into how NF-κB transcriptional specificity is determined.

In principle, NF-κB-GFP reporter cells could also be used to identify inhibitors of NF-κB. For this type of screen, it is essential that the reporter is not expressed at steady-state and the destabilized GFP reporter would be preferred. After stimulation, cells would be washed, and cells that remain green would be sorted and collected. The stimulation conditions and the timing of the sort would need to be optimized. One difficulty that may be encountered with a screen for inhibitors is compensation for the loss of one inhibitor by another.

While our screens have focused on regulators of NF-κB, similar screens could be performed for regulators of other transcription factors. There are approximately 1,391 human sequence specific DNA binding transcription factors, many of which have binding site profiles that have been described (Jolma et al., 2013; Vaquerizas et al., 2009). My results suggest that screening for NF-κB regulators in KBM7 cells may be complicated by the presence of the *BCR-ABL* fusion oncogene. Other signaling pathways may be less affected by this mutation and may be more amenable for study in KBM7 cells.

The recent development of clustered, regularly interspaced, short palindromic repeats (CRISPR)–CRISPR-associated (Cas) systems permit cheap and rapid genome engineering in cells and mice. Already groups have exploited CRISPR-Cas9 to perform genome-wide screens in multiple cell types (Koike-Yusa et al., 2014; Shalem et al., 2014; Wang et al., 2014). Human haploid genetic screens are currently limited to two cell types. In contrast, there seems to be no limit to the type of cell that CRISPR-Cas9 could be applied to. CRISPR-Cas9 screens can also be applied in negative and positive selections. The CRISPR-Cas9 screens published to date have only used cell viability and proliferation as selection criteria. As with human haploid screens, transcriptional reporters will allow CRISPR-Cas9 screens to study pathways that do not affect cell viability or proliferation. Thus many of the lessons learned from the development of human haploid reporter screens could be applied to CRISPR-Cas9 reporter screens.

Leucine-rich repeat-containing 8 (LRRC8) proteins

LRRC8D and *LRRC8A* were initially identified as hits in a screen for inhibitors of NF-κB. It was subsequently demonstrated that *LRRC8D* is required for the import of blasticidin, the selecting agent used in the screen, and not for the regulation of NF-κB. Further functional and molecular characterization of LRRC8D have contributed to a greater understanding of how the antibiotic blasticidin is imported into mammalian cells. Our studies also support the existence of functional homology between LRRC8D and pannexins, a family of communication channels that share sequence homology with LRRC8 family members. This work provides a starting point for understanding how LRRC8A and LRRC8C are involved in lymphocyte and adipocyte development, respectively.

LRRC8B, LRRC8D, and LRRC8E have not been implicated in any physiological processes to date. The creation of knock-out mice may provide clues to their function. CRISPR-Cas9 genome engineering allows the rapid generation of mice with mutations in genes of interest. We have used this approach to create mice containing a homozygous 17 bp deletion in *LRRC8D* that creates an early stop codon in the gene. The predicted mutant protein would be 174 amino acids in length and the last 40 amino acids would be of a mutant sequence. This mutant protein would only encode the first predicted transmembrane domain of LRRC8D and is likely non-functional. Future characterization of *LRRC8D* mutant mice may help elucidate the physiological function of *LRRC8D*.

Antibodies against LRRC8 family members would be useful reagents to have on hand as they would allow the study of the endogenous proteins. Present immunofluorescence and co-immunoprecipitation experiments have made use of overexpressed epitope-tagged versions of LRRC8 family members. As overexpression of proteins can result in artifacts, repeating the experiment with antibodies against the endogenous proteins would be worthwhile. Isolation of antibodies that can promote opening or closing of LRRC8D-containing channels would facilitate the study of channel function.

Since LRRC8D did not evolve to import a toxic molecule, there are likely physiological substrates that have yet to be identified. Untargeted mass spectrometry of cell extracts from wild-type and LRRC8D-deficient cells could be applied to identify metabolites that are enriched in wild-type cells. Given that wild-type cells, but not LRRC8D-deficient cells can import blasticidin at steady-state, other small molecules may

also be imported passively through LRRC8D. It would be important in such an experiment to incubate the cells in a solution that contains the physiological substrate(s) that are imported. Since fetal bovine serum (FBS) is rich in metabolites, incubating the cells in medium that contains a high percentage of FBS prior to extraction would be a good starting point. While this is not a trivial approach, LC/MS-based metabolomics have successfully identified substrates for the transporters ABCC2 and SLC22A2 (Krumpochova et al., 2012; Taubert et al., 2007). It may be more difficult to identify metabolites that are exported by LRRC8D because their concentrations in the media are likely to be low. Overexpressing LRRC8D and partner proteins in cells and incubating the cells in a small volume of solution may help increase the concentration of exported metabolites. However, there still remains the challenging issue of selectively removing any salt or buffer included in the cell media from the metabolite-containing sample prior to LC/MS. Since pannexins export ATP out of apoptotic cells, it may be worth exploring, in a targeted manner, whether LRRC8D transports ATP (Chekeni et al., 2010; Qu et al., 2011). CellTiter-Glo could be used to measure ATP levels in cell extracts and media of wild-type and LRRC8D-deficient cells. Crude RT-PCR experiments have suggested that LRRC8D expression is induced by phytohemagglutinin (PHA) in peripheral blood mononucleated cells (PBMC) and by LPS in monocytes, suggesting that PHA and LPS may regulate LRRC8D function (Kubota et al., 2004). Thus, it may be worthwhile to also attempt the above strategies before and after stimulation with PHA and LPS.

We demonstrated that LRRC8D can stably interact with LRRC8A, LRRC8B, and LRRC8C, but it remains to be determined whether they interact in one large complex or in multiple complexes of distinct stoichiometry and composition. The observation that LRRC8A and LRRC8D are ubiquitously expressed, but LRRC8B, LRRC8C, and LRRC8E have more selective expression, suggests they may not be present in one complex at all times (Abascal and Zardoya, 2012). LRRC8C expression was elevated during the adipogenesis of 3T3-L1 cells, but the expression levels of the other LRRC8 family members did not change, suggesting that in certain physiological contexts complexes may be enriched for particular LRRC8 family members. Co-localization studies, channel reconstitution in *Xenopus* oocytes, and observations of overlap in substrates transported by each LRRC8 may help address these points.

Pannexins are comprised of four transmembrane domains and do not possess a LRR domain (Penuela et al., 2013). It is unclear what function the LRR domain plays in

LRRC8 proteins, but it is undoubtedly important for the function of LRRC8A. Truncation of just the last 2.5 LRR motifs in one allele of *LRRC8A* results in an absence of peripheral B cells (Sawada et al., 2003). The study of deletion mutants may provide insight into the function of this domain. While it is possible that the LRR domain is required for the interaction of channel constituents, the pannexins can oligomerize into channels without a LRR domain. Perhaps instead the LRR domain mediates interaction with a cellular protein. This interaction could regulate channel opening or closing, control channel substrate specificity, or recruit signaling proteins that interact with the transported substrates. The interaction of the LRR domain of LRRC8 proteins and other proteins may be transient or occur only under certain physiological contexts. Nonetheless, co-immunoprecipitation/mass spectrometry experiments could be attempted with full-length and LRR deletion mutants in the presence of cross-linkers or various stimuli.

Many questions remain surrounding the function of LRRC8 proteins. My work demonstrating that LRRC8D is required for the transport of a small molecule will help guide future studies on this family of proteins.

References

Abascal, F., and Zardoya, R. (2012). LRRC8 proteins share a common ancestor with pannexins, and may form hexameric channels involved in cell-cell communication. Bioessays.

Andrade, M.A., Petosa, C., O'Donoghue, S.I., Müller, C.W., and Bork, P. (2001). Comparison of ARM and HEAT protein repeats. J Mol Biol *309*, 1–18.
Baltimore, D. (2011). NF-κB is 25. Nat Immunol *12*, 683–685.

Chekeni, F.B., Elliott, M.R., Sandilos, J.K., Walk, S.F., Kinchen, J.M., Lazarowski, E.R., Armstrong, A.J., Penuela, S., Laird, D.W., Salvesen, G.S., et al. (2010). Pannexin 1 channels mediate "find-me" signal release and membrane permeability during apoptosis. Nature *467*, 863–867.

Corish, P., and Tyler-Smith, C. (1999). Attenuation of green fluorescent protein half-life in mammalian cells. Protein Eng. *12*, 1035–1040.

Groves, M.R., Hanlon, N., Turowski, P., Hemmings, B.A., and Barford, D. (1999). The Structure of the Protein Phosphatase 2A PR65/A Subunit Reveals the Conformation of Its 15 Tandemly Repeated HEAT Motifs. Cell *96*, 99–110.

Jolma, A., Yan, J., Whitington, T., Toivonen, J., Nitta, K.R., Rastas, P., Morgunova, E., Enge, M., Taipale, M., Wei, G., et al. (2013). DNA-binding specificities of human transcription factors. Cell *152*, 327–339.

Koike-Yusa, H., Li, Y., Tan, E.-P., Del Castillo Velasco-Herrera, M., and Yusa, K. (2014). Genome-wide recessive genetic screening in mammalian cells with a lentiviral CRISPR-guide RNA library. Nat Biotech *32*, 267–273.

Krumpochova, P., Sapthu, S., Brouwers, J.F., de Haas, M., de Vos, R., Borst, P., and van de Wetering, K. (2012). Transportomics: screening for substrates of ABC transporters in body fluids using vesicular transport assays. Faseb J. *26*, 738–747.

Kubota, K., Kim, J.Y., Sawada, A., Tokimasa, S., Fujisaki, H., Matsuda-Hashii, Y., Ozono, K., and Hara, J. (2004). LRRC8 involved in B cell development belongs to a novel family of leucine-rich repeat proteins. FEBS Lett *564*, 147–152.

Lander, E.S., Linton, L.M., Birren, B., Nusbaum, C., Zody, M.C., Baldwin, J., Devon, K., Dewar, K., Doyle, M., FitzHugh, W., et al. (2001). Initial sequencing and analysis of the human genome. Nature *409*, 860–921.

Nelson, D.E., Ihekwaba, A.E.C., Elliott, M., Johnson, J.R., Gibney, C.A., Foreman, B.E., Nelson, G., See, V., Horton, C.A., Spiller, D.G., et al. (2004). Oscillations in NF-kappaB signaling control the dynamics of gene expression. Science *306*, 704–708.

Neuwald, A.F., and Hirano, T. (2000). HEAT repeats associated with condensins, cohesins, and other complexes involved in chromosome-related functions. Genome Res.

10, 1445–1452.

Penuela, S., Gehi, R., and Laird, D.W. (2013). The biochemistry and function of pannexin channels. Biochim Biophys Acta *1828*, 15–22.

Qu, Y., Misaghi, S., Newton, K., Gilmour, L.L., Louie, S., Cupp, J.E., Dubyak, G.R., Hackos, D., and Dixit, V.M. (2011). Pannexin-1 is required for ATP release during apoptosis but not for inflammasome activation. The Journal of Immunology *186*, 6553–6561.

Sawada, A., Takihara, Y., Kim, J.Y., Matsuda-Hashii, Y., Tokimasa, S., Fujisaki, H., Kubota, K., Endo, H., Onodera, T., Ohta, H., et al. (2003). A congenital mutation of the novel gene LRRC8 causes agammaglobulinemia in humans. J Clin Invest *112*, 1707–1713.

Shalem, O., Sanjana, N.E., Hartenian, E., Shi, X., Scott, D.A., Mikkelsen, T.S., Heckl, D., Ebert, B.L., Root, D.E., Doench, J.G., et al. (2014). Genome-Scale CRISPR-Cas9 Knockout Screening in Human Cells. Science *343*, 84–87.

Taubert, D., Grimberg, G., Stenzel, W., and Schömig, E. (2007). Identification of the Endogenous Key Substrates of the Human Organic Cation Transporter OCT2 and Their Implication in Function of Dopaminergic Neurons. PLoS ONE *2*, e385.

Vaquerizas, J.M., Kummerfeld, S.K., Teichmann, S.A., and Luscombe, N.M. (2009). A census of human transcription factors: function, expression and evolution. Nat Rev Genet *10*, 252–263.

Venter, J.C., Adams, M.D., Myers, E.W., Li, P.W., Mural, R.J., Sutton, G.G., Smith, H.O., Yandell, M., Evans, C.A., Holt, R.A., et al. (2001). The sequence of the human genome. Science *291*, 1304–1351.

Wang, T., Wei, J.J., Sabatini, D.M., and Lander, E.S. (2014). Genetic screens in human cells using the CRISPR-Cas9 system. Science *343*, 80–84.

Appendix 1

Proteolytic cleavage in an endolysosomal compartment is required for activation of Toll-like receptor 9

Boyoun Park [1], Melanie M Brinkmann [1], Eric Spooner [1], Clarissa C Lee [1], You-Me Kim [2] & Hidde L Ploegh [1]

[1] Whitehead Institute for Biomedical Research, Massachusetts Institute of Technology, Cambridge, MA, USA.

[2] Novartis Institutes for Biomedical Research, Cambridge, MA, USA.

nature
immunology

Proteolytic cleavage in an endolysosomal compartment is required for activation of Toll-like receptor 9

Boyoun Park[1], Melanie M Brinkmann[1], Eric Spooner[1], Clarissa C Lee[1], You-Me Kim[2] & Hidde L Ploegh[1]

Toll-like receptors (TLRs) activate the innate immune system in response to pathogens. Here we show that TLR9 proteolytic cleavage is a prerequisite for TLR9 signaling. Inhibition of lysosomal proteolysis rendered TLR9 inactive. The carboxy-terminal fragment of TLR9 thus generated included a portion of the TLR9 ectodomain, as well as the transmembrane and cytoplasmic domains. This cleavage fragment bound to the TLR9 ligand CpG DNA and, when expressed in *Tlr9−/−* dendritic cells, restored CpG DNA–induced cytokine production. Although cathepsin L generated the requisite TLR9 cleavage products in a cell-free *in vitro* system, several proteases influenced TLR9 cleavage in intact cells. Lysosomal proteolysis thus contributes to innate immunity by facilitating specific cleavage of TLR9.

Toll-like receptors (TLRs) are essential sensors of microbial infection in multicellular hosts, and TLR engagement promotes the initiation of adaptive immune responses[1,2]. The TLR family consists of 10 members in humans and 13 in mice[3,4]. TLR1, TLR2, TLR4, TLR5 and TLR6 localize to the plasma membrane and are involved in the recognition of microbial products or lipid components[5–9]. TLR3, TLR7 (A002299) and TLR9 (A002301) are located in intracellular compartments and recognize pathogen-derived double-stranded RNA, single-stranded RNA and unmethylated CpG DNA, respectively[10–15]. The intracellular localization of TLR9 is critical for the discrimination of self and non-self nucleic acids[16]. After stimulation of cells with CpG DNA, TLR9 redistributes from the endoplasmic reticulum to lysosomes, where a signaling cascade is triggered by recruitment of the MyD88 adaptor molecule[14,17].

The papain-like lysosomal cysteine protease family, which includes the main thiol proteases cathepsin B and cathepsin L, is important in the degradation of endocytosed and intracellular proteins[18]. At the same time, compounds that block lysosomal acidification, such as chloroquine or bafilomycin A, inhibit CpG DNA–driven signaling and responses[19]. Lysosomal proteolysis in general[20] and cathepsin K specifically[21] have also been linked to TLR9 signaling, but the molecular mechanisms underlying their involvement remain to be elucidated.

RESULTS

Cathepsin-mediated cleavage of TLR9

To investigate whether cathepsin activity is required for TLR responses, we exposed the RAW mouse macrophage cell line to pepstatin A, an inhibitor of aspartic proteases, or to z-FA-fmk, a cysteine protease inhibitor that blocks cathepsin activity; we then exposed these cells to agonists of TLR4 (lipopolysaccharide (LPS)),

TLR7 (imiquimod) and TLR9 (CpG DNA). We found that z-FA-fmk considerably inhibited the production of tumor necrosis factor (TNF) by RAW macrophages stimulated with CpG DNA but did not influence TNF release after exposure to LPS or imiquimod (**Fig. 1a**). Thus, lysosomal cysteine proteases inhibited by z-FA-fmk are involved in the responsiveness of TLR9 but not TLR4 or TLR7.

To establish how cathepsin activity controls TLR9 responses, we explored the fate of newly synthesized TLR9. We generated a RAW macrophage derivative that stably expressed TLR9 tagged at the carboxyl (C) terminus with Myc (TLR9-Myc) and exposed it to z-FA-fmk or DMSO. We then labeled cells for 2 h with [35S]methionine and cysteine, followed by a chase for 6 h, after which we immunoprecipitated TLR9-Myc with a Myc-specific antibody. To improve electrophoretic resolution, we digested the immunoprecipitates with peptide–*N*-glycosidase F (Endo F), which eliminates carbohydrate heterogeneity. In the antibody to Myc (anti-Myc) immunoprecipitates of DMSO-treated cells, we detected two distinct polypeptides of 65 and 45 kilodaltons (kDa; **Fig. 1b**) that were not present in the immunoprecipitates of cells labeled in the presence of z-FA-fmk (**Fig. 1b**). We then denatured the initial anti-Myc immunoprecipitates and reimmunoprecipitated them with anti-Myc to retrieve TLR9-Myc. We detected the 65-kDa polypeptide in such reimmunoprecipitates from cells treated with DMSO but not those from cells exposed to z-FA-fmk (**Fig. 1b**). However, we noted similar rates of TLR9 synthesis during labeling. As we were able to retrieve the 65-kDa polypeptide with the Myc-specific antibody, we concluded that it was derived from TLR9.

To explore the nature of the 65- and 45-kDa polypeptides, we treated RAW macrophages expressing TLR9-Myc with DMSO or z-FA-fmk, immunoprecipitated TLR9 with anti-Myc, resolved glycosidase-digested proteins by SDS-PAGE and visualized proteins by silver
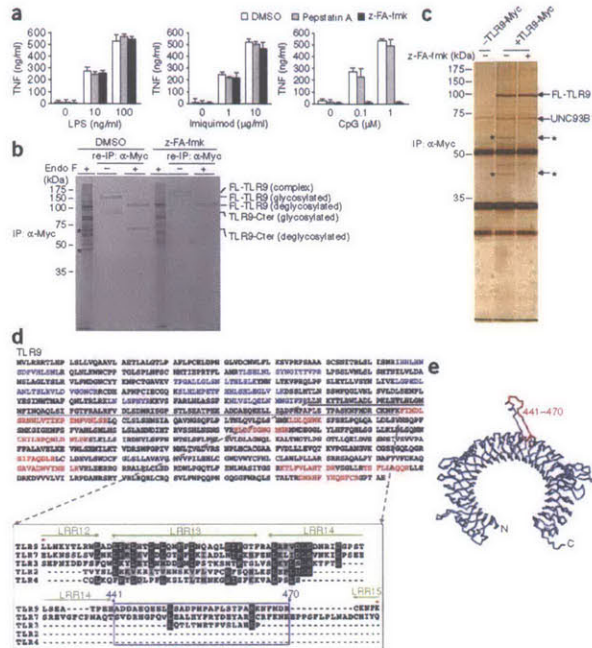
Figure 1 TLR9 is cleaved into two distinct polypeptides by cathepsins. (a) TNF production by RAW macrophages treated with pepstatin A, z-FA-fmk or DMSO, followed by incubation with LPS, imiquimod or CpG DNA. (b) SDS-PAGE of immunoprecipitates of TLR9-Myc–expressing RAW macrophages pretreated with DMSO or z-FA-fmk: radioactively labeled proteins were immunoprecipitated (IP) with anti-Myc (α-Myc); 10% of each sample was digested with Endo F and resolved by SDS-PAGE, and the remaining 90% was denatured and then reimmuno-precipitated (re-IP) with anti-Myc and left untreated (−) or treated with Endo F (+) and resolved by SDS-PAGE. *, 45-kDa and 65-kDa TLR9 cleavage fragments. FL-TLR9, full-length TLR9; TLR9-Cter, C-terminal fragment of TLR9. Samples were analyzed in duplicate for each condition. (c) Silver staining of proteins immunoprecipitated by anti-Myc from TLR9-Myc–expressing RAW macrophages treated with DMSO (−) or z-FA-fmk (+). *, polypeptides of 65 and 45 kDa analyzed by liquid chromatography–tandem mass spectrometry. (d) Top, mouse TLR9 sequence, with peptides identified by liquid chromatography–tandem mass spectrometry in c in blue (N-terminal) and red (C-terminal). No peptides were identified in the region encompassing residues 378–475 (underlined). Bottom, alignment of the region encompassing the cleavage site(s) of TLR9 (residues 378–475) with sequences of other TLRs. Residues 441–470 (blue outline) are part of a flexible loop. Green, LRRs. (e) Model of the TLR9 ectodomain based on the crystal structure of the TLR3 ectodomain. Red, predicted cathepsin cleavage site (441–470). Data are representative of four (a; average and s.d.) or two (b,c) independent experiments.

staining. We detected full-length TLR9 (about 100 kDa) in cells treated with DMSO or z-FA-fmk and detected the two polypeptides of 65 kDa and 45 kDa in cells treated with DMSO but not those treated with z-FA-fmk (**Fig. 1c**). We detected interaction between the polytopic membrane protein UNC93B1 and TLR9, critical for the translocation of TLR9 to lysosomes[22,23], in cells treated with DMSO or z-FA-fmk (**Fig. 1c** and **Supplementary Fig. 1a** online). We unambiguously identified the 65-kDa and 45-kDa polypeptides as the C-terminal and amino (N)-terminal fragments of TLR9, respectively, by mass spectrometry (**Fig. 1d** and **Supplementary Fig. 1b**). The identification of the 45-kDa polypeptide as the N-terminal fragment of TLR9 explains why we did not retrieve it by reimmunoprecipitation with anti-Myc (**Fig. 1b**). Thus, its appearance in the initial anti-Myc immunoprecipitates suggests that the N-terminal fragment interacted with full-length TLR9, with the C-terminal cleavage fragment or with both (**Fig. 1b**). Fragmentation of TLR9 was readily detectable after 3 h of chase, a time frame consistent with delivery of TLR9 to lysosomes (**Supplementary Fig. 2** online).

Identification of cleavage site(s) in the ectodomain of TLR9

To identify the likely site(s) of cleavage in TLR9, we determined the C-terminal boundary of the N-terminal segment and the N-terminal boundary of the C-terminal fragment on the basis of the unambiguous presence of peptides from these fragments as identified by mass spectrometry (**Fig. 1d** and **Supplementary Fig. 1a**). Our analysis confined the location of possible cleavage site(s) as being a region

encompassing amino acids 378–475 of TLR9 (**Fig. 1d**). Because the leucine-rich repeat (LRR) regions, some of which are stabilized by disulfide bonds, form a tightly packed hydrophobic core, these regions should be less susceptible to proteolysis[24]. Secondary-structure prediction programs designated residues 441–470, which are situated between LRR14 and LRR15, as being part of a flexible loop that could render TLR9 susceptible to proteolysis (**Fig. 1d**). On the basis of published TLR structures[24,25], we assume that the LRRs of TLRs generally take on a fairly similar fold and that LRR14 and LRR15 of TLR9 can thus be used to buttress the intervening segment of TLR9. Molecular modeling showed the presence of residues 441–470, which are contained in the putative cleavage region, in an extended loop (**Fig. 1e**).

Only in the presence of z-FA-fmk did we detect an additional species of TLR9 that migrated more slowly (**Figs. 1b** and **2a**). Glycosidase digestion showed that this form had acquired partial resistance to Endo H (**Fig. 2a**), consistent with passage through the Golgi apparatus. Because the cathepsin inhibitor z-FA-fmk was required for its visualization, this form of TLR9 is probably cleaved in lysosomes. The finding that it was normally cleaved and thus eliminated would account for the earlier failure to detect this Endo H–resistant form of TLR9 (refs. 22,23).

Endolysosomal localization of TLR9 cleavage

To determine if the endolysosomal compartment is the location of TLR9 cleavage, we assessed the effect of z-FA-fmk on the expression, maturation and stability of wild-type TLR9 and the TLR9 chimeras
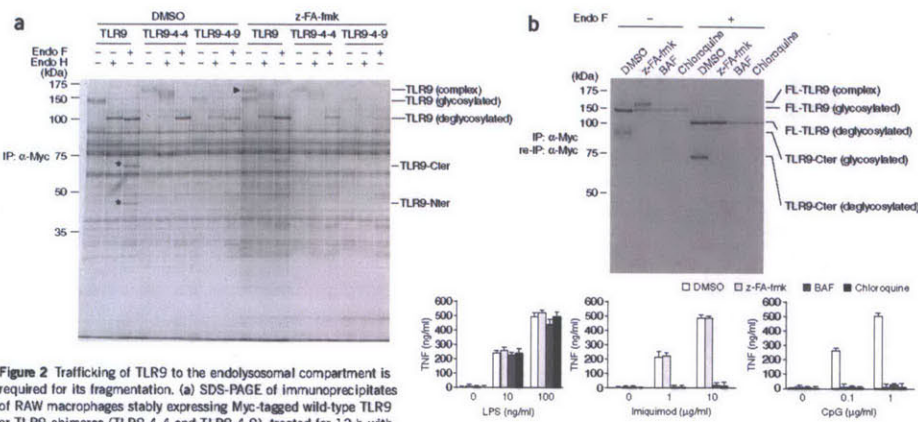
Figure 2 Trafficking of TLR9 to the endolysosomal compartment is required for its fragmentation. (a) SDS-PAGE of immunoprecipitates of RAW macrophages stably expressing Myc-tagged wild-type TLR9 or TLR9 chimeras (TLR9-4-4 and TLR9-4-9), treated for 12 h with DMSO or 10 μM z-FA-fmk, metabolically labeled for 1.5 h and chased for 6 h; TLRs recovered by immunoprecipitation with anti-Myc were treated with Endo H or Endo F (above lanes). Arrowhead, mature, Endo H–resistant TLR9; *, C- and N-terminal TLR9 cleavage fragments. (b) SDS-PAGE (top) of immunoprecipitates of TLR9-Myc–expressing RAW macrophages incubated for 10 h with DMSO or z-FA-fmk (10 μM) or for 4 h with bafilomycin (BAF; 5 μg/ml) or chloroquine (5 μM), then metabolically labeled for 1 h, followed by a chase period of 6 h; proteins were immunoprecipitated and reimmunoprecipitated with anti-Myc and immunoprecipitates were left untreated (−) or treated with Endo F (+). Below, enzyme-linked immunosorbent assay of TNF secretion by RAW macrophages incubated for 12 h with DMSO or z-FA-fmk (10 μM) or for 4 h with bafilomycin (5 μg/ml) or chloroquine (5 μM), then stimulated for 2 h with increasing concentrations of LPS, imiquimod or CpG DNA. Data are representative of three independent experiments (average and s.d. in b, below).

TLR9-4-4 and TLR9-4-9 (**Fig. 2a**). TLR9-4-4 contains the transmembrane and cytoplasmic region of TLR4, whereas TLR9-4-9 contains only the transmembrane region of TLR4 (ref. 22). These TLR9 chimeras fail to interact with UNC93B1 and therefore do not reach the lysosomal compartment, the presumed location of CpG DNA recognition and TLR9 signaling[22,23]. Unlike wild-type TLR9, neither TLR9-4-4 nor TLR9-4-9 yielded the two distinct fragments (**Fig. 2a**). These findings suggest that localization to the endolysosomal compartment is required for TLR9 cleavage.

As TLR7 is also located in the endolysosomal compartment, we sought to determine whether TLR7, like TLR9, undergoes proteolytic processing. In the absence of the cathepsin inhibitor, in conditions in which the TLR9 cleavage products were readily detected, we retrieved only full-length TLR7 (**Supplementary Fig. 3** online). In addition, we did not detect a mature Endo H–resistant TLR7 species in the presence of z-FA-fmk, as we did for TLR9 (**Supplementary Fig. 3**). Next we used the vacuolar H⁺ ATPase inhibitor bafilomycin A and the weak base chloroquine to block endosomal acidification and thus, indirectly, lysosomal protease activity[19]. Both compounds, like z-FA-fmk, blocked cleavage of TLR9 as well as CpG DNA–driven production of TNF (**Fig. 2b**). In contrast, bafilomycin A and chloroquine but not z-FA-fmk suppressed imiquimod-driven production of TNF. Thus, we concluded that fragmentation of TLR9 by lysosomal proteases is inhibited by interference with lysosomal acidification; in contrast, TLR7 shows no signs of such lysosomal cleavage.
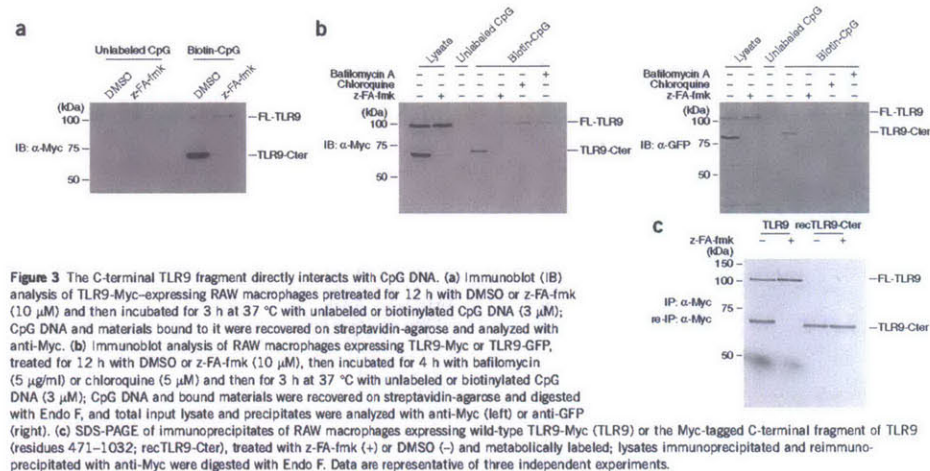
Influence of cleavage on TLR9 function

We next analyzed the interaction between CpG DNA and TLR9 in the presence and absence of z-FA-fmk (**Fig. 3**). We pretreated RAW cells expressing TLR9-Myc with z-FA-fmk, followed by incubation with unlabeled CpG DNA or biotinylated CpG DNA (biotin-CpG). We recovered biotin-CpG and materials bound to it with streptavidin-agarose and assessed the presence of coprecipitated TLR9-Myc by immunoblot analysis with anti-Myc. In the absence of the cathepsin inhibitor, we noted a strong interaction of the C-terminal TLR9 fragment with CpG DNA and weak but detectable binding between CpG DNA and full-length TLR9 (**Fig. 3a**). As expected, given the absence of the C-terminal TLR9 cleavage fragment in lysates of cells treated with z-FA-fmk, we did not detect binding of the C-terminal TLR9 fragment to CpG DNA in z-FA-fmk-treated cells (**Fig. 3a**). Notably, z-FA-fmk had no effect on the interaction between full-length TLR9 and CpG DNA, but the association between full-length TLR9 and biotin-CpG seemed to be much weaker than the interaction between CpG DNA and the C-terminal TLR9 fragment (**Fig. 3a**). TLR9 molecules tagged with green fluorescent protein (GFP) showed fragmentation and binding to CpG DNA similar to that of Myc-tagged TLR9 (**Fig. 3b**). A recombinantly expressed TLR9 fragment encompassing TLR9 residues 471–1032 was not cleaved further (**Fig. 3c**). This recombinant C-terminal fragment, when expressed in isolation, also bound to biotin-CpG more strongly than full-length Myc-tagged TLR9 did (**Fig. 4a**).

Next we sought to determine if fragmentation of TLR9 by cathepsins is critical for subsequent TLR9 signal transduction. We investigated the fragmentation of TLR9 and its interaction of CpG DNA in RAW cells stably expressing either Myc-tagged wild-type TLR9 or TLR9Δ441–470, a TLR9 deletion mutant lacking the proposed cleavage region (**Fig. 4a,b**). TLR9Δ441–470 was not cleaved but was still able to bind biotin-CpG (**Fig. 4a,b**). These findings suggested no gross structural alteration in the structure of the TLR9Δ441–470 mutant protein. To analyze the functional capacity of TLR9Δ441–470, we measured its ability to restore CpG DNA–induced TNF production in bone marrow–derived dendritic cells (BMDCs) from Tlr9⁻/⁻ mice. We

ARTICLES

a

b

Figure 3 The C-terminal TLR9 fragment directly interacts with CpG DNA. (a) Immunoblot (IB) analysis of TLR9-Myc–expressing RAW macrophages pretreated for 12 h with DMSO or z-FA-fmk (10 μM) and then incubated for 3 h at 37 °C with unlabeled or biotinylated CpG DNA (3 μM); CpG DNA and materials bound to it were recovered on streptavidin-agarose and analyzed with anti-Myc. (b) Immunoblot analysis of RAW macrophages expressing TLR9-Myc or TLR9-GFP, treated for 12 h with DMSO or z-FA-fmk (10 μM), then incubated for 4 h with bafilomycin (5 μg/ml) or chloroquine (5 μM) and then for 3 h at 37 °C with unlabeled or biotinylated CpG DNA (3 μM); CpG DNA and bound materials were recovered on streptavidin-agarose and digested with Endo F, and total input lysate and precipitates were analyzed with anti-Myc (left) or anti-GFP (right). (c) SDS-PAGE of immunoprecipitates of RAW macrophages expressing wild-type TLR9-Myc (TLR9) or the Myc-tagged C-terminal fragment of TLR9 (residues 471–1032; recTLR9-Cter), treated with z-FA-fmk (+) or DMSO (–) and metabolically labeled; lysates immunoprecipitated and reimmuno-precipitated with anti-Myc were digested with Endo F. Data are representative of three independent experiments.
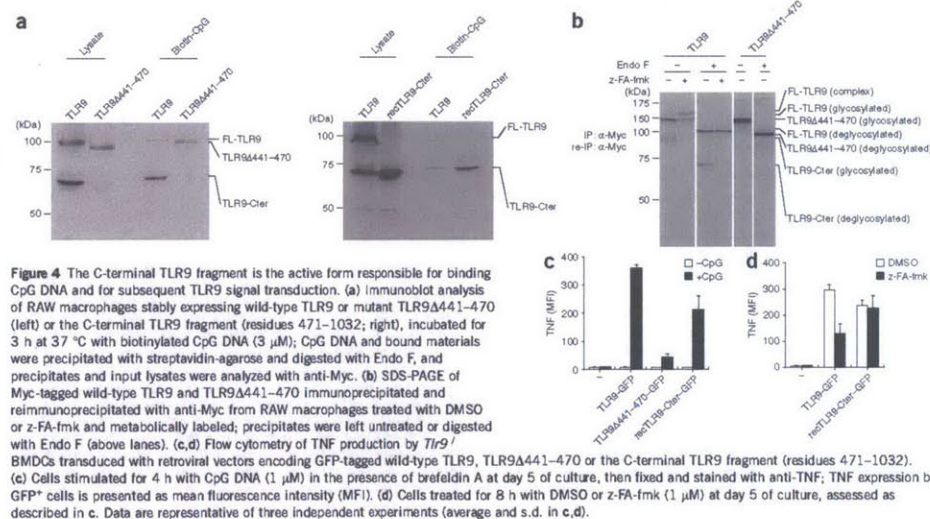
tagged wild-type TLR9, the C-terminal cleavage fragment of TLR9 and TLR9Δ441–470 with GFP and expressed these by retroviral transduction in *Tlr9*^{−/−} BMDCs, then exposed these cells to CpG DNA and measured TNF production in GFP^{+} cells by flow cytometry (**Fig. 4c**). BMDCs transduced with the TLR9Δ441–470 mutant produced less TNF in response to CpG DNA stimulation than did cells expressing wild-type TLR9 (**Fig. 4c**). As the transmembrane segment and cytoplasmic tail of TLR9Δ441–470 are identical to those of full-length

TLR9, and UNC93B1 bound wild-type TLR9 and TLR9Δ441–470 to a similar degree (data not shown), we believe that trafficking properties were unaffected by the deletion of residues 441–470.

C-terminal TLR9 fragment restores *Tlr9*^{−/−} BMDC function

We next investigated whether the C-terminal fragment, which retained a portion of the ectodomain encompassing LRR15–LRR26 and contained the full transmembrane and cytoplasmic domains, was on its

a

b

Figure 4 The C-terminal TLR9 fragment is the active form responsible for binding CpG DNA and for subsequent TLR9 signal transduction. (a) Immunoblot analysis of RAW macrophages stably expressing wild-type TLR9 or mutant TLR9Δ441–470 (left) or the C-terminal TLR9 fragment (residues 471–1032; right), incubated for 3 h at 37 °C with biotinylated CpG DNA (3 μM); CpG DNA and bound materials were precipitated with streptavidin-agarose and digested with Endo F, and precipitates and input lysates were analyzed with anti-Myc. (b) SDS-PAGE of Myc-tagged wild-type TLR9 and TLR9Δ441–470 immunoprecipitated and reimmunoprecipitated with anti-Myc from RAW macrophages treated with DMSO or z-FA-fmk and metabolically labeled; precipitates were left untreated or digested with Endo F (above lanes). (c,d) Flow cytometry of TNF production by *Tlr9*^{−/−} BMDCs transduced with retroviral vectors encoding GFP-tagged wild-type TLR9, TLR9Δ441–470 or the C-terminal TLR9 fragment (residues 471–1032). (c) Cells stimulated for 4 h with CpG DNA (1 μM) in the presence of brefeldin A at day 5 of culture, then fixed and stained with anti-TNF; TNF expression by GFP^{+} cells is presented as mean fluorescence intensity (MFI). (d) Cells treated for 8 h with DMSO or z-FA-fmk (1 μM) at day 5 of culture, assessed as described in c. Data are representative of three independent experiments (average and s.d. in c,d).
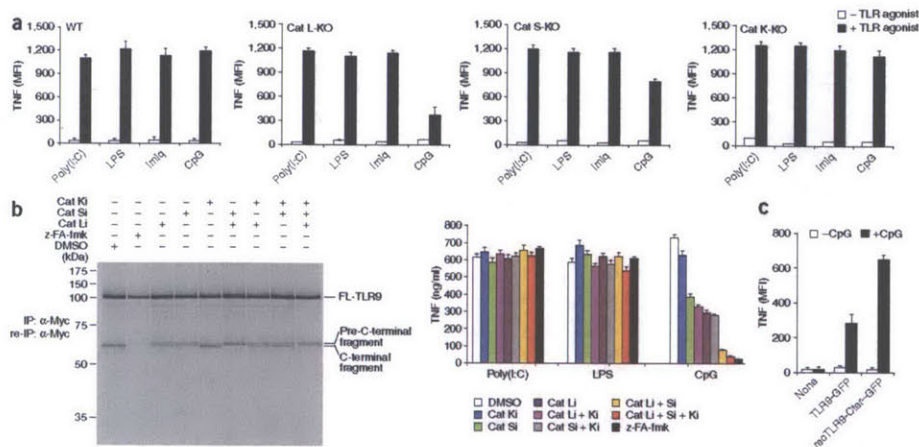
Figure 5 TLR9 cleavage requires many lysosomal proteases. (a) Flow cytometry of intracellular TNF in BMDCs from wild-type mice or mice lacking cathepsin L (Cat L-KO), cathepsin S (Cat S-KO) or cathepsin K (Cat K-KO), stimulated for 4 h with polyinosinic-polycytidylic acid (poly(I:C); 100 μg/ml), LPS (1 μg/ml), imiquimod (Imiq; 10 μg/ml) or CpG DNA (1 μM) in the presence of brefeldin A at day 6 of culture, then fixed and stained with anti-TNF. (b) SDS-PAGE (left) of immunoprecipitates of TLR9-Myc–expressing RAW macrophages pretreated for 12 h with DMSO, z-FA-fmk (10 μM) or the selective cathepsin L inhibitors Clik195 and Clik148 (Cat Li; 10 μM), the cathepsin S inhibitor LHVS (Cat Si; 10 nM), cathepsin K inhibitor II (Cat Ki; 1 μM) or combinations thereof, then metabolically labeled for 1.5 h, followed by a chase period of 5 h; TLR9 immunoprecipitated and reimmunoprecipitated from lysates with anti-Myc was digested with Endo F. Right, enzyme-linked immunosorbent assay of TNF secreted by RAW macrophages treated for 12 h with DMSO, z-FA-fmk or cathepsin inhibitors (key) and stimulated for 2 h with TLR agonists (horizontal axis). (c) Flow cytometry of TNF in cathepsin L–deficient BMDCs left untransduced (None) or transduced with retroviral vector encoding GFP-tagged wild-type TLR9 or C-terminal TLR9 fragment (471–1032) at day 1 of culture, then stimulated for 4 h at day 6 with CpG DNA (1 μM) in the presence of brefeldin A, fixed and stained with anti-TNF; data represent TNF in GFP$^+$ (transduced) cells. Data are representative of two (a,c) or three (b) independent experiments (average and s.d.).

own sufficient for binding to CpG DNA and initiating TLR9 signal transduction. In RAW macrophages, recombinant C-terminal TLR9 fragments tagged at the C terminus with either Myc or GFP interacted strongly with biotin-CpG, as demonstrated by the recovery of the C-terminal TLR9 fragment on streptavidin-agarose (**Fig. 3b**). Neither the expression nor the molecular size of the recombinant C-terminal fragment was affected by z-FA-fmk (**Fig. 3c**). *Tlr9*$^{-/-}$ BMDCs transduced with a retrovirus encoding the recombinant GFP-tagged C-terminal fragment of TLR9 regained responsiveness to CpG DNA stimulation, as indicated by TNF production (**Fig. 4c**). TNF synthesis elicited by CpG DNA stimulation of *Tlr9*$^{-/-}$ BMDCs expressing the GFP-tagged C-terminal fragment of TLR9 was not affected by treatment with z-FA-fmk (**Fig. 4d**). In contrast, TNF production facilitated by the expression of GFP-tagged wild-type TLR9 in *Tlr9*$^{-/-}$ BMDCs was inhibited by z-FA-fmk (**Fig. 4d**). The greater sensitivity of BMDCs to cytotoxic effects of z-FA-fmk did not allow us to use the inhibitor concentrations readily tolerated by RAW cells and their derivatives to achieve full inhibition of TNF production. Nevertheless, we conclude that the C-terminal TLR9 fragment on its own is sufficient to bind CpG DNA and initiate signaling.

Multistep TLR9 cleavage

If indeed residues 441–470 are correctly modeled as a flexible loop (**Fig. 1e**), then any of a number of proteases could presumably cleave it, as has been noted for other proteins activated by proteolysis, such as flu hemagglutinin, cholera toxin and various proenzymes, including lysosomal hydrolases. Similarly, although the involvement of

lysosomal proteolysis in major histocompatibility class II–restricted antigen presentation is immediately evident from the inhibitory effects of a broad protease blockade, with very few exceptions, it has been difficult to link any particular protease to the processing of a specific antigen[26,27]. For the same reasons, it may be difficult to determine which members of the cathepsin family of lysosomal proteases cleave TLR9. After genetic ablation or pharmacological inhibition of a single cathepsin, any of several cysteine proteases could 'pick up the slack', thereby explaining the greater inhibitory potency of the broadly specific inhibitors over more narrowly targeted compounds[28,29]. Also, mice lacking multiple cathepsins have more severely deleterious phenotypes than those of mice lacking a single cathepsin[30]. Nonetheless, we examined the TLR responsiveness of BMDCs from mice lacking individual cathepsins. Cathepsin L–deficient BMDCs and, to a lesser extent, cathepsin S–deficient BMDCs produced less TNF in response to CpG DNA (**Fig. 5a**). We noted normal TNF production in response to CpG DNA by BMDCs from cathepsin K–deficient mice, which seemed at variance with a published report[21] in which cathepsin K–deficient BMDCs failed to respond to CpG DNA stimulation, as assessed by their lower production of interleukin 12.

We next examined the effects of a series of selective cathepsin inhibitors on the pattern of TLR9 cleavage in and TNF production by RAW cells. We found that z-FA-fmk, but not any of the more narrowly specific cathepsin inhibitors, completely suppressed formation of the 65-kDa C-terminal TLR9 fragment itself (**Fig. 5b**). Cleavage in the presence of the cathepsin K inhibitor was indistinguishable from cleavage in the presence of DMSO (**Fig. 5b**). Selective inhibition of

5

Appendix 1: Proteolytic cleavage in an endolysosomal compartment is required for activation of Toll-like receptor 9

Figure 6 Cathepsin L cleaves TLR9 *in vitro* but fails to cleave the TLR9 deletion mutant lacking the region encompassing the putative cathepsin cleavage site(s). (a) SDS-PAGE of wild-type TLR9 or the TLR9 deletion mutant TLR9Δ441–470 transcribed and translated *in vitro* in the presence of microsomes and [^{35}S]methionine plus either 2 mM dithiothreitol (DTT) or 2 mM oxidized glutathione (GSSG); microsomes were pelleted and lysed and recombinant cathepsin L was added for 2 h at 37 °C, followed by analysis of 10% of the total volume of the *in vitro* transcription and translation reaction. *, C- and N-terminal TLR9 fragments. (b) SDS-PAGE of

Myc-tagged wild-type TLR9 or C-terminal TLR9 fragment (residues 471–1032) transcribed and translated *in vitro* in the presence of microsomes and [^{35}S]methionine; microsomes were pelleted and lysed, and 10% was immunoprecipitated with anti-Myc, then digested with EndoF, and the other 90% was incubated for 2 h at 37 °C with recombinant cathepsin L (0.2 μM), then incubated for 2 h with biotinylated CpG DNA (5 μM), incubated with streptavidin-agarose and digested with Endo F. Data are representative of two independent experiments.
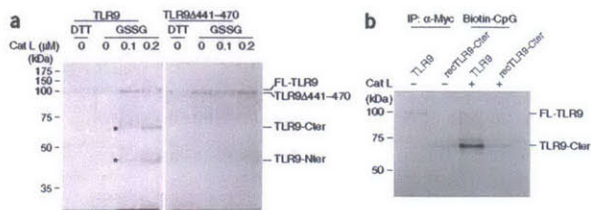
cathepsin L or cathepsin S resulted in the appearance of a doublet composed of a slightly larger band in addition to the 65-kDa band (**Fig. 5b**). We called the upper band the 'pre-C-terminal fragment'. The cathepsin K inhibitor, when combined with other inhibitors, failed to produce an additive effect (**Fig. 5b**). However, combining the cathepsin S– and cathepsin L–selective inhibitors resulted in enrichment of the pre-C-terminal fragment relative to the C-terminal fragment (**Fig. 5b**). The pre-C-terminal fragment seemed to be inactive, as we noted a strict inverse correlation between its presence and TNF production (**Fig. 5b**). Partial conversion of full-length TLR9 to the pre-C-terminal and C-terminal fragments yielded intermediate amounts of TNF. The slight difference in apparent molecular weight suggested that at most a few dozen residues distinguished the active C-terminal fragment from the inactive TLR9 pre-C-terminal fragment (**Fig. 5b**). These data suggest that at least two cleavage events occur to convert full-length TLR9 into its active form (**Supplementary Fig. 4** online). In addition, introduction of the C-terminal TLR9 fragment into cathepsin L–deficient BMDCs restored CpG DNA-driven production of TNF (**Fig. 5c**). Wild-type TLR9 restored TNF production to a limited extent, consistent with the limited inhibition of TNF production of untransduced cathepsin L–deficient BMDCs (**Fig. 5a,c**). We conclude that more than a single lysosomal protease is involved in cleavage of TLR9, with an important function for cathepsin L.

To further support the idea that cathepsin L can cleave TLR9 at the proposed cleavage site, we incubated radiochemically pure TLR9, produced by *in vitro* translation in the presence of properly redox-buffered microsomes[31], with purified cathepsin L (**Fig. 6a**). Cathepsin L produced the C-terminal fragment of TLR9 *in vitro* (**Fig. 6a**), and this C-terminal fragment bound to biotin-CpG (**Fig. 6b**). However, the TLR9 deletion mutant TLR9Δ441–470 was not cleaved by cathepsin L *in vitro* (**Fig. 6a**). Our results collectively establish that TLR9 undergoes cleavage in an endolysosomal compartment, a step that is important for TLR9 to execute its proper function.

DISCUSSION

The involvement of the endolysosomal compartment in proper functioning of the nucleic acid–sensing TLRs (TLR3, TLR7 and TLR9) is well documented[11–16], but exactly how this environment contributes to the receipt and transmission of signals through these TLRs has not been established. We have now demonstrated that TLR9 underwent proteolytic cleavage, executed by cysteine proteases, in the endolysosomal compartment. On a molar basis, the C-terminal cleavage fragment of TLR9 bound CpG DNA more strongly than did full-length TLR9, although full-length TLR9 did bind CpG DNA.

The broadly specific inhibitor z-FA-fmk was most effective at blocking this cleavage and, accordingly, abrogated TNF production in cells exposed to the TLR9 agonist CpG DNA. Our data are consistent with the involvement of more than one protease in this cleavage reaction, because we noted a blunted rather than a completely blocked TNF response to CpG DNA in BMDCs deficient in cathepsin L or cathepsin S. Furthermore, a combination of inhibitors selective for cathepsin L and cathepsin S not only blocked TNF production in response to CpG DNA but also yielded a cleavage intermediate, the pre-C-terminal fragment, whose abundance was inversely correlated with TNF production. The expression of only the C-terminal fragment in *Tlr9*^{−/−} BMDCs restored their ability to produce TNF, as also noted for cathepsin L–deficient BMDCs. We hypothesize that the absence of cleavage in the presence of chloroquine and bafilomycin A is best explained by higher pH or less proteolytic activity.

The delivery of TLR9 to endolysosomal compartments requires its interaction with UNC93B1, mediated through the transmembrane segment of TLR9 (ref. 22). Eliminating this interaction by substituting the transmembrane segment of TLR9 causes TLR9 to traffic incorrectly to the surface[16], and mutating the gene encoding UNC93B1 abolishes trafficking of TLR9 to the endolysosomal compartment[23]. The ability of a chimera consisting of the extracellular domain of TLR9 and the transmembrane and cytoplasmic domains of TLR4, which localizes to the cell surface, to induce signal transduction after CpG DNA binding might be attributed to the recruitment of adaptors other than MyD88 to the TLR4 cytoplasmic tail[16,32].

We did not find any inhibition of TNF production in cathepsin K–deficient BMDCs or by imposition of a cathepsin K blockade, in contrast to an earlier study that showed less production of interleukin 12 by cathepsin K–deficient BMDCs in response to CpG DNA[21]. We further determined that responses requiring the engagement of TLR7 were not affected by z-FA-fmk, unlike the blockade in upregulation of CD86 and B cell proliferation reported earlier[20]. The production of interleukin 12 may require the involvement of cathepsin K at steps 'downstream' of TLR9 engagement, which could explain the observed discrepancy. Likewise, the surface expression of CD86 and steps that control B cell proliferation may require lysosomal protease involvement for reasons other than cleavage of the TLRs involved.

We obtained no evidence that TLR7 is cleaved in a z-FA-fmk–sensitive way, and we have been unable to detect cleavage fragments of TLR7. This raises the issue of why signaling through TLR7, or through TLR3, for that matter, is nonetheless sensitive to the inclusion of lysosomotropic agents. Several of the TLRs are known to act together with partner proteins, such as CD14 and MD2 for TLR4 (refs. 33,34),

CD36 for TLR1, TLR2 and TLR6 (ref. 35), or dectin-1 for TLR2 (ref. 36). We hypothesize that the activity of TLR3 and TLR7 may require cofactors whose involvement necessitates a proteolytic cleavage, or at least includes a pH-sensitive step, that is affected by the inclusion of lysosomotropic agents.

The evolutionary importance of TLR9 cleavage is as yet unclear. Why should TLR9 be unique among lysosomal TLRs in requiring this mode of activation? The C-terminal cleavage fragment of TLR9 was able to bind CpG DNA and accomplish signal transduction even when synthesized in the absence of the N-terminal portion of TLR9. A search for interaction partners of the N-terminal cleavage fragment might elucidate yet other aspects of TLR9 biology. Regardless of the identity of the TLR9 convertase(s) and the exact function of the cleavage products generated, full innate immunity requires lysosomal proteolysis no less than adaptive immunity does.

METHODS

Reagents. Imiquimod (R837) and polyinosinic-polycytidylic acid were from Invivogen; 1826 CpG DNA and 1826 biotinylated CpG DNA (5′-Bio-TsCsCsAsTsgsAsCsgsTsTsCsCsTsgsAsCsgsTsT) were from TIB Molbiol; and LPS (*Escherichia coli* serotype 026:B6) and brefeldin A were from Sigma. Endo H and Endo F were from New England Biolabs. Monoclonal anti-Myc (9B11), rabbit polyclonal anti-rabbit GFP (ab290) and rabbit polyclonal anti-TLR7 (IMG-5632) were from Cell Signaling, Abcam and Imgenex, respectively. Streptavidin-agarose beads were from Pierce. Bafilomycin, chloroquine, z-FA-fmk (benzyloxycarbonyl–phenylalanine-alanine–fluoromethylketone) and glutathione disulfide were from Sigma, and the cathepsin B inhibitor CA-074Me ((L-3-*trans*-(propylcarbamoyl)oxirane-2-carbonyl)-L-isoleucyl-L-proline methyl ester) was from Calbiochem. The selective cathepsin inhibitors Clik195 and Clik148 (cathepsin L), LHVS (cathepsin S) and cathepsin K inhibitor II (cathepsin K; Calbiochem) were provided by G.-P. Shi[37].

Mice and cell lines. C57BL/6 mice were from Charles River Laboratories; *Tlr9−/−* mice were from A. Marshak-Rothstein. All animals were maintained in specific pathogen-free conditions according to guidelines of the committee for animal care at the Whitehead Institute. Mouse RAW 264.7 macrophages (TIB-71; American Type Culture Collection) and human embryonic kidney cells (HEK293T; CRL-11268; American Type Culture Collection) were cultured in DMEM supplemented with 10% (vol/vol) heat-inactivated FCS and penicillin-streptomycin. Cells were grown at 37 °C in humidified air with 5% CO₂. Mice deficient in cathepsin L, cathepsin S and cathepsin K were provided by G.-P. Shi.

DNA cloning. All mouse TLR9 constructs were fused at the C terminus to Myc or GFP. Wild-type TLR9 and TLR9 chimeras have been described[22]. The TLR9 deletion mutant lacking residues 441–470 was generated by sequential PCR with the primers 5′-CTGTCAGAAGCCACCCCTGAAGAGTGTAAGAACTT CAAGTTCACCATGGACCTG-3′ (forward) and 5′-CAGGTCCATGGTGAAC TTGAAGTTCTTACACTCTTCAGGGGTGGCTTCTGAGAC-3′ (reverse). The recombinant C-terminal TLR9 fragment encompassing residues 471–1032 was generated by PCR with the primers 5′-GGGGTACCTGTAAGAACTTC AAGTTCACCATGGACCTG-3′ (forward) and 5′-AGCTTTGTTTAAACTTTA CAAGTCCTCTTCAGAAATGAGCTTTTGCTCTTCTGCTGTAGGTCCCCGG CAGA-3′ (reverse). The C-terminal TLR9 fragment encompassing residues 471–1032 was fused at the N terminus with the H-2Kᵇ signal sequence (MVPCTLLLLAAALAPTQTRA). All constructs were cloned into pcDNA3.1(+) (Invitrogen) or the retroviral pMSCV vector (Clontech) and were verified by sequencing.

Preparation of BMDCs. BMDCs were prepared as described[58].

Pulse-chase analysis, immunoprecipitation and Endo H–Endo F assay. RAW macrophages (1 × 10⁷) were 'starved' for 50 min in medium lacking methionine and cysteine (starvation medium), then were labeled with a mixture of [³⁵S]methionine and [³⁵S]cysteine (0.1 mCi/nl; Perkin Elmer) in starvation medium supplemented with dialyzed heat-inactivated FCS, followed by a chase in complete medium with or without 10 μM inhibitor. Cells were lysed for 1 h at 4 °C with 1% (vol/vol) Nonidet-P40 in PBS supplemented with protease inhibitors (Roche). After lysates were precleared with protein G–Sepharose (Sigma-Aldrich), primary antibodies and protein G–Sepharose were added to supernatants, followed by incubation at 4 °C. The protein G–Sepharose beads were washed five times with 0.1% (vol/vol) Nonidet-P40 in PBS. Proteins were eluted from the beads by boiling in SDS sample buffer and were separated by SDS-PAGE, and polypeptides were visualized by fluorography. Where indicated, samples were digested for 3 h at 37 °C with Endo H and Endo F.

Coimmunoprecipitation and immunoblot analysis. Cells were lysed in 1% (vol/vol) digitonin (Calbiochem) in buffer containing 25 mM HEPES, 100 mM NaCl, 10 mM CaCl₂ and 5 mM MgCl₂, pH 7.6, supplemented with 0.5 mM phenylmethylsulfonylfluoride and leupeptin. Lysates were precleared for 1 h at 4 °C with protein G–Sepharose (Sigma-Aldrich). For immunoprecipitation, samples were incubated for 12 h at 4 °C with the appropriate antibodies before protein G beads were added for 3 h. Beads were washed four times with 0.1% (vol/vol) digitonin, and bound proteins were eluted by boiling in SDS sample buffer or 1% (vol/vol) SDS. Proteins were separated by 10% SDS-PAGE, were transferred to nitrocellulose membranes, were blocked for 2 h with 5% (wt/vol) skim milk in PBS with 0.1% (vol/vol) Tween-20 and were probed for 4 h with the appropriate antibodies. Membranes were washed three times with PBS with 0.1% (vol/vol) Tween-20 and were incubated for 1 h with horseradish peroxidase–conjugated streptavidin. Proteins were visualized with an enhanced chemiluminescence detection reagent.

Large-scale affinity purification and mass spectrometry. After coimmuno-precipitation, eluted samples were separated by SDS-PAGE and polypeptides were visualized by silver staining. Bands of interest were excised, were lysed with trypsin and were analyzed by tandem mass spectrometry.

Retroviral transduction. HEK293T cells were transfected with plasmids encoding VSV-G and Gag-Pol, as well as pMSCV-TLR9-Myc, pMSCV-TLR9-4-4-Myc, pMSCV-TLR9-4-9-Myc, pMSCV-TLR9Δ441–470 or pMSCV-TLR9 471–1032. At 24 h and 48 h after transfection, medium containing viral particles was collected, was filtered through a 0.45-μm membrane and was added to RAW macrophages or BMDCs at day 1 of BMDC culture. The next day, cells were given fresh media.

In vitro transcription and translation. Myc-tagged wild-type TLR9, TLR9Δ441–470 or the C-terminal TLR9 fragment of residues 471–1032 cloned into the pcDNA3.1(+) vector (1 μg) was transcribed and translated for 1 h at 30 °C *in vitro* with the TNT T7 Quick Coupled Transcription/Translation system (Promega) in the presence of microsomes and 10 μCi [³⁵S]methionine (Perkin Elmer) in a total volume of 50 μl. Microsomes were pelleted by centrifugation for 4 min at 17,000g and were lysed in 20 μl cathepsin activation buffer (1% (vol/vol) Nonidet-P40, 50 mM sodium acetate, pH 5.5, 3 mM cysteine and 1 mM EDTA). Recombinant cathepsin L (Sigma) was immediately added to the microsomes at a concentration of 0.1–0.2 μM and incubated for 2 h at 37 °C, followed by incubation for 2 h at 37 °C with biotinylated CpG DNA (5 μM). Reactions were diluted to a final volume of 1 ml with 1% (vol/vol) Nonidet-P40 lysis buffer with protease inhibitors, and TLR9 proteins were immunoprecipitated with anti-Myc or were incubated with streptavidin agarose and separated by SDS-PAGE.

Intracellular TNF assay. *Tlr9−/−* BMDCs expressing either wild-type or mutant TLR9 were cultured for 5 d and were stimulated for 4 h with CpG DNA (1 μM) in the presence of brefeldin A (10 μg/ml). Cells were fixed for 10 min at 20 °C with 4% (vol/vol) formaldehyde and were made permeable by incubation for 10 min with 0.5% (wt/vol) saponin in flow cytometry buffer (PBS with 2% (wt/vol) BSA and 0.05% (wt/vol) sodium azide). Cells were stained for 30 min with Alexa Fluor 647–conjugated anti-TNF (MP6-XT22; 557730; BD Biosciences). Fluorescence intensity was measured with LSR I flow cytometer (BD Biosciences). Data were collected with CellQuest software (BD Biosciences) and were analyzed with FlowJo software (TreeStar).

TNF enzyme-linked immunosorbent assay. RAW macrophages were stimulated for 2 h with increasing concentrations of the TLR agonists LPS (TLR4),

ARTICLES

imiquimod (TLR7) or CpG DNA (TLR9). Conditioned medium was collected and was analyzed by enzyme-linked immunosorbent assay with hamster antibody to mouse or rat TNF (557516; BD Biosciences) as a capture antibody and biotin-labeled rabbit anti-mouse as a secondary antibody (557432; BD Biosciences).

Homology modeling. A multiple sequence alignment containing the target sequence (*Mus musculus* TLR9; National Center for Biotechnology Information accession number NP_112455) and the template sequence (*Mus musculus* TLR3; National Center for Biotechnology Information accession number NP_569054) was generated by the ClustalW program. The resulting alignment and the structure of the *Mus musculus* TLR3 ectodomain (Protein Data Base accession code 3ciy, chain A) were used to generate a structural model of the *Mus musculus* TLR9 ectodomain with the Swiss-Model automated comparative protein modeling server[39].

Accession codes. UCSD-Nature Signaling Gateway (http://www.signaling-gateway.org): A002299 and A002301.

Note: Supplementary information is available on the Nature Immunology website.

1. Takeda, K., Kaisho, T. & Akira, S. Toll-like receptors. *Annu. Rev. Immunol.* **21**, 335–376 (2003).
2. Janeway, C.A. Jr & Medzhitov, R. Innate immune recognition. *Annu. Rev. Immunol.* **20**, 197–216 (2002).
3. Kawai, T. & Akira, S. TLR signaling. *Cell Death Differ.* **13**, 816–825 (2006).
4. Takeda, K. & Akira, S. Toll-like receptors in innate immunity. *Int. Immunol.* **17**, 1–14 (2005).
5. Poltorak, A. *et al.* Defective LPS signaling in C3H/HeJ and C57BL/10ScCr mice: mutations in Tlr4 gene. *Science* **282**, 2085–2088 (1998).
6. Takeuchi, O. *et al.* Differential roles of TLR2 and TLR4 in recognition of gram-negative and gram-positive bacterial cell wall components. *Immunity* **11**, 443–451 (1999).
7. Takeuchi, O. *et al.* Discrimination of bacterial lipoproteins by Toll-like receptor 6. *Int. Immunol.* **13**, 933–940 (2001).
8. Ozinsky, A. *et al.* The repertoire for pattern recognition of pathogens by the innate immune system is defined by cooperation between toll-like receptors. *Proc. Natl. Acad. Sci. USA* **97**, 13766–13771 (2000).
9. Hayashi, F. *et al.* The innate immune response to bacterial flagellin is mediated by Toll-like receptor 5. *Nature* **410**, 1099–1103 (2001).
10. Hemmi, H. *et al.* Small anti-viral compounds activate immune cells via the TLR7 MyD88-dependent signaling pathway. *Nat. Immunol.* **3**, 196–200 (2002).
11. Diebold, S.S., Kaisho, T., Hemmi, H., Akira, S. & Reis e Sousa, C. Innate antiviral responses by means of TLR7-mediated recognition of single-stranded RNA. *Science* **303**, 1529–1531 (2004).
12. Heil, F. *et al.* Species-specific recognition of single-stranded RNA via Toll-like receptor 7 and 8. *Science* **303**, 1526–1529 (2004).
13. Hemmi, H. *et al.* A Toll-like receptor recognizes bacterial DNA. *Nature* **408**, 740–745 (2000).
14. Latz, E. *et al.* TLR9 signals after translocating from the ER to CpG DNA in the lysosome. *Nat. Immunol.* **5**, 190–198 (2004).
15. Nishiya, T., Kajita, E., Miwa, S. & Defranco, A.L. TLR3 and TLR7 are targeted to the same intracellular compartments by distinct regulatory elements. *J. Biol. Chem.* **280**, 37107–37117 (2005).
16. Barton, G.M., Kagan, J.C. & Medzhitov, R. Intracellular localization of Toll-like receptor 9 prevents recognition of self DNA but facilitates access to viral DNA. *Nat. Immunol.* **7**, 49–56 (2006).
17. Leifer, C.A. *et al.* TLR9 is localized in the endoplasmic reticulum prior to stimulation. *J. Immunol.* **173**, 1179–1183 (2004).
18. Kominami, E., Ueno, T., Muno, D. & Katunuma, N. The selective role of cathepsins B and D in the lysosomal degradation of endogenous and exogenous proteins. *FEBS Lett.* **287**, 189–192 (1991).
19. Honda, K. *et al.* Spatiotemporal regulation of MyD88-IRF-7 signalling for robust type-I interferon induction. *Nature* **434**, 1035–1040 (2005).
20. Matsumoto, F. *et al.* Cathepsins are required for Toll-like receptor 9 responses. *Biochem. Biophys. Res. Commun.* **367**, 693–699 (2008).
21. Asagiri, M. *et al.* Cathepsin K-dependent toll-like receptor 9 signaling revealed in experimental arthritis. *Science* **319**, 624–627 (2008).
22. Brinkmann, M.M. *et al.* The interaction between the ER membrane protein UNC93B and TLR3, 7, and 9 is crucial for TLR signaling. *J. Cell Biol.* **177**, 265–275 (2007).
23. Kim, Y.M., Brinkmann, M.M., Paquet, M.E. & Ploegh, H.L. UNC93B1 delivers nucleotide-sensing toll-like receptors to endolysosomes. *Nature* **452**, 234–238 (2008).
24. Choe, J., Kelker, M.S. & Wilson, I.A. Crystal structure of human Toll-like receptor 3 (TLR3) ectodomain. *Science* **309**, 581–585 (2005).
25. Jin, M.S. & Lee, J.O. Structures of the Toll-like receptor family and its ligand complexes. *Immunity* **29**, 182–191 (2008).
26. Villadangos, J.A. & Ploegh, H.L. Proteolysis in MHC class II antigen presentation: who's in charge? *Immunity* **12**, 233–239 (2000).
27. Lennon-Dumenil, A.M., Bakker, A.H., Wolf-Bryant, P., Ploegh, H.L. & Lagaudriere-Gesbert, C. A closer look at proteolysis and MHC-class-II-restricted antigen presentation. *Curr. Opin. Immunol.* **14**, 15–21 (2002).
28. Greenbaum, D.C. *et al.* Small molecule affinity fingerprinting. A tool for enzyme family subclassification, target identification, and inhibitor design. *Chem. Biol.* **9**, 1085–1094 (2002).
29. Bogyo, M., Verhelst, S., Bellingard-Dubouchaud, V., Toba, S. & Greenbaum, D. Selective targeting of lysosomal cysteine proteases with radiolabeled electrophilic substrate analogs. *Chem. Biol.* **7**, 27–38 (2000).
30. Felbor, U. *et al.* Neuronal loss and brain atrophy in mice lacking cathepsins B and L. *Proc. Natl. Acad. Sci. USA* **99**, 7883–7888 (2002).
31. Huppa, J.B. & Ploegh, H.L. In vitro translation and assembly of a complete T cell receptor-CD3 complex. *J. Exp. Med.* **186**, 393–403 (1997).
32. Kawai, T. *et al.* Lipopolysaccharide stimulates the MyD88-independent pathway and results in activation of IFN-regulatory factor 3 and the expression of a subset of lipopolysaccharide-inducible genes. *J. Immunol.* **167**, 5887–5894 (2001).
33. Wright, S.D., Ramos, R.A., Tobias, P.S., Ulevitch, R.J. & Mathison, J.C. CD14, a receptor for complexes of lipopolysaccharide (LPS) and LPS binding protein. *Science* **249**, 1431–1433 (1990).
34. Shimazu, R. *et al.* MD-2, a molecule that confers lipopolysaccharide responsiveness on Toll-like receptor 4. *J. Exp. Med.* **189**, 1777–1782 (1999).
35. Triantafilou, M. *et al.* Membrane sorting of toll-like receptor (TLR)-2/6 and TLR2/1 heterodimers at the cell surface determines heterotypic associations with CD36 and intracellular targeting. *J. Biol. Chem.* **281**, 31002–31011 (2006).
36. Rogers, N.C. *et al.* Syk-dependent cytokine induction by Dectin-1 reveals a novel pattern recognition pathway for C type lectins. *Immunity* **22**, 507–517 (2005).
37. Yang, M. *et al.* Cathepsin L activity controls adipogenesis and glucose tolerance. *Nat. Cell Biol.* **9**, 970–977 (2007).
38. Maehr, R. *et al.* Asparagine endopeptidase is not essential for class II MHC antigen presentation but is required for processing of cathepsin L in mice. *J. Immunol.* **174**, 7066–7074 (2005).
39. Liu, L. *et al.* Structural basis of Toll-like receptor 3 signaling with double-stranded RNA. *Science* **320**, 379–381 (2008).

Appendix 2

Accessory molecules for Toll-like receptors and their function

Clarissa C. Lee*, Ana M. Avalos* and Hidde L. Ploegh

Whitehead Institute for Biomedical Research, Massachusetts Institute of Technology, Cambridge, Massachusetts 02142, USA
*These authors contributed equally to this work.

Accessory molecules for Toll-like receptors and their function

Clarissa C. Lee*, Ana M. Avalos* and Hidde L. Ploegh

Abstract | Toll-like receptors (TLRs) are essential components of the innate immune system. Accessory proteins are required for the biosynthesis and activation of TLRs. Here, we summarize recent findings on TLR accessory proteins that are required for cell-surface and endosomal TLR function, and we classify these proteins based on their function as ligand-recognition and delivery cofactors, chaperones and trafficking proteins. Because of their essential roles in TLR function, targeting of such accessory proteins may benefit strategies aimed at manipulating TLR activation for therapeutic applications.

Pattern-recognition receptors (PRRs) are germline-encoded innate immune receptors that were originally reported as sensors for pathogen-associated molecular patterns (PAMPs)[1]. PRRs can also recognize endogenous molecules that are released in response to stress or tissue damage, thus behaving as sensors of alarmins. PRRs therefore sense PAMPs and alarmins, which together constitute damage-associated molecular patterns (DAMPs)[2]. PRR engagement promotes the activation of innate and adaptive immune responses[1]. Members of the Toll-like receptor (TLR) family are PRRs that recognize pathogen-derived macromolecules, ranging from bacterial and yeast cell wall components to viral and bacterial nucleic acids. TLR ligation leads to the activation of nuclear factor-κB (NF-κB) and interferon-regulatory factors (IRFs), and these transcription factors then induce the production of pro-inflammatory cytokines and type I interferons (IFNs), respectively.

Humans express ten functional TLRs (TLR1 to TLR10), whereas twelve TLRs (TLR1 to TLR9 and TLR11 to TLR13) have been identified in mice. Ligands have been determined for all TLRs except for human TLR10, mouse TLR12 and mouse TLR13. TLR1, TLR2, TLR4, TLR5, TLR6 and TLR11 reside at the plasma membrane, where they recognize molecular components located on the surface of pathogens. By contrast, TLR3, TLR7, TLR8 and TLR9 are found intracellularly, where they mediate the recognition of nucleic acids. Thus, the subcellular distribution of TLRs correlates, to a substantial extent, with the compartments in which their ligands are found (TABLE 1).

TLRs are type I transmembrane proteins composed of an ectodomain that contains leucine-rich repeats, a single transmembrane domain and a cytoplasmic Toll/IL-1 receptor (TIR) domain that is involved in

Whitehead Institute for Biomedical Research, Massachusetts Institute of Technology, Cambridge, Massachusetts 02142, USA. Correspondence to H.L.P. e-mail: ploegh@wi.mit.edu
These authors contributed equally to this work.
doi:10.1038/nn3151
Published online
3 February 2012

the recruitment of signalling adaptor molecules. TLRs form heterodimers or homodimers as a means of triggering a signal. Most TLRs form homodimers, with a few exceptions. For example, TLR2 forms heterodimers with TLR1 or TLR6, which enables differential recognition of lipopeptides: TLR1–TLR2 recognizes triacylated lipopeptides, whereas TLR2–TLR6 responds to diacylated lipopeptides (TABLE 1).

Extracellular and endosomal TLRs have similar ectodomain sequences, a feature that is in sharp contrast with the diversity of the ligands that they recognize. One mode of ligand discrimination relies on the differences in the residues present in the ectodomains of distinct TLRs. The leucine-rich repeat modules located in the ectodomains of TLRs are each composed of 20–30 amino acids and contain the consensus sequence LxxLxLxxN. TLRs have different amino acid compositions within these modules, leading to variations in structural conformation that allow for ligand interaction[3]. Amino acid variations and the formation of heterodimers can only provide a limited platform for the recognition of the varied set of TLR ligands. Thus, another mechanism that reflects the complexity and diversity of TLR ligand composition must exist to ensure proper detection of PAMPs and discrimination between self and non-self. Specific accessory proteins or cofactors can fulfil that role. A given TLR dimer can bind to cofactors that deliver molecules of a particular composition while avoiding other ligands. These cofactors can also have roles in ensuring proper TLR folding in the endoplasmic reticulum (ER), localization to the appropriate subcellular compartment and protein processing, all of which ensure that TLRs reach their assigned subcellular compartments to bind to ligands and initiate signalling. Thus, given

Table 1 | Localization and ligands of TLRs

TLR	Subcellular localization	Physiological ligands	Synthetic ligands
TLR1–TLR2	Plasma membrane	Triacylated lipopeptides	Pam$_3$CSK$_4$
TLR2	Plasma membrane	Peptidoglycan, phospholipomannan, tGPI-mucins, haemagglutinin, porins, lipoarabinomannan, glucuronoxylomannan, HMGB1	ND
TLR2–TLR6	Plasma membrane	Diacylated lipopeptides, LTA, zymosan	FSL1, MALP2, Pam$_2$CSK$_4$
TLR3	Endosome	dsRNA	Poly:C
TLR4	Plasma membrane	LPS, VSV glycoprotein G, RSV fusion protein, MMTV envelope protein, mannan, glucuronoxylomannan, glycosylinositolphospholipids, HSP60, HSP70, fibrinogen, nickel, HMGB1	ND
TLR4–TLR6	Plasma membrane	OxLDL, amyloid-β fibrils	ND
TLR5	Plasma membrane	Flagellin	ND
TLR7	Endosome	ssRNA	Imidazoquinoline compounds: imiquimod, resiquimod, loxoribine
TLR8	Endosome	ssRNA	Resiquimod
TLR9	Endosome	DNA, haemozoin	CpG-A, CpG-B and CpG-C ODNs
TLR11 (mouse)	Plasma membrane	Profilin	ND

dsRNA, double-stranded RNA; FSL1, S-(2,3-bispalmitoyloxypropyl)-CGDPKHSPKSF; HMGB1, high-mobility group box 1 protein; HSP, heat-shock protein; LPS, lipopolysaccharide; LTA, lipoteichoic acid; MALP2, macrophage-activating lipopeptide of 2 kDa; MMTV, mouse mammary tumour virus; ND, not determined; ODN, oligodeoxynucleotide; oxLDL, oxidized low-density lipoprotein; poly:C, polyinosinic–polycytidylic acid; RSV, respiratory syncytial virus; ssRNA, single-stranded RNA; tGPI-mucin, *Trypanosoma cruzi* glycosylphosphatidylinositol-anchored mucin-like glycoprotein; TLR, Toll-like receptor; VSV, vesicular stomatitis virus.

the observed differences in ligand binding and signalling outcomes among TLRs, accessory proteins may modulate various aspects of TLR function.

For the purpose of this Review, we use the terms 'accessory protein' and 'cofactor' synonymously, and we define molecules as such when they fulfil the following roles: they are required for TLR function; they interact with a TLR or a TLR ligand; and their ability to facilitate the interaction of a TLR with a ligand has been experimentally confirmed. This definition aims to focus the Review on bona fide TLR cofactors, thereby excluding scaffolding or adaptor proteins required for signalling (such as myeloid differentiation primary-response protein 88 (MYD88) and TIR domain-containing adaptor protein inducing IFNβ (TRIF); reviewed in REFS 4,5), as well as molecules involved in crosstalk between signalling pathways (reviewed in REF. 6) and negative regulators (reviewed in REFS 4,7). We also discuss certain molecules that are essential for TLR functions (although their roles as cofactors are less well defined than those of the other accessory molecules that we describe) and that may also have roles in signalling crosstalk (BOX 1). A separate category comprises receptors that can interact with TLRs and may passively modulate TLR functions (BOX 2). Owing to space constraints, we do not discuss the sequence and structure of TLRs (which are reviewed in REF. 3), the possible crosstalk between TLRs and cytosolic innate immune receptors, or TLR signalling (which are reviewed in REFS 4,5,8–11).

Cofactors for surface TLRs

LBP in ligand delivery to surface TLRs. LPS-binding protein (LBP) is a 481-amino-acid acute-phase protein that binds with high affinity to lipopolysaccharide (LPS) derived from the outer membrane of Gram-negative bacteria[12]. This interaction facilitates the disaggregation of LPS and its presentation to CD14, an accessory protein that, among other functions, mediates TLR4 responsiveness to LPS[12,13] (FIG. 1). LBP can also bind to lipoteichoic acid (LTA), peptidoglycan and lipopeptides and transfer them to CD14, suggesting that LBP may assist not only in the function of TLR4, but also in the function of TLR1, TLR2 and TLR6 (REFS 14–16). *Lbp$^{-/-}$* mice are highly susceptible to infection with the Gram-negative bacterium *Salmonella enterica* subsp. *enterica* serovar Typhimurium compared with *Lbp$^{+/-}$* mice[17]. LBP also has a role in the *in vivo* immune response to Gram-positive pneumococci, as leukocyte influx into the cerebrospinal fluid (the hallmark of bacterial meningitis) following challenge with pneumococci was drastically reduced in *Lbp$^{-/-}$* mice compared with that in *Lbp$^{+/-}$* mice[18]. LBP thus mediates innate immune responses to PAMPs derived from both Gram-negative and Gram-positive bacteria.

MD2 in ligand recognition by TLR4. MD2 (also known as LY96) is a 160-amino-acid glycosylated soluble protein that associates with the extracellular domain of TLR4 and is required for TLR4 expression on the

Acute-phase protein
A member of a group of proteins — including C-reactive protein, serum amyloid A, fibrinogen and a 1-acid glycoprotein — that are secreted into the blood in increased or decreased quantities by hepatocytes in response to trauma, inflammation or disease. These proteins can be inhibitors or mediators of inflammatory processes.

REVIEWS

cell surface[19,20]. MD2 is necessary for TLR4-dependent responses to LPS *in vivo*[20], and *Md2*^{−/−} B cells, macrophages and dendritic cells (DCs) are hyporesponsive to LPS. *Md2*^{−/−} mice were shown to survive LPS-induced endotoxin shock and were more susceptible to *S.* Typhimurium than wild-type mice, thereby demonstrating a phenotype identical to that of *Tlr4*^{−/−} mice[20]. The crystal structure of TLR4–MD2 in complex with *Escherichia coli* LPS shows how MD2 facilitates TLR4 function[21]: LPS buries five of its six lipid chains into the hydrophobic pocket of MD2. Two MD2–LPS complexes are essential for bridging two TLR4 molecules[21] (FIG. 1). Of the TLRs whose structures have been determined in complex with a ligand (namely, TLR1–TLR2, TLR2–TLR6, TLR3 and TLR4), TLR4 is unique in that it requires an accessory molecule for ligand binding[2]. As the two molecules of TLR4 in the TLR4–MD2 heterodimer have limited direct interaction, MD2 is essential for both the ligand binding and the dimerization of TLR4 (REF. 21).

Ligand discrimination by CD36. CD36 is a 472-amino-acid double-spanning membrane glycoprotein of the scavenger receptor class B family that is found in lipid rafts[22,23]. CD36 was first implicated in the function of TLR2–TLR6 heterodimers by a genetic screen that generated a mouse homozygous for a loss-of-function allele of *Cd36* (*Cd36*[obl/obl])[24]. *Cd36*[obl/obl] macrophages showed an impaired production of tumour necrosis factor (TNF) in response to two TLR2–TLR6 ligands — namely, LTA and the *R*-stereoisomer of the diacylated lipopeptide MALP2 (*R*-MALP2) — but not to Pam₂CSK₄, Pam₃CSK₄, LPS, peptidoglycan, zymosan A, resiquimod, polyinosinic–polycytidylic acid (polyI:C) or CpG DNA[24]. Thus, CD36 enhances immune responses to some TLR2–TLR6 ligands but not to others (FIG. 1). *In vivo*, deficiency in CD36 results in an increased susceptibility to infection by the Gram-positive bacterium *Staphylococcus aureus*[24,25].

CD36 also mediates inflammatory responses to oxidized low-density lipoprotein (oxLDL) and amyloid-β fibrils through the assembly of a TLR4–TLR6 heterodimer[26]. *Tlr4*^{−/−}, *Tlr6*^{−/−} and *Cd36*^{−/−} macrophages and microglial cells failed to upregulate inflammatory mediators in response to oxLDL and fibrillar amyloid-β peptide (Aβ₁₋₄₂), respectively[26]. Human embryonic kidney 293 (HEK293) cells expressing TLR4, TLR6 and CD36 induced a higher level of expression of an NF-κB–luciferase reporter gene in response to oxLDL or Aβ₁₋₄₂ than HEK293 cells lacking CD36, suggesting that TLR4, TLR6 and CD36 function together to mediate responses to oxLDL and amyloid-β[26]. Indeed, stimulation of THP1 monocytes with oxLDL or Aβ₁₋₄₂ enhanced the association of TLR4–TLR6 with CD36 (REF. 26). Whether the TLR4–TLR6–CD36 complex recognizes and responds to PAMPs in addition to endogenous ligands remains to be determined.

How CD36 mediates the function of TLR2–TLR6 and TLR4–TLR6 is not completely understood, but the carboxyl terminus of CD36 seems to have an important role. A CD36 mutant that has a substitution of tyrosine 463 (CD36[Y463F]) failed to induce the activation of NF-κB or to mediate TLR4–TLR6 dimerization in response to oxLDL[26]. An interaction between CD36 and the tyrosine kinase LYN was shown to require residues 460–463 of CD36, and inhibition of LYN kinase activity impaired the association of CD36 with TLR4–TLR6 and blocked NF-κB activation in response to oxLDL[26]. Recruitment of LYN to the C-terminus of CD36 is thus important for the formation of a functional TLR4–TLR6–CD36 signalling complex[26]. The Y463F mutation in CD36 also abrogated CD36-mediated NF-κB activation in response to the ligand LTA[25]. Therefore, the recruitment of LYN to CD36 may also be important for the formation of a signalling-competent TLR2–TLR6–CD36 complex. A C464S mutation in CD36 also abrogates NF-κB activation in response to LTA[25]. Given that CD36 undergoes palmitoylation on residue 464, this

Lipid rafts
Structures that are proposed to arise from phase separation of different plasma membrane lipids as a result of the selective coalescence of certain lipids on the basis of their physical properties. This results in the formation of distinct and stable lipid domains in membranes that might provide a platform for membrane-associated protein organization.

Box 2 | Receptor-modulators of TLR responses

In contrast to the accessory proteins described in the main text, 'passive' receptor cofactors of Toll-like receptor (TLR) responses are membrane bound and do not necessarily interact with TLRs or their ligands. These receptors modulate TLR functions by passively delivering TLR agonists to their receptors as a result of intracellular trafficking.

B cell receptor

Antigen recognition through the B cell receptor (BCR) triggers the B cell responses required for an adaptive immune response. Immune complexes comprised of IgG and chromatin extracts induce the proliferation of autoreactive B cells that express a BCR specific for IgG; this B cell activation was shown to be dependent on myeloid differentiation primary-response protein 88 (MYD88) and was blocked by TLR9 inhibitors[51]. In addition, immune complexes containing CG-rich mammalian DNA sequences activated autoreactive B cells in a TLR9-dependent manner[62,93]. Furthermore, RNA-containing immune complexes can trigger TLR7 activation through a similar mechanism[94]. BCR ligation has been shown to affect the trafficking of TLR9. BCR stimulation leads to TLR9 trafficking to an autophagosome-like compartment[95], and TLR9 activation by ligands delivered by the BCR results in a different cytokine profile from that induced by CpG DNA-mediated TLR9 stimulation in the absence of a BCR stimulus[96]. Future studies should aim to clarify the crosstalk pathways that link BCR activation with the trafficking and/or activation of TLRs in B cells.

RAGE

Receptor for advanced glycation end-products (RAGE) was the first reported receptor for high-mobility group box 1 protein (HMGB1)[97]. RAGE was originally characterized as a receptor for adducts of proteins, lipids and nucleic acids that are produced non-enzymatically in highly oxidative environments. RAGE ligation leads to nuclear factor-κB (NF-κB) activation and pro-inflammatory cytokine production, which is self-sustained and therefore dysregulated[98]. RAGE was shown to modulate TLR9 functions in plasmacytoid dendritic cells, in which the addition of HMGB1 potentiated CpG-induced production of interferon-α in a RAGE-dependent manner[40]. Whether HMGB1 loaded with RNA can trigger TLR3 or TLR7 responses through RAGE remains to be determined.

signalling defect may be attributed to the inability of CD36[C464S] to be properly targeted to lipid rafts[27]. Thus, fine-tuning of CD36-mediated TLR assembly and responses to ligands depend on the localization of CD36 to plasma membrane microdomains, where it can interact with downstream components.

CD14: a cofactor for several TLRs. CD14 is a 375-amino-acid glycoprotein composed of leucine-rich repeats that is present in a soluble form in the blood or as a glycosylphosphatidylinositol (GPI)-anchored membrane protein on myeloid cells. CD14 interacts with multiple TLR ligands and enhances their ability to activate TLRs (FIG. 1). Direct binding studies using recombinant CD14 show that CD14 has the unusual ability to bind to a variety of microbial products (and their synthetic analogues), including LPS, peptidoglycan, Pam₂CSK₄, polyI:C and CpG DNA[14,28–31]. The crystal structure of CD14 shows it to be a dimer, and the two subunits together form a horseshoe-shaped structure that is reminiscent of the structure of the ectodomains of TLRs. The amino terminus of each subunit is equipped with a hydrophobic pocket, which is the principal component of the LPS-binding site in CD14 (REF. 32). The CD14 binding sites for different TLR ligands appear to overlap, as LPS can compete with DNA and peptidoglycan, LTA can compete with peptidoglycan, and double-stranded DNA can (partially) compete with polyI:C for CD14 binding[14,28,30]. How CD14 can bind to ligands with such different molecular compositions remains to be established, and crystal structures of CD14 in complex with ligands would help to address this question.

CD14 was first implicated in TLR4-mediated immune responses. At doses of LPS or Gram-negative bacteria that kill wild-type mice, *Cd14⁻/⁻* mice survive and produce negligible amounts of TNF and interleukin-6 (IL-6)[33]. In response to LPS, CD14 is required for

TRIF-dependent signalling and, at low doses of LPS, for MYD88-dependent signalling[13,34]. It has been shown that CD14 can chaperone LPS from LBP to TLR4–MD2 at the cell surface, and new evidence demonstrates that CD14 also mediates the LPS-induced endocytosis of TLR4, resulting in the delivery of TLR4 to a compartment from which it can engage TRIF-dependent signalling[34–37]. Thus, for TLR4 activation, CD14 facilitates both ligand delivery and TLR4 endocytosis.

CD14 also enhances immune responses to the endosomal TLR ligands polyI:C, imiquimod and CpG DNA[28,30]. CD14 probably promotes the general internalization of nucleic acids, as the addition of soluble CD14 increased the internalization of polyI:C by Chinese hamster ovary (CHO) cells, and *Cd14⁻/⁻* macrophages internalized less CpG DNA than wild-type macrophages[28,30]. However, responses to polyI:C, imiquimod and CpG DNA are not completely abrogated in the absence of CD14, suggesting the existence of additional factors that can mediate their delivery[28,30]. Although CD14 has been shown to associate with TLR3, TLR7 and TLR9 (REFS 28,30), it is unclear whether CD14 mediates the trafficking of these endosomal TLRs, as it does for TLR4, or whether it just mediates ligand trafficking.

Reflecting its ability to bind to diverse ligands, CD14 also mediates TNF production in response to the TLR2–TLR6 ligands MALP2, LTA, zymosan A and Pam₂CSK₄. Moreover, CD14 participates in TLR-mediated immune responses to various viruses, including respiratory syncytial virus (RSV; which activates CD14 through its fusion protein), vesicular stomatitis virus (VSV; which activates CD14 through its glycoprotein G), human cytomegalovirus (HCMV) and influenza A virus[13,28,38–40]. How exactly CD14 is involved in these processes remains to be determined but, as shown for LPS and nucleic acids, CD14 may mediate the interaction of ligands with several TLRs.
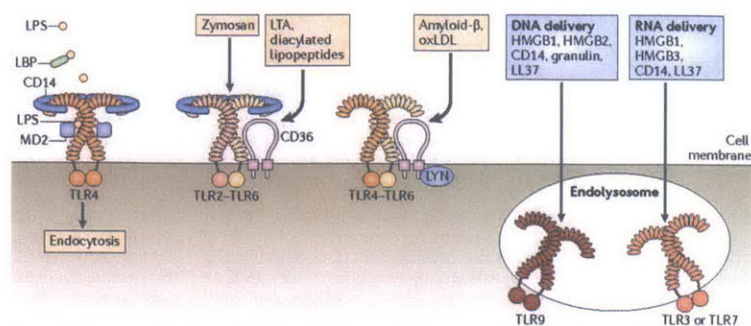
REVIEWS

Figure 1 | Accessory molecules mediate ligand binding and delivery to surface and endosomal TLRs.
The Toll-like receptor 2 (TLR2)–TLR6 heterodimer uses CD14 to respond to zymosan and both CD14 and CD36 to respond to lipoteichoic acid (LTA) and diacylated lipopeptides. LPS-binding protein (LBP) binds to lipopolysaccharide (LPS) and presents it to CD14, which is required for TIR domain-containing adaptor protein inducing IFNβ (TRIF)-dependent signalling in response to LPS and, at low doses of LPS, for myeloid differentiation primary-response protein 88 (MYD88)-dependent signalling. MD2 is necessary for TLR4 to bind to LPS and homodimerize. CD36 is needed for the TLR4–TLR6 heterodimer to respond to the altered self components amyloid-β and oxidized low-density lipoprotein (oxLDL). Endosomal TLRs also use cofactors for nucleic acid delivery. CD14 and high-mobility group box (HMGB) proteins bind to double-stranded RNA, single-stranded RNA and DNA, and mediate the delivery of these nucleic acids to TLR3, TLR7 and TLR9, respectively. LL37 binds to both RNA and DNA and delivers them to TLR7 and TLR8 (in the case of RNA) or TLR9 (for DNA). Granulin binds only to DNA and mediates DNA delivery to TLR9. Signalling from TLRs culminates in the activation of transcription factors — namely, activator protein 1, nuclear factor-κB and interferon-regulatory factors — and the production of pro-inflammatory cytokines and type I interferons (not shown).

Delivery of TLR ligands by TRIL. TLR4 interactor with leucine-rich repeats (TRIL) is a type I transmembrane protein of 811 amino acids that contains 12 predicted leucine-rich repeats in its extracellular domain. TRIL is highly expressed in the brain and its expression can be induced by LPS and polyI:C[41,42]. TRIL colocalizes with early endosomal markers in the human astrocytoma cell line U373 but was found on the surface of HEK293 cells, suggesting that TRIL may have cell type-specific localization patterns[41,42]. Knockdown experiments demonstrated that TRIL mediates TLR3 and TLR4 signalling, but not TLR2 or TLR9 signalling[41,42]. TRIL co-immunoprecipitates with LPS, TLR3 and TLR4, suggesting an involvement for TRIL in ligand delivery[41,42]. Future studies should clarify whether TRIL, like CD14, is involved in mediating ligand delivery to TLR3 and TLR4 and whether TRIL has a specialized function in the brain.

Ligand delivery to endosomal TLRs

Granulin delivers CpG DNA to TLR9. Granulin is a cysteine-rich glycosylated multifunctional protein that is produced as a result of proteolytic processing of its 593-amino-acid precursor, progranulin, by the serine proteases elastase and proteinase 3 (also known as myeloblastin)[43,44]. Multiple cell types constitutively secrete progranulin, and it is present at high levels in serum[43-45]. Granulin fragments were shown to interact with full-length TLR9 by immunoprecipitation from RAW264.7 macrophages treated with the broad cysteine protease inhibitor Z-FA-FMK. Addition of exogenous progranulin enhanced TNF secretion by RAW264.7 macrophages in

response to synthetic oligodeoxynucleotides (ODNs) of the CpG-B and CpG-C classes, and mice deficient in progranulin (*Grn*⁻/⁻ mice) had a defect in TNF production[45]. *Grn*⁻/⁻ bone marrow-derived macrophages (BMDMs) were less able to bind to CpG DNA than their wild-type counterparts, and this defect could be corrected by the addition of exogenous progranulin. Progranulin binds not only to CpG ODNs, but also to ODNs with inhibitory activity, suggesting that granulin binds to ODNs in a sequence-independent manner. The binding of CpG ODNs to the C-terminus of TLR9 was impaired in *Grn*⁻/⁻ mice; thus, granulin may facilitate the delivery of CpG DNA to lysosomal compartments (FIG. 1). The inhibition of elastase activity reduced TNF responses to CpG DNA, suggesting that the processing of progranulin into its fragments is required for its contribution to TLR9 signalling[45]. Taken together, these results demonstrate that granulin helps to deliver CpG DNA to the appropriate compartment to promote TLR9 responses. It is still unclear whether granulins interact with a surface receptor, whether they can bind to double-stranded DNA, and what determines the enhancement of TLR9 responses to CpG-B and CpG-C but not CpG-A ODNs. Future studies should aim to clarify these issues and also determine which forms of granulin are required for TLR9 activation.

HMGB1-mediated delivery of RNA and DNA. Members of the high-mobility group box (HMGB) family are nuclear proteins associated with chromatin that are involved in making DNA available for the regulation of transcription[46]. The most-studied

member of this family is HMGB1, which mediates its pro-inflammatory functions through interactions with its receptors — TLR2, TLR4 and receptor for advanced glycation end-products (RAGE) — and has a role in sterile inflammation (injury) and infection[47]. HMGB1 is a 215-amino-acid soluble protein composed of two DNA-binding domains containing basic amino acids (the A and B boxes) and an acidic tail, and it binds to DNA in a sequence-independent manner. HMGB1 displays pro-inflammatory functions once secreted by the cell, and this activity led to the exploration of whether HMGB1 could deliver ligands to TLR9 and other endosomal TLRs.

HMGB1 was described as a TLR9 cofactor based on its ability to bind to CpG DNA, to interact with TLR9 and to enhance the delivery of TLR9 to endosomal compartments in response to CpG DNA. Exogenous addition of HMGB1 enhances the production of IFNα and pro-inflammatory cytokines in response to CpG DNA in DCs and macrophages[48,49]. IFNα secretion was dependent on the interaction of HMGB1 with RAGE[49], which is a 'passive' receptor cofactor of TLR9 (BOX 2). An absence of HMGB1 decreases the ability of CpG DNA to upregulate the expression of type I IFNs and the secretion of pro-inflammatory cytokines (such as IL-6, TNF and IL-12p40) by DCs[48]. In patients with lupus, HMGB1 forms complexes with nucleosomes that circulate in the blood as a result of increased apoptosis. Such HMGB1–nucleosome complexes induce pro-inflammatory cytokine production by peripheral blood mononuclear cells[50]. Immune complexes containing mammalian DNA, HMGB1 and IgG can activate autoreactive B cells in a TLR9-dependent manner[49,51]. HMGB1 binds to both CG-rich and CG-poor DNA, but only the delivery by the B cell receptor of CG-rich mammalian DNA — in the form of HMGB1–DNA–IgG immune complexes — promotes TLR9-dependent B cell activation[52] (BOX 2). Therefore, HMGB1 is required for TLR9 responses to CpG DNA and may exacerbate autoimmune disease owing to its ability to bind DNA.

HMGB proteins may be universal mediators of innate immune responses to nucleic acids. HMGB1 binds to both DNA and RNA, and the closely related proteins HMGB2 and HMGB3 bind to DNA and RNA, respectively. HMGB proteins are required for type I IFN and pro-inflammatory cytokine production in response to RNA (through TLR3 and TLR7) and DNA (through TLR9)[53]. Although direct binding of HMGB proteins to these TLRs was not demonstrated in this study, an absence of HMGB protein function decreased responses to DNA and RNA. HMGB proteins are thus required for normal inflammatory immune responses to nucleic acids[53]. However, it is not clear how HMGB proteins distinguish between DNA and RNA. Furthermore, how can these proteins resist degradation once outside of the cell? Is their binding to nucleic acids regulated? If HMGB proteins are implicated in 'promiscuous sensing' of nucleic acids, then what prevents immune responses to self DNA and self RNA? Future studies should address these questions to further clarify the role of HMGB proteins in responses to nucleic acids.

Sterile inflammation
An inflammatory response triggered by tissue damage in the absence of infection.

Amphipathic peptide
A peptide that contains hydrophilic and hydrophobic domains, which allow the peptide to interact both with charged residues and with lipophilic structures.

Endosomes
Vesicles of the endocytic pathway that transport proteins from the plasma membrane and the Golgi compartment and have a mildly acidic pH.

Paralogue
A homologous gene that resulted from a gene duplication event.

LL37-mediated ligand delivery to endosomal TLRs. LL37 has been reported to be a TLR9 cofactor and has been implicated in the delivery of self DNA to TLR9 in plasmacytoid DCs (pDCs)[54]. LL37 is a 37-amino-acid amphipathic peptide that is activated through the cleavage of its precursor, cathelicidin antimicrobial peptide, by a serine protease[55,56]. LL37–DNA complexes are resistant to degradation by DNases; they are internalized by pDCs and subsequently localize to early endosomes, from where they mediate TLR9-dependent IFNα production[54]. Patients with psoriasis — a skin autoimmune disease characterized by local activation of DCs and T cells — have an infiltration of pDCs in the skin and high expression levels of LL37 in keratinocytes[55]. LL37 drives pDC activation and IFNα production in psoriasis by binding to DNA that is released by injured cells. There is no evidence for a direct interaction between LL37 and TLR9, suggesting that LL37 may serve mostly as a DNA-delivery molecule in situations of cell injury. LL37 has also been shown to form complexes with self RNA and to deliver these complexes to pDCs to initiate TLR7- and TLR8-dependent IFN production. LL37–self RNA complexes are also found in psoriatic skin lesions[57]. Thus, LL37 — like HMGB proteins — can bind to self nucleic acids to mediate their delivery to endosomal TLRs. Whether LL37 is important for host defence in the context of TLR-driven responses remains to be established.

TLR chaperones and trafficking factors

TLR folding by GRP94 and PRAT4A. Glucose-regulated protein of 94 kDa (GRP94; also known as gp96 and endoplasmin) is an 803-amino-acid ER paralogue of the heat-shock protein 90 (HSP90) chaperone, which mediates protein folding. GRP94 is ubiquitously expressed and exists as an obligate soluble homodimer, with each subunit composed of an N-terminal ATP-binding domain, a highly charged middle domain and a C-terminal dimerization domain[58]. The viability of B cells, macrophages and embryonic stem cells does not require GRP94; thus, GRP94 is not essential for global protein quality control in the ER[59–62].

So far, a limited number of targets have been identified for GRP94, including integrins, platelet glycoprotein complexes and TLRs[58–60,62,63]. GRP94 is necessary for the function of TLR1, TLR2, TLR4, TLR5, TLR7 and TLR9, but not that of TLR3 (REFS 59,60,62). GRP94 co-immunoprecipitates with TLR1, TLR2, TLR4 and TLR9; moreover, it is required for the surface expression of TLR1, TLR2 and TLR4 and for the maturation and cleavage of TLR9 (REFS 60,62,64). Thus, GRP94 mediates the folding and maturation of TLRs to allow them to exit the ER. Exactly at what stage GRP94 intervenes in TLR folding, and how, is not known. Until recently, it was unclear whether the function of GRP94 — like that of HSP90 — required co-chaperones. Recent evidence suggests that PRAT4A (protein associated with TLR4 A) may fulfil that role.

PRAT4A is a ubiquitous and highly conserved soluble 276-amino-acid protein found in the ER lumen that was identified as a protein that co-immunoprecipitates with TLR4 (REF. 65). Bone marrow-derived DCs (BMDCs),

REVIEWS

macrophages and B cells isolated from *Prat4a⁻/⁻* mice produced lower levels of cytokines than control cells in response to ligands for TLR1, TLR2, TLR4, TLR7 and TLR9, but not following stimulation with ligands for TLR3, a phenotype similar to that of *Grp94* conditional-knockout mice[66]. Small hairpin RNA (shRNA)-mediated knockdown of PRAT4A expression in B cell lines impeded the passage of TLR1 and TLR4 through the Golgi and prevented ligand-induced trafficking of TLR9 from the ER to endolysosomes[66]. Thus, PRAT4A, like GRP94, is important for the maturation of multiple TLRs in the ER. However, it is not a chaperone for general membrane glycoprotein synthesis, as PRAT4A-deficient BMDCs showed normal surface expression of CD14, MHC class I molecules and CD11c[66].

PRAT4A and GRP94 work together to ensure the proper folding of TLRs (FIG. 2). PRAT4A and GRP94 can interact directly *in vitro*[64], and amino acid substitutions in GRP94 (E103A) and PRAT4A (M145K) that prevent the exit of TLRs from the ER also prevent GRP94 and PRAT4A from associating *in vivo*[60,64,67]. Knockdown of PRAT4A expression impaired the association of GRP94 with TLR9 and, similarly, knockdown of GRP94 expression disrupted PRAT4A–TLR9 binding[64], indicating that PRAT4A and GRP94 are dependent on each other for their interactions with TLR9. For other TLRs, a similar folding mechanism may operate.

As an ER luminal protein, GRP94 interacts with the ectodomains of TLRs; this has been confirmed by co-immunoprecipitation of GRP94 with fusion proteins that contain the ectodomain of TLR4, TLR9 or TLR11 fused to the transmembrane domain of the platelet-derived growth factor receptor[64]. Such fusion proteins of TLR4, TLR9 and TLR11 were expressed on the cell surface of wild-type pre-B cells but not GRP94-deficient pre-B cells[64]. Similar results were found when measuring the surface expression of TLR fusion proteins on RAW264.7 cells transduced with *Prat4a*-targeted shRNA[64]. Thus, both GRP94 and PRAT4A are required to mediate the proper folding of TLR ectodomains, so that the TLRs can exit the ER.

Both GRP94 and PRAT4A are essential for the folding of several TLRs, but many questions remain. What features of the folding, dimerization and/or stability of TLRs (except TLR3) dictate a need for GRP94 and PRAT4A? Notwithstanding its structural similarity to the other TLRs, does TLR3 require a different set of specialized chaperones in place of GRP94 and PRAT4A, or is it inherently less dependent on chaperones? The structural motif in TLRs that is recognized by GRP94 and PRAT4A remains to be molecularly defined, and this leaves open the possibility of identifying additional client proteins through a search for proteins that contain the relevant motif(s). Together, these results suggest that TLRs have unique folding requirements compared with other glycoproteins (BOX 3).
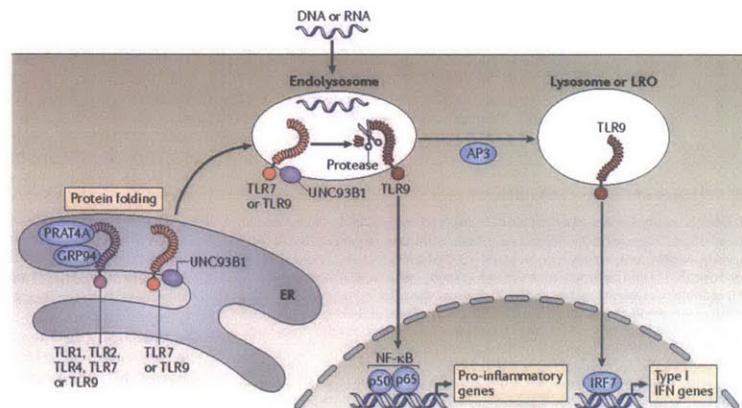

Figure 2 | ER chaperones and trafficking and processing factors for TLRs. The endoplasmic reticulum (ER) luminal chaperones glucose-regulated protein of 94 kDa (GRP94) and protein associated with TLR4 A (PRAT4A) are responsible for the proper folding and function of Toll-like receptor 1 (TLR1), TLR2, TLR4, TLR7 and TLR9, but not TLR3. The ER membrane protein uncoordinated 93 homolog B1 (UNC93B1) is required for the translocation of TLR7 and TLR9 to endolysosomes, where these TLRs are cleaved by cathepsins and asparagine endopeptidase. The cleaved TLRs bind to their ligands (RNA or DNA), which trigger the recruitment of signalling components, leading to nuclear factor-κB (NF-κB)-dependent production of pro-inflammatory cytokines. The adaptor protein 3 (AP3) complex mediates the translocation of TLR9 to lysosome-associated membrane glycoprotein 2 (LAMP2)-expressing lysosomes or lysosome-related organelles (LROs), where the interferon-regulatory factor 7 (IRF7) signalling pathway is initiated, leading to the expression of type I interferon (IFN) genes.

121

Lysosomes
Organelles involved in protein degradation that have a low pH and correspond to the last step of the endocytic pathway.

Lysosome-related organelles
(LROs). Cell type-specific compartments that share properties with lysosomes but have specialized functions. LROs include melanosomes, lytic granules, MHC class II compartments, platelet-dense granules, basophil granules and azurophil granules.

Endosomal TLR trafficking by UNC93B1. Uncoordinated 93 homolog B1 (UNC93B1) is a 598-amino-acid ER-resident glycoprotein that is predicted to span the membrane 12 times[68]. Mice homozygous for a missense mutation (H412R) located in the ninth predicted transmembrane domain of UNC93B1 (known as 3d mice) have impaired signalling via TLR3, TLR7 and TLR9 and show an increased susceptibility to various viral and bacterial pathogens[68]. Similarly, cells from human patients with mutations that result in truncated *UNC93B1* transcripts have defective TLR3, TLR7, TLR8 and TLR9 signalling[69]. Thus, UNC93B1 is required for endosomal TLR responses (FIG. 2).

Co-immunoprecipitation experiments show that UNC93B1 interacts with TLR3, TLR7, TLR8, TLR9 and TLR13, but not with TLR4, and its interaction with TLRs is eliminated by the H412R mutation[70]. Replacement of the transmembrane domain of TLR3 or TLR9 with that of TLR4 resulted in a TLR chimaera that was unable to interact with UNC93B1, whereas replacement of the transmembrane domain of TLR4 with that of TLR3 or TLR9 resulted in chimeric proteins that could interact with UNC93B1. The transmembrane domain of endosomal TLRs thus controls association with UNC93B1 (REF. 70). Ligand-induced trafficking of UNC93B1, TLR7 and TLR9 to CpG-containing endolysosomal compartments is defective in BMDCs from 3d mice[71]. Therefore, nucleic acid-sensing TLRs must interact with UNC93B1 via their transmembrane domains so that UNC93B1 can mediate their delivery to endolysosomes, where they can bind and respond to their respective ligands.

UNC93B1 discriminates between various nucleic acid-sensing TLRs. A D34A missense mutation in UNC93B1 renders TLR7 hyperresponsive and TLR9 hyporesponsive, whereas TLR3 is unaffected. This is due to a stronger association between this UNC93B1 mutant and TLR7 (REF. 72). Mice homozygous for

the *Unc93b1*[D34A] allele die prematurely owing to systemic inflammation[73]. TLR7 is responsible for the pathologies of the *Unc93b1*[D34A/D34A] mice, because *Unc93b1*[D34A/D34A]*Tlr7*^{−/−} mice showed normal survival and splenic cell numbers. Increased trafficking of TLR7 to endolysosomes in the absence of ligand was observed in *Unc93b1*[D34A/D34A] stem cell-derived DCs compared with the levels in wild-type DCs[73]. The D34A mutation in UNC93B1 thus leads to aberrant trafficking and activation of TLR7.

The role of UNC93B1 in TLR biology is intriguing. How the cell perceives and processes the signals that are initially required for the trafficking of UNC93B1–TLR complexes from the ER to their endolysosomal destination remains unknown. Are there small numbers of functional nucleic acid-sensing TLRs at the cell surface that could transmit this signal? Are additional nucleic acid sensors involved? It is also becoming apparent that the intracellular distribution of nucleic acid-sensing TLRs mediated by UNC93B1 may differ between cell types. For example, in B cells from transgenic mice that express green fluorescent protein-linked TLR9, TLR9 was shown to preferentially localize to an endolysosomal compartment even in the absence of any obvious stimulation (A.M.A., M. M. Brinkmann and H.L.P., unpublished observations). Also, how TLR–UNC93B1 oligomeric structures assemble in the ER remains a 'black box'.

Divergence of TLR9 responses by AP3. Adaptor protein 3 (AP3) is a required component of the trafficking machinery for TLR9. Members of the adaptor protein family are tetrameric complexes that mediate the sorting of membrane proteins in the secretory and endocytic pathways[74]. AP3 — which consists of the subunits δ, μ3A, β3A and σ3 — recruits cargo proteins into endosomes for delivery to lysosomes and lysosome-related organelles[74]. Compared with control cells, BMDMs lacking the β3A subunit of AP3 (*Ap3b1*^{−/−} BMDMs) had reduced IFN expression in response to CpG-A ODNs complexed with the cationic lipid DOTAP (DOTAP–CpG-A), polyI:C or LPS[75]. pDCs from mice with mutations in *Ap3b1* show a similar defect in IFN production in response to CpG-A ODNs, VSV or influenza virus[75,76]. Following treatment of AP3-deficient BMDMs with DOTAP–CpG-A, TLR9 was not observed in lysosome-associated membrane glycoprotein 2 (LAMP2)-expressing compartments at 6 hours post-stimulation, suggesting a role for AP3 in recruiting TLR9 to lysosomes or lysosome-related organelles[75]. Furthermore, the recruitment of IRF7 to lysosomes containing CpG-A ODNs was impaired in AP3-deficient BMDMs[75]. Thus, the failure of TLR9 to reach LAMP2^{+} compartments and the lack of IRF7 recruitment are responsible for the defective IFN response in AP3-deficient BMDMs.

These findings contrast with observations made at earlier time points (such as 90 minutes post-stimulation), when CpG-A ODNs are observed in endosomes of pDCs[77,78]. DOTAP-mediated retention of CpG-A ODNs in endosomes of macrophages, which do not

---

Box 3 | Unique folding of TLRs in the ER

Several proteins associate with Toll-like receptors (TLRs) early in the course of their biosynthesis. These include chaperones — such as glucose-regulated protein of 94 kDa (GRP94) and protein associated with TLR4 A (PRAT4A), which are soluble proteins that reside in the lumen of the endoplasmic reticulum (ER) — as well as ER membrane proteins that possess multiple membrane-spanning segments (such as uncoordinated 93 homolog B1 (UNC93B1)). Some of these proteins, including GRP94, clearly assist in the biogenesis of glycoproteins other than TLRs. Others, such as UNC93B1, appear to be far more selective for TLRs. Little is known about the oligomeric states of these TLR-associated proteins themselves, but the current incomplete picture that has emerged is that of a highly complex launching pad that prepares TLRs for their release from the ER in a properly assembled form. Other accessory molecules may not associate with TLRs until they have reached their final destination.
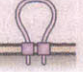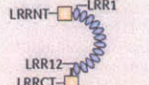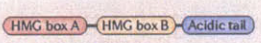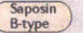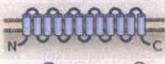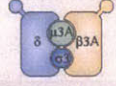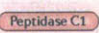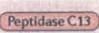
The proper assembly of multiprotein complexes such as the T cell receptor is a prerequisite for their exit from the ER, a concept referred to as architectural editing. This means that the absence of a single subunit compromises assembly, egress from the ER and hence surface display. A similar concept may apply to the formation of signalling-competent TLR assemblies. However, we have little mechanistic information on how each of the proteins discussed in this article participates in the generation of active TLRs. This, clearly, is an area in need of further exploration.

Appendix 2: Accessory molecules for Toll-like receptors and their function

normally produce IFNs, promoted the recruitment of IRF7 and MYD88 to CpG-A ODN-containing endosomes and the expression of IFNs[78]. Thus, the endosomal compartment was thought to be crucial for IFN production. It is necessary to reconcile these findings with the observation that AP3-mediated trafficking of TLR9 to LAMP2+ compartments is necessary for IFN production by BMDMs stimulated with DOTAP–CpG-A. Further trafficking studies thus need to be conducted to clarify this point and to determine whether AP3 is also involved in the trafficking of TLR3, TLR4 or TLR7.

Table 2 | Accessory molecules for TLR function

Name	Protein domain structure	Localization	Interacting TLR	Interacting ligand	Refs
Mediators of ligand delivery and/or recognition					
LBP	BPI1 — BPI2	Secreted	None demonstrated	LPS	12
MD2	ML	Plasma membrane	TLR4	LPS	19–21
CD36		Plasma membrane, Golgi	TLR2, TLR4, TLR6	FSL1, LTA, oxLDL, amyloid-β fibrils	23,26, 99–101
CD14	LRR1 — LRR11	Secreted, plasma membrane (GPI-linked), endolysosomes	TLR2, TLR3, TLR4, TLR7, TLR8, TLR9	LPS, peptidoglycan, Pam$_3$CSK$_4$, polyI:C, CpG DNA	14,23,29–31, 102,103
TRIL	LRRNT — LRR1, LRR12, LRRCT	Plasma membrane, early endosomes	TLR3, TLR4	LPS	41,42
Progranulin	P-G-F-B-A-C-D-E Granulin domain	Secreted, endolysosomes	TLR9	CpG-A, CpG-B, CpG-C and inhibitory ODNs	45
HMGB1	HMG box A — HMG box B — Acidic tail	Nucleus, cytoplasm, can be secreted following TLR ligation	TLR9, possibly TLR3 and TLR7	CpG-A ODNs, CpG-B ODNs, DNA, RNA	48,49,53
LL37	Amphipathic helix-bend-helix	Early endosomes	Possibly TLR7 and TLR9	Mammalian DNA, mammalian RNA	54,57
Chaperones					
GRP94	ATP-binding domain, Charged domain, Dimerization domain	ER	TLR1, TLR2, TLR4, TLR9	None demonstrated	58,60,62,64
PRAT4A	Saposin B-type	ER	TLR1, TLR2, TLR4, TLR9	None demonstrated	64–67
Molecules that facilitate the trafficking of endosomal TLRs					
UNC93B1	N — C	ER, endolysosomes	TLR3, TLR7, TLR8, TLR9, TLR13	None demonstrated	68,70,71
AP3	δ, μ3A, β3A, σ3	TGN, endolysosomes, LROs	TLR9	None demonstrated	75
TLR-processing enzymes					
Cathepsins	Peptidase C1	Endosomes, lysosomes	TLR9, possibly TLR3 and TLR7	None demonstrated	79,80,84
AEP	Peptidase C13	Endosomes, lysosomes	TLR9, possibly TLR3 and TLR7	None demonstrated	83,84

AEP, asparagine endopeptidase; AP3, adaptor protein 3; BPI1, BPI/LBP/CETP N-terminal domain; BPI2, BPI/LBP/CETP C-terminal domain; ER, endoplasmic reticulum; FSL1, S-(2,3-bispalmitoyloxypropyl)-CGDPKHSPKSF; GPI, glycosylphosphatidylinositol; GRP94, glucose-regulated protein of 94 kDa; HMGB1, high-mobility group box 1 protein; LBP, LPS-binding protein; LPS, lipopolysaccharide; LRO, lysosome-related organelle; LRR, leucine-rich repeat; LRRCT, LRR C-terminal domain; LRRNT, LRR N-terminal domain; LTA, lipoteichoic acid; ML, MD2-related lipid-recognition domain; ODN, oligodeoxynucleotide; oxLDL, oxidized low-density lipoprotein; polyI:C, polyinosinic–polycytidylic acid; PRAT4A, protein associated with TLR4 A; TGN, trans-Golgi network; TLR, Toll-like receptor; TRIL, TLR4 interactor with leucine-rich repeats; UNC93B1, uncoordinated 93 homolog B1.

123

TLR processing factors

TLR9 undergoes proteolytic processing following its arrival at endolysosomal compartments, and possibly also in early endosomes that are endowed with a low pH and proteases[79,80]. Proteases that process TLRs must interact with them, at least transiently, and are thus considered cofactors. The endosomal–lysosomal complement of proteases is composed mostly of cathepsins. Cathepsins were first implicated in TLR9 function when it was found that inhibition of cathepsin K ameliorated disease in an adjuvant-induced mouse model of arthritis, and cathepsin K deficiency resulted in a decreased BMDC cytokine response to CpG DNA but not to TLR3, TLR7, TLR8 or TLR2–TLR6 ligands[81]. By functional cDNA cloning, cathepsin B, cathepsin L, cathepsin S and cathepsin F were identified as factors associated with TLR9 function in a B cell line. Furthermore, the inhibition of these cathepsins by small molecules blocked TLR3-, TLR7- and TLR9-mediated responses in primary B cells[82]. The combined action of cathepsin L and cathepsin S results in cleavage of TLR9 (REF. 80), an event required for signalling[79,80]. Inhibitors for individual cathepsins failed to fully inhibit cleavage and TLR-driven responses[79,84]; the activity of multiple cathepsins is therefore required for full TLR9 activity. Asparagine endopeptidase (AEP; also known as legumain) is a lysosomal protease that cleaves C-terminal to asparagine residues. AEP can cleave TLR9 and thus mediates its activation in DCs[83]. Therefore, AEP and cathepsins appear to have redundant and/or sequential roles in the cleavage of TLR9 in different types of antigen-presenting cells[84].

Proteolytic processing has also been reported for TLR3 and TLR7 (REFS 79,84), and cleavage may therefore be a general occurrence for endosomal TLR activation. However, the partial inhibition of TLR cleavage and activation that is achieved by inhibitors of cathepsin and AEP suggests that proteolysis, although important, may not be essential for the activation of TLR3 and TLR7 (REF. 84). A differential requirement for either AEP or cathepsins in the proteolytic conversion and activation of TLR9 probably reflects variations in protease expression in different tissues and cell types. A better understanding of the regulation of TLR3, TLR7 and TLR9 cleavage and function demands a cell type-specific exploration of the proteases required for activation. However, it remains to be established whether these results can be generalized to other species, including humans.

Cofactors and advances in TLR biology

The identification of new TLR accessory molecules and the elucidation of their mechanisms of action have led to a greater understanding of TLR biology. From a biological perspective, ligand discrimination by different TLRs can be accomplished through the use of different cofactors that aid in the specificity of ligand recognition. However, many accessory proteins (exemplified by UNC93B1 and CD14) appear to be used by several TLRs, suggesting an additional layer of complexity in the mechanisms by which TLRs distinguish one ligand from another (TABLE 2).

Many questions still remain regarding the role of cofactors in different aspects of TLR biosynthesis, trafficking, ligand recognition and activation.

The involvement of UNC93B1 in the trafficking of signalling-competent TLR3, TLR7 and TLR9 and how this polytopic protein regulates its interactions with its client TLRs is incompletely understood. The emerging picture is that the role of UNC93B1 is more complex than merely serving as a delivery platform for endosomal TLRs. Much remains to be learnt about the assembly of UNC93B1–TLR complexes in the ER, their exit sites and their targeting to organelles for proper TLR function. Trafficking factors such as AP3 are important for compartment-specific regulation of TLR signalling. But are all cells subject to this differential TLR distribution? With the discovery of AP3 as a cell- and compartment-specific cofactor — together with the recent identification of viperin (also known as RSAD2) as a possible TLR7 and TLR9 signalling adaptor molecule specific for the production of IFNα[85] — this area of TLR biology is coming into focus.

The ability of surface TLRs to sense a wide variety of diverse ligands contrasts with the restricted specificity of endosomal TLRs (TABLE 1). Is this due to the presence of more surface TLR cofactors for ligand discrimination or to the variety of extracellular PAMPs found in nature? The more-restricted pattern of endosomal TLR ligand recognition probably evolved as an adaptation to prevent the recognition of self nucleic acids that mimic those of microbial origin. The use of cofactors for ligand recognition makes a special case for TLR7 and TLR8: their activation by small molecules such as the imidazoquinolines is not easily reconciled with the mode of natural ligand binding to other TLRs, and the existance of a TLR7- or TLR8-associated cofactor would be an obvious solution to this conundrum. Importantly, it also remains to be determined how ubiquitous cofactors (such as granulin and HMGB1, which can potentially carry pro-inflammatory endogenous nucleic acids) enter cells and reach TLR-containing compartments.

Conclusions and future perspectives

The TLR field has rapidly evolved since the initial discovery of receptors that recognize widely different PAMPs but contain structurally conserved ectodomains. Many molecules that contribute to ligand discrimination and receptor signalling have been identified, and such molecules have different roles, for example as cofactors, signalling adaptors and molecules, and regulators of TLR function. The final result of TLR specificity and activation must stem from a combination of such mediators, resulting in complex signalling platforms.

Because of their contributions to TLR function, the study of cofactors that help to activate TLRs yields the obvious dividend of a better understanding of TLR pathways that control innate and adaptive immunity. Whether such knowledge can be applied to devise new therapies is impossible to gauge, but the elucidation of additional means of manipulating TLRs remains a highly desirable goal. We may thus anticipate important advances in our understanding of the roles of TLR accessory proteins.

REVIEWS

1. Janeway, C. A. Jr & Medzhitov, R. Introduction: the role of innate immunity in the adaptive immune response. *Semin. Immunol.* **10**, 349–350 (1998).
2. Bianchi, M. E. DAMPs, PAMPs and alarmins: all we need to know about danger. *J. Leukoc. Biol.* **81**, 1–5 (2007).
3. Kang, J. Y. & Lee, J.-O. Structural biology of the Toll-like receptor family. *Annu. Rev. Biochem.* **80**, 917–941 (2011).
4. Kawai, T. & Akira, S. The role of pattern-recognition receptors in innate immunity: update on Toll-like receptors. *Nature Immunol.* **11**, 373–384 (2010).
5. O'Neill, L. A. & Bowie, A. G. The family of five: TIR-domain-containing adaptors in Toll-like receptor signalling. *Nature Rev. Immunol.* **7**, 353–364 (2007).
6. Trinchieri, G. & Sher, A. Cooperation of Toll-like receptor signals in innate immune defence. *Nature Rev. Immunol.* **7**, 179–190 (2007).
7. Liew, F. Y., Xu, D., Brint, E. K. & O'Neill, L. A. Negative regulation of Toll-like receptor-mediated immune responses. *Nature Rev. Immunol.* **5**, 446–458 (2005).
8. Schroder, K. & Tschopp, J. The inflammasomes. *Cell* **140**, 821–832 (2010).
9. Takeuchi, O. & Akira, S. Pattern recognition receptors and inflammation. *Cell* **140**, 805–820 (2010).
10. Ting, J. P., Duncan, J. A. & Lei, Y. How the noninflammasome NLRs function in the innate immune system. *Science* **327**, 286–290 (2010).
11. Tschopp, J. & Schroder, K. NLRP3 inflammasome activation: the convergence of multiple signalling pathways on ROS production? *Nature Rev. Immunol.* **10**, 210–215 (2010).
12. Ulevitch, R. J. & Tobias, P. S. Receptor-dependent mechanisms of cell stimulation by bacterial endotoxin. *Annu. Rev. Immunol.* **13**, 437–457 (1995).
13. Jiang, Z. *et al.* CD14 is required for MyD88-independent LPS signaling. *Nature Immunol.* **6**, 565–570 (2005).
14. Dziarski, R., Tapping, R. I. & Tobias, P. S. Binding of bacterial peptidoglycan to CD14. *J. Biol. Chem.* **273**, 8680–8690 (1998).
15. Schroder, N. W. *et al.* Lipopolysaccharide binding protein binds to triacylated and diacylated lipopeptides and mediates innate immune responses. *J. Immunol.* **173**, 2683–2691 (2004).
16. Schroder, N. W. *et al.* Lipoteichoic acid (LTA) of *Streptococcus pneumoniae* and *Staphylococcus aureus* activates immune cells via Toll-like receptor (TLR)-2, lipopolysaccharide-binding protein (LBP), and CD14, whereas TLR-4 and MD-2 are not involved. *J. Biol. Chem.* **278**, 15587–15594 (2003).
17. Jack, R. S. *et al.* Lipopolysaccharide-binding protein is required to combat a murine Gram-negative bacterial infection. *Nature* **389**, 742–745 (1997).
18. Weber, J. R. *et al.* Recognition of pneumococcal peptidoglycan: an expanded, pivotal role for LPS binding protein. *Immunity* **19**, 269–279 (2003).
19. Shimazu, R. *et al.* MD-2, a molecule that confers lipopolysaccharide responsiveness on Toll-like receptor 4. *J. Exp. Med.* **189**, 1777–1782 (1999).
20. Nagai, Y. *et al.* Essential role of MD-2 in LPS responsiveness and TLR4 distribution. *Nature Immunol.* **3**, 667–672 (2002).
21. Park, B. S. *et al.* The structural basis of lipopolysaccharide recognition by the TLR4–MD-2 complex. *Nature* **458**, 1191–1195 (2009).
    This paper is the first description of the crystal structure of a TLR in complex with its ligand and an accessory molecule.
22. Calvo, D., Dopazo, J. & Vega, M. A. The CD36, CLA-1 (CD36L1), and LIMPII (CD36L2) gene family: cellular distribution, chromosomal location, and genetic evolution. *Genomics* **25**, 100–106 (1995).
23. Triantafilou, M. *et al.* Membrane sorting of Toll-like receptor (TLR)-2/6 and TLR2/1 heterodimers at the cell surface determines heterotypic associations with CD36 and intracellular targeting. *J. Biol. Chem.* **281**, 31002–31011 (2006).
24. Hoebe, K. *et al.* CD36 is a sensor of diacylglycerides. *Nature* **433**, 523–527 (2005).
25. Stuart, L. M. *et al.* Response to *Staphylococcus aureus* requires CD36-mediated phagocytosis triggered by the COOH-terminal cytoplasmic domain. *J. Cell Biol.* **170**, 477–485 (2005).
26. Stewart, C. R. *et al.* CD36 ligands promote sterile inflammation through assembly of a Toll-like receptor 4 and 6 heterodimer. *Nature Immunol.* **11**, 155–161 (2010).
27. Tao, N., Wagner, S. J. & Lublin, D. M. CD36 is palmitoylated on both N- and C-terminal cytoplasmic tails. *J. Biol. Chem.* **271**, 22315–22320 (1996).
28. Baumann, C. L. *et al.* CD14 is a coreceptor of Toll-like receptors 7 and 9. *J. Exp. Med.* **207**, 2689–2701 (2010).
29. Hailman, E. *et al.* Lipopolysaccharide (LPS)-binding protein accelerates the binding of LPS to CD14. *J. Exp. Med.* **179**, 269–277 (1994).
30. Lee, H. K., Dunzendorfer, S., Soldau, K. & Tobias, P. S. Double-stranded RNA-mediated TLR3 activation is enhanced by CD14. *Immunity* **24**, 153–163 (2006).
    This paper provided the first concrete evidence that CD14 is important for endosomal TLRs in addition to surface TLRs.
31. Nakata, T. *et al.* CD14 directly binds to triacylated lipopeptides and facilitates recognition of the lipopeptides by the receptor complex of Toll-like receptors 2 and 1 without binding to the complex. *Cell. Microbiol.* **8**, 1899–1909 (2006).
32. Kim, J. I. *et al.* Crystal structure of CD14 and its implications for lipopolysaccharide signaling. *J. Biol. Chem.* **280**, 11347–11351 (2005).
33. Haziot, A. *et al.* Resistance to endotoxin shock and reduced dissemination of Gram-negative bacteria in CD14-deficient mice. *Immunity* **4**, 407–414 (1996).
34. Zanoni, I. *et al.* CD14 controls the LPS-induced endocytosis of Toll-like receptor 4. *Cell* **147**, 868–880 (2011).
    This was the first description of LPS-induced trafficking of TLR4 by CD14.
35. Akashi-Takamura, S. & Miyake, K. TLR accessory molecules. *Curr. Opin. Immunol.* **20**, 420–425 (2008).
36. da Silva Correia, J., Soldau, K., Christen, U., Tobias, P. S. & Ulevitch, R. J. Lipopolysaccharide is in close proximity to each of the proteins in its membrane receptor complex: transfer from CD14 to TLR4 and MD-2. *J. Biol. Chem.* **276**, 21129–21135 (2001).
37. Gioannini, T. L. *et al.* Isolation of an endotoxin–MD-2 complex that produces Toll-like receptor 4-dependent cell activation at picomolar concentrations. *Proc. Natl Acad. Sci. USA* **101**, 4186–4191 (2004).
38. Compton, T. *et al.* Human cytomegalovirus activates inflammatory cytokine responses via CD14 and Toll-like receptor 2. *J. Virol.* **77**, 4588–4596 (2003).
39. Georgel, P. *et al.* Vesicular stomatitis virus glycoprotein G activates a specific antiviral Toll-like receptor 4-dependent pathway. *Virology* **362**, 304–313 (2007).
40. Kurt-Jones, E. A. *et al.* Pattern recognition receptors TLR4 and CD14 mediate response to respiratory syncytial virus. *Nature Immunol.* **1**, 398–401 (2000).
41. Carpenter, S. *et al.* TRIL, a functional component of the TLR4 signaling complex, highly expressed in brain. *J. Immunol.* **183**, 3989–3995 (2009).
42. Carpenter, S., Wochal, P., Dunne, A. & O'Neill, L. A. Toll-like receptor 3 (TLR3) signaling requires TLR4 interactor with leucine-rich repeats (TRIL). *J. Biol. Chem.* **286**, 38795–38804 (2011).
43. Kessenbrock, K. *et al.* Proteinase 3 and neutrophil elastase enhance inflammation in mice by inactivating antiinflammatory progranulin. *J. Clin. Invest.* **118**, 2438–2447 (2008).
44. Zhu, J. *et al.* Conversion of proepithelin to epithelins: roles of SLPI and elastase in host defense and wound repair. *Cell* **111**, 867–878 (2002).
45. Park, B. *et al.* Granulin is a soluble cofactor for Toll-like receptor 9 signaling. *Immunity* **34**, 505–513 (2011).
    Here, granulin was shown to have an essential role in ligand delivery for TLR9 activation.
46. Lotze, M. T. & Tracey, K. J. High-mobility group box 1 protein (HMGB1): nuclear weapon in the immune arsenal. *Nature Rev. Immunol.* **5**, 331–342 (2005).
47. Andersson, U. & Tracey, K. J. HMGB1 is a therapeutic target for sterile inflammation and infection. *Annu. Rev. Immunol.* **29**, 139–162 (2011).
48. Ivanov, S. *et al.* A novel role for HMGB1 in TLR9-mediated inflammatory responses to CpG-DNA. *Blood* **110**, 1970–1981 (2007).
49. Tian, J. *et al.* Toll-like receptor 9-dependent activation by DNA-containing immune complexes is mediated by HMGB1 and RAGE. *Nature Immunol.* **8**, 487–496 (2007).
    This work first reported a role for HMGB1 in delivering DNA to TLR9.
50. Urbonaviciute, V. *et al.* Induction of inflammatory and immune responses by HMGB1–nucleosome complexes: implications for the pathogenesis of SLE. *J. Exp. Med.* **205**, 3007–3018 (2008).
51. Leadbetter, E. A. *et al.* Chromatin–IgG complexes activate B cells by dual engagement of IgM and Toll-like receptors. *Nature* **416**, 603–607 (2002).
52. Avalos, A. M. *et al.* RAGE-independent autoreactive B cell activation in response to chromatin and

HMGB1/DNA immune complexes. *Autoimmunity* **43**, 103–110 (2010).
53. Yanai, H. *et al.* HMGB proteins function as universal sentinels for nucleic-acid-mediated innate immune responses. *Nature* **462**, 99–103 (2009).
54. Lande, R. *et al.* Plasmacytoid dendritic cells sense self-DNA coupled with antimicrobial peptide. *Nature* **449**, 564–569 (2007).
    This paper demonstrated the role of LL37 in DNA delivery to TLR9 in pDCs.
55. Gilliet, M. & Lande, R. Antimicrobial peptides and self-DNA in autoimmune skin inflammation. *Curr. Opin. Immunol.* **20**, 401–407 (2008).
56. Zanetti, M., Gennaro, R. & Romeo, D. The cathelicidin family of antimicrobial peptide precursors: a component of the oxygen-independent defense mechanisms of neutrophils. *Ann. NY Acad. Sci.* **832**, 147–162 (1997).
57. Ganguly, D. *et al.* Self-RNA–antimicrobial peptide complexes activate human dendritic cells through TLR7 and TLR8. *J. Exp. Med.* **206**, 1983–1994 (2009).
58. Yang, Y. & Li, Z. Roles of heat shock protein gp96 in the ER quality control: redundant or unique function? *Mol. Cells* **20**, 173–182 (2005).
59. Liu, B. & Li, Z. Endoplasmic reticulum HSP90b1 (gp96, grp94) optimizes B-cell function via chaperoning integrin and TLR but not immunoglobulin. *Blood* **112**, 1223–1230 (2008).
60. Randow, F. & Seed, B. Endoplasmic reticulum chaperone gp96 is required for innate immunity but not cell viability. *Nature Cell Biol.* **3**, 891–896 (2001).
61. Wanderling, S. *et al.* GRP94 is essential for mesoderm induction and muscle development because it regulates insulin-like growth factor secretion. *Mol. Biol. Cell* **18**, 3764–3775 (2007).
62. Yang, Y. *et al.* Heat shock protein gp96 is a master chaperone for Toll-like receptors and is important in the innate function of macrophages. *Immunity* **26**, 215–226 (2007).
63. Staron, M. *et al.* Heat-shock protein gp96/grp94 is an essential chaperone for the platelet glycoprotein Ib-IX-V complex. *Blood* **117**, 7136–7144 (2011).
64. Liu, B. *et al.* Folding of Toll-like receptors by the HSP90 paralogue gp96 requires a substrate-specific cochaperone. *Nature Commun.* **1**, 79 (2010).
    This paper shows that GRP94 and PRAT4A work together to chaperone TLRs.
65. Wakabayashi, Y. *et al.* A protein associated with Toll-like receptor 4 (PRAT4A) regulates cell surface expression of TLR4. *J. Immunol.* **177**, 1772–1779 (2006).
66. Takahashi, K. *et al.* A protein associated with Toll-like receptor (TLR) 4 (PRAT4A) is required for TLR-dependent immune responses. *J. Exp. Med.* **204**, 2963–2976 (2007).
67. Kiyokawa, T. *et al.* A single base mutation in the PRAT4A gene reveals differential interaction of PRAT4A with Toll-like receptors. *Int. Immunol.* **20**, 1407–1415 (2008).
68. Tabeta, K. *et al.* The *Unc93b1* mutation 3d disrupts exogenous antigen presentation and signaling via Toll-like receptors 3, 7 and 9. *Nature Immunol.* **7**, 156–164 (2006).
69. Casrouge, A. *et al.* Herpes simplex virus encephalitis in human UNC-93B deficiency. *Science* **314**, 308–312 (2006).
70. Brinkmann, M. M. *et al.* The interaction between the ER membrane protein UNC93B and TLR3, 7, and 9 is crucial for TLR signaling. *J. Cell Biol.* **177**, 265–275 (2007).
71. Kim, Y. M., Brinkmann, M. M., Paquet, M. E. & Ploegh, H. L. UNC93B1 delivers nucleotide-sensing Toll-like receptors to endolysosomes. *Nature* **452**, 234–238 (2008).
    This paper provides evidence for the role of UNC93B1 in the trafficking of endosomal TLRs.
72. Fukui, R. *et al.* Unc93B1 biases Toll-like receptor responses to nucleic acid in dendritic cells toward DNA- but against RNA-sensing. *J. Exp. Med.* **206**, 1339–1350 (2009).
73. Fukui, R. *et al.* Unc93B1 restricts systemic lethal inflammation by orchestrating Toll-like receptor 7 and 9 trafficking. *Immunity* **35**, 69–81 (2011).
74. Nakatsu, F. & Ohno, H. Adaptor protein complexes as the key regulators of protein sorting in the post-Golgi network. *Cell Struct. Funct.* **28**, 419–429 (2003).
75. Sasai, M., Linehan, M. M. & Iwasaki, A. Bifurcation of Toll-like receptor 9 signaling by adaptor protein 3. *Science* **329**, 1530–1534 (2010).
    This study was the first to demonstrate that AP3 has a role in TLR9-dependent IFN responses.

REVIEWS

76. Blasius, A. L. et al. Slc15a4, AP-3, and Hermansky-Pudlak syndrome proteins are required for Toll-like receptor signaling in plasmacytoid dendritic cells. Proc. Natl Acad. Sci. USA 107, 19973–19978 (2010).
77. Guiducci, C. et al. Properties regulating the nature of the plasmacytoid dendritic cell response to Toll-like receptor 9 activation. J. Exp. Med. 203, 1999–2008 (2006).
78. Honda, K. et al. Spatiotemporal regulation of MyD88–IRF-7 signalling for robust type-I interferon induction. Nature 434, 1035–1040 (2005).
79. Ewald, S. E. et al. The ectodomain of Toll-like receptor 9 is cleaved to generate a functional receptor. Nature 456, 658–662 (2008).
80. Park, B. et al. Proteolytic cleavage in an endolysosomal compartment is required for activation of Toll-like receptor 9. Nature Immunol. 9, 1407–1414 (2008).
References 79 and 80 demonstrate the cleavage requirement for TLR9 activation by CpG DNA.
81. Asagiri, M. et al. Cathepsin K-dependent Toll-like receptor 9 signaling revealed in experimental arthritis. Science 319, 624–627 (2008).
82. Matsumoto, F. et al. Cathepsins are required for Toll-like receptor 9 responses. Biochem. Biophys. Res. Commun. 367, 693–699 (2008).
83. Sepulveda, F. E. et al. Critical role for asparagine endopeptidase in endocytic Toll-like receptor signaling in dendritic cells. Immunity 31, 737–748 (2009).
This is the first demonstration of a role for AEP in TLR9 activation in primary DCs.
84. Ewald, S. E. et al. Nucleic acid recognition by Toll-like receptors is coupled to stepwise processing by cathepsins and asparagine endopeptidase. J. Exp. Med. 208, 643–651 (2011).
85. Saitoh, T. et al. Antiviral protein Viperin promotes Toll-like receptor 7- and Toll-like receptor 9-mediated type I interferon production in plasmacytoid dendritic cells. Immunity 34, 352–363 (2011).

86. Gerold, G. et al. A Toll-like receptor 2–integrin β3 complex senses bacterial lipopeptides via vitronectin. Nature Immunol. 9, 761–768 (2008).
87. Kagan, J. C. & Medzhitov, R. Phosphoinositide-mediated adaptor recruitment controls Toll-like receptor signaling. Cell 125, 943–955 (2006).
88. Gantner, B. N., Simmons, R. M., Canavera, S. J., Akira, S. & Underhill, D. M. Collaborative induction of inflammatory responses by dectin-1 and Toll-like receptor 2. J. Exp. Med. 197, 1107–1117 (2003).
89. Nagai, Y. et al. The radioprotective 105/MD-1 complex links TLR2 and TLR4/MD-2 in antibody response to microbial membranes. J. Immunol. 174, 7043–7049 (2005).
90. Divanovic, S. et al. Negative regulation of Toll-like receptor 4 signaling by the Toll-like receptor homolog RP105. Nature Immunol. 6, 571–578 (2005).
91. Blumenthal, A. et al. RP105 facilitates macrophage activation by Mycobacterium tuberculosis lipoproteins. Cell Host Microbe 5, 35–46 (2009).
92. Uccellini, M. B. et al. Autoreactive B cells discriminate CpG-rich and CpG-poor DNA and this response is modulated by IFN-α. J. Immunol. 181, 5875–5884 (2008).
93. Viglianti, G. A. et al. Activation of autoreactive B cells by CpG dsDNA. Immunity 19, 837–847 (2003).
94. Lau, C. M. et al. RNA-associated autoantigens activate B cells by combined B cell antigen receptor/Toll-like receptor 7 engagement. J. Exp. Med. 202, 1171–1177 (2005).
95. Chaturvedi, A., Dorward, D. & Pierce, S. K. The B cell receptor governs the subcellular location of Toll-like receptor 9 leading to hyperresponses to DNA-containing antigens. Immunity 28, 799–809 (2008).
96. Avalos, A. M. et al. Differential cytokine production and bystander activation of autoreactive B cells in response to CpG-A and CpG-B oligonucleotides. J. Immunol. 183, 6262–6268 (2009).
97. Hori, O. et al. The receptor for advanced glycation end products (RAGE) is a cellular binding site for amphoterin. Mediation of neurite outgrowth and co-expression of

rage and amphoterin in the developing nervous system. J. Biol. Chem. 270, 25752–25761 (1995).
98. Bierhaus, A. et al. Understanding RAGE, the receptor for advanced glycation end products. J. Mol. Med. 83, 876–886 (2005).
99. Boullier, A. et al. The binding of oxidized low density lipoprotein to mouse CD36 is mediated in part by oxidized phospholipids that are associated with both the lipid and protein moieties of the lipoprotein. J. Biol. Chem. 275, 9163–9169 (2000).
100. Coraci, I. S. et al. CD36, a class B scavenger receptor, is expressed on microglia in Alzheimer's disease brains and can mediate production of reactive oxygen species in response to β-amyloid fibrils. Am. J. Pathol. 160, 101–112 (2002).
101. Jimenez-Dalmaroni, M. J. et al. Soluble CD36 ectodomain binds negatively charged diacylglycerol ligands and acts as a co-receptor for TLR2. PLoS ONE 4, e7411 (2009).
102. Yang, R. B., Mark, M. R., Gurney, A. L. & Godowski, P. J. Signaling events induced by lipopolysaccharide-activated Toll-like receptor 2. J. Immunol. 163, 639–643 (1999).
103. Muta, T. & Takeshige, K. Essential roles of CD14 and lipopolysaccharide-binding protein for activation of Toll-like receptor (TLR)2 as well as TLR4 reconstitution of TLR2- and TLR4-activation by distinguishable ligands in LPS preparations. Eur. J. Biochem. 268, 4580–4589 (2001).

FURTHER INFORMATION
Hidde L.Ploegh's homepage: http://jura.wi.mit.edu/ploegh/
ALL LINKS ARE ACTIVE IN THE ONLINE PDF

126